universität wien

DIPLOMARBEIT

Titel der Diplomarbeit

Penetration of Hydroxypyridinones through the Blood-Brain Barrier based on a cell monolayer system

angestrebter akademischer Grad

Magistra der Pharmazie (Mag.pharm.)

Verfasserin:	Elisabeth Priester
Matrikel-Nummer:	0500824
Studienrichtung /Studienzweig (lt. Studienblatt):	Pharmazie
Betreuer:	O. Univ.-Prof. DI Mag. Dr. Christian Noe

Wien, am 27.5.2010

Acknowledgements

First I'd like to thank Prof. Dr. Robert Hider from King's College London and Prof. Dr. Christian Noe from the University of Vienna for giving me the chance to do this project in London. A very special thanks goes to Dr. Hannelore Kopelent-Frank who did an amazing job coordinating my stay and always knew what to do.

I also want to thank Dr. Sarah Thomas for having me in her group and for supporting me in so many ways. Christopher Watson, who answered all my questions, regardless of their simplicity, was the best supervisor I could have gotten throughout this whole project. Furthermore, I would like to thank Sourav Roy who introduced me into the mysteries of HPLC and helped me analyse my chromatograms. Murat Dogruel and Mehmet Fidanboylu made sure that there was enough fun besides the work in the lab, thank you for that.

I would also like to thank all my friends and my family for their support, especially my parents who kept their expectations high so that I could reach for them.

Thank you Martin for your amazing and loving support through all the years.

TABLE OF CONTENTS

List of figures

List of tables

List of Abbreviations

ABC – ATP-binding cassette

AJ – adherens junction

ATP – adenosine triphosphate

AUC – area under the curve

BBB – blood-brain barrier

BCRP – breast cancer resistance protein

CNS – central nervous system

CP20 – deferiprone

DMSO – dimethylsulfoxide

GABA - γ-aminobutyric acid

GLUT – glucose transporter

HEPES – 4-(2-hydroxyethyl)-1-piperazineethanesulfonic acid

HPLC – high pressure liquid chromatography

hTERT – human telomerase reverse transcriptase

JAM – junctional adhesion molecule

M - molar

MRP – multidrug resistance-associated protein

MTT - (3-(4,5-dimethylthiazol-2-yl)-2,5-diphenyl tetrazolium bromide

PBS – phosphate-buffered saline

PgP – P-glycoprotein

PSA – polar surface area

SLC – solute carrier

TEER – transendothelial electrical resistance

TJ – tight junction

ZO – zonula occludens

1 Introduction:

1.1 The Blood-Brain Barrier

1.1.1 Function of the Blood-Brain Barrier

The Blood-Brain Barrier (BBB) is a complex structure of capillary endothelial cells which prevents damaging and toxic substances from getting into the brain. However, it also differentiates between substrates required by the central nervous system (CNS) and unwanted agents such as xenobiotics and microorganisms (Mensch, Oyarzabal et al. 2009). It also makes sure the brain is cleared of metabolites, waste products and unwanted molecules (Abbott, Ronnback et al. 2006). Additionally, the BBB plays an important role in maintaining the homeostatic regulation of the brain microenvironment, being an essential requirement for the healthy activity of the neurons (Abbott 2002). This function is especially important as changes in the ionic composition of the blood that occur after meals or exercise, would significantly damage synaptic and axonal signalling. Subsequently, the BBB separates two pools of neurotransmitters, peripheral and central, making it possible for the body to use similar agents in different concentrations without having an effect on each other (Abbott, Ronnback et al. 2006).

1.1.2 History

The first empirical observation of the BBB was documented by Paul Ehrlich, a German scientist and physician, in 1885. He intravenously injected dyes which are used for vital staining in cells, in rats and discovered that they would stain all the organs of the body except for the brain. However Ehrlich did not draw the right conclusion as he thought the brain had less affinity to the dye than the other parts of the body. His student Edwin Goldmann continued the experiments and injected Trypan blue intravenously. He made the same observation, but additionally he performed experiments where he injected the dye into the cerebrospinal fluid. Importantly only the brain and the CSF were dyed, the other organs were unstained. Upon this result, Goldmann presumed some kind of barrier must

exist between the blood and the brain. But he was not the only one, who had a closer look at this matter, Max Lewandowsky, a German neurologist, performed experiments with Potassium hexocyanidoferrate(II) and was the first to introduce the term “Blood-Brain Barrier”. In the 1930s a differentiation between BBB and blood-CSF barrier was made, but it was not until the 1960s that scanning electron microscopy gave proof of the existence of the BBB.

1.1.3 Structure and cell types

The BBB is formed mainly by three different cell types (Fig. 1): endothelial cells, which line the cerebral capillaries, astrocytes, to envelope the capillary endothelium and in between pericytes, which work as connective tissue. Due to their interaction in health and injury they are seen as a functional unit, called the neurovascular unit (Cecchelli, Berezowski et al. 2007). The cerebral endothelial cells are different from those in the periphery in two main ways. Firstly they form tight junctions, a key element of the BBB which gives the BBB its physical “barrier” properties, and secondly they have a relatively low rate of fluid-endocytosis (Rubin, Hall et al. 1991). Additionally, they lack fenestrations and have increased mitochondrial content (Hawkins and Davis 2005). All of these features ensure the barrier function of the BBB.

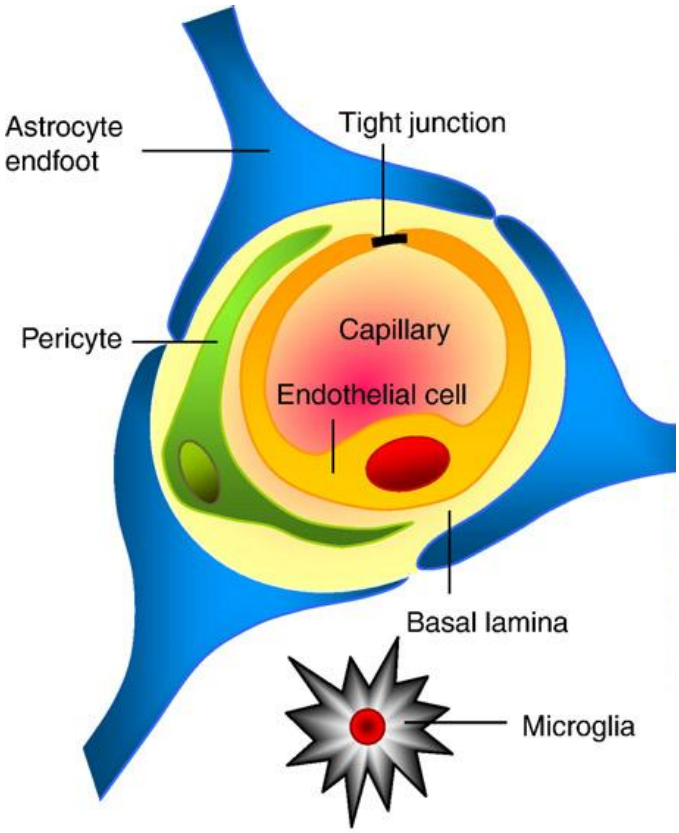

Fig. 1 schematic representation of the neurovascular unit, modified from (Abbott, Patabendige et al. 2010)

Astrocyte endfeet cover more than 99% of the endothelial cells’ abluminal side. They play an important role in the differentiation of the BBB and heighten the restrictive barrier. In vitro

studies have proved that endothelial cells have an increased transendothelial electrical resistance (TEER) when co-cultured with astrocytes. The TEER displays the tightness of a cell layer (see section 1.1.4) and is used to characterise the ion permeability in cerebral blood vessels but also epithelia (Butt, Jones et al. 1990). The increased TEER can be partially explained by the induction of tight junctional properties by soluble astrocytic paracrine factors. However, the role of the astrocytic endfeet in maintaining BBB integrity is not yet fully understood. Furthermore astrocytes can also modulate enzymes and transporter systems such as the multi-drug resistance efflux transporter Pgp (P-glycoprotein) and the brain glucose transporter GLUT-1 (Smith and Gumbleton 2006).

Other than the endothelial cells and the astrocytes, pericytes, the third component of the neurovascular unit, have also yet to have their role in the BBB uncovered. They can be seen as the smooth muscle cell of the unit and appear to stabilize it. In addition to providing structural integrity, they apparently play a role in the regulation of the cerebral blood flow (Smith and Gumbleton 2006). In pathological conditions e.g. hypoxia or brain injury, where the BBB integrity is decreased, pericytes migrate away from the microvessels. Therefore it is assumed that these two phenomena are related, but it has not yet been verified if the pericyte migration has a causative role in BBB deficiency (Hawkins and Davis 2005). Further pericytes seem to play a key role in the formation of new vessels and they express a variety of metabolising enzymes and scavenging receptors which distinguishes their role as an enzymatic barrier and in neuroimmunity (Smith and Gumbleton 2006).

1.1.4 Features of the BBB – junctional complexes

The BBB has several characteristics which give the highly specialised endothelium strong barrier. First of all the tight junctions (TJs) and in addition adherens junctions (AJs) ensure that there is very limited paracellular traffic of molecules, only small gaseous molecules like O_2 and CO_2 can pass the BBB freely (Abbott, Ronnback et al. 2006). The presence of gap junctions has not yet been confirmed (Hawkins and Davis 2005). Consequently, most of the substances which cross the BBB have to take a transcellular pathway and use transporters or other ways (see 1.1.5) as the route of simple diffusion is not available for all of them

(Hawkins and Davis 2005). Also waste products from the brain require efflux into the blood and specific mechanisms exist at the BBB to allow for this.

Tight junctions are the bridging elements that link the endothelial cells and therefore provide a solid bloodvessel (Stamatovic, Keep et al. 2008).

By using the method of freeze-fracture techniques the morphological structure of the TJs can be seen. These replicas show the complexity and the association with the inner (P-face) or outer (E-face) lipidic layer of the membrane. As a result it is visible, that in brain capillaries, the TJs associate in the same degree with both faces, whereas TJs in peripheral endothelial cells prefer the E-face. This observation is another proof for the tightness of the barrier (Wolburg, Noell et al. 2009).

The TJs have a very complex structure (Fig. 2) formed by various plasma membrane proteins to link and connect the endothelial cells. The most important ones are the claudins, occludin, junctional adhesion molecules (JAMs) and cytoplasmic proteins, such as zonula occludens proteins (ZO) and cingulin (Ueno 2009).

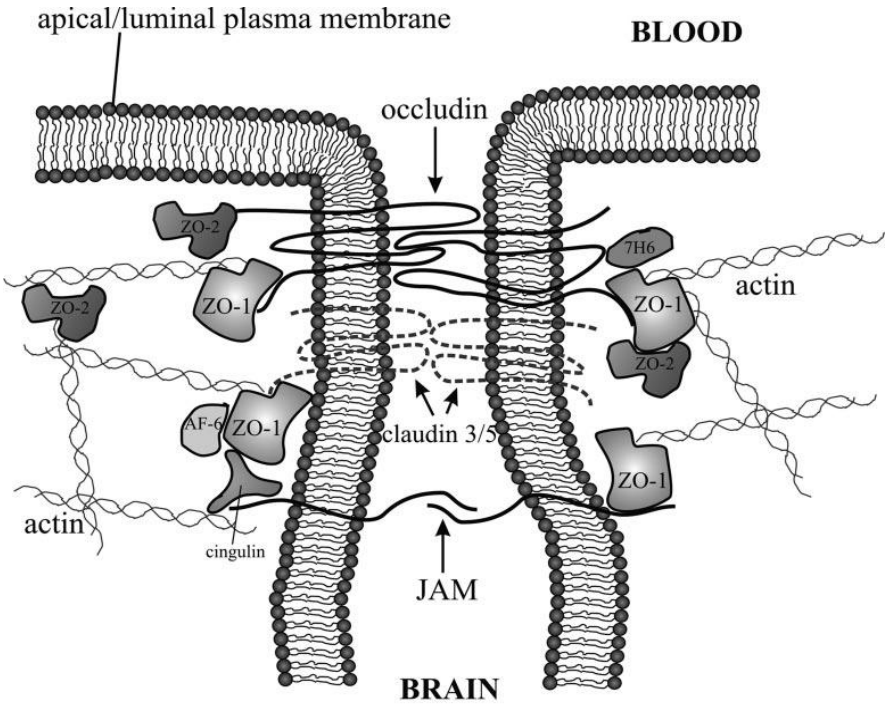

Fig. 2 Representation of the main elements forming a tight junction. Modified from (Hawkins and Davis 2005)

Claudins are the core element of the TJs, they enable the high TEER and form the principal hurdle (Hawkins and Davis 2005; Bernacki, Dobrowolska et al. 2008). To date 24 different claudins have been described in mammals, their size varies between 20 and 24 kDa, but structurally they show the same elements: two extracellular loops, four transmembrane domains and both C- and N-Terminus in the cytoplasm (Stamatovic, Keep et al. 2008). The extracellular loops correspond with each other in both a homophilic and a heterophilic way (Hawkins and Davis 2005). One of them controls paracellular charge selectivity whereas the other one is a receptor for a bacterial toxin. In the cytoplasm the C-Terminus links the protein with ZO-1, ZO-2 and ZO-3 (Hawkins and Davis 2005; Bernacki, Dobrowolska et al. 2008). Of the mentioned 24 claudins, the BBB shows claudin-1, claudin-3 and claudin-5, although the presence of claudin-1 has been questioned recently (Hawkins and Davis 2005).

In addition to this “backbone”, occludin, another transmembrane, protein helps to maintain the barrier. It was the first to be discovered and shares some structural features but no sequence homology with the claudin family (Wolburg, Noell et al. 2009). Occludin has a size of around 65 kDa and its structure includes four transmembrane regions, two extracellular loops and one intracellular short turn. Both C- and N-terminus are situated in the cytoplasm. The two extracellular loops again provide the TEER and the adhesion between the cells. At the C-terminal end it is connected with ZO-1, ZO-2 and ZO-3, the N-terminus is important for the role of an adhesion molecule (Stamatovic, Keep et al. 2008). Nevertheless, it has been proved in various studies, that a deficiency of occludin does not influence the formation of TJs. It has more of a regulatory purpose although a reduced expression correlates with disrupted BBB function in several diseases (Hawkins and Davis 2005).

The third element of the TJs, providing with bonding character are the junctional adhesion molecules (JAMs). Their exact function in the grown BBB is still largely unknown, but it is assumed that they play a role in the early attachment of vicinal cells membranes (Hawkins and Davis 2005). JAMs belong to the group of immunoglobulins with a size of about 40 kDa. Structurally they have a single transmembrane domain, which is linked to an extracellular strand with two loops (Bernacki, Dobrowolska et al. 2008). The C-terminal end is in the cytoplasm again, but the N-terminus lies in the extracellular space (Stamatovic, Keep et al. 2008). Three types have been distinguished: JAM-1, -2 and -3 (Bernacki, Dobrowolska et al. 2008).

Finally there is the group of cytoplasmic proteins, for instance zonula occludens proteins or cingulin. In general they help maintaining the tight junctions and provide structural support. ZOs (ZO-1, -2 and -3 are known by now) are linking with claudins, occludin and JAM, Cingulin on the other hand binds to ZOs and myosin. Altogether they connect the transmembrane proteins with the cytoskeleton (Bernacki, Dobrowolska et al. 2008).

Adherens junctions have the same purpose as well as arbitrating the adhesion of the endothelial cells to each other, upholding their contact and initiating cell polarity. The major component of AJ is vascular endothelial (VE)-cadherin, a Ca^{2+}-regulated protein, which mediates cell-cell adhesion of bordering cells by homophilic interaction of the extracellular domains of proteins (Hawkins and Davis 2005). Cadherin is linked with catenin and other related proteins. In that way the membrane proteins are, through the cytoplasmic proteins, connected with the actin cytoskeleton, which is the backbone of the cell (Ueno 2009).

Though the AJs contribute to the tightness, it is the tight junctions that provide most of it. Characteristics here are the high transendothelial electrical resistance (TEER) of about 1500 – 2000 $\Omega.cm^2$, peripheral capillaries show a TEER of 3 – 33 $\Omega.cm^2$, and the dependence on a stable Ca^{2+} concentration to maintain the integrity (Bernacki, Dobrowolska et al. 2008; Stamatovic, Keep et al. 2008). Therefore changes in the electrolyte household can influence the barrier delicately and decrease permeability. On the contrary elevated cATP levels in the cell induce the forming of fusion points and fasten TJs (Bernacki, Dobrowolska et al. 2008).

1.1.5 Pathways across the BBB and their mechanisms

Due to the above-mentioned physiologically restricting structure, most of the pathways across the BBB are transporter-mediated.

Paracellular transport is highly restrictive and it is controlled by electrochemical, hydrostatic and osmotic gradients. In cases of higher paracellular transport the junctional complexes are being altered and form minute intercellular gaps (Stamatovic, Keep et al. 2008). This situation can occur in case of stroke or epileptogenic foci (Abbott, Patabendige et al. 2010). In a situation like that albumin (and other plasma proteins), fluids and leukocytes are able to pass the barrier (Stamatovic, Keep et al. 2008).

On the other hand transcellular pathways can be classified in passive diffusion, transport proteins, receptor-mediated transcytosis and adsorptive transcytosis (Fig. 3).

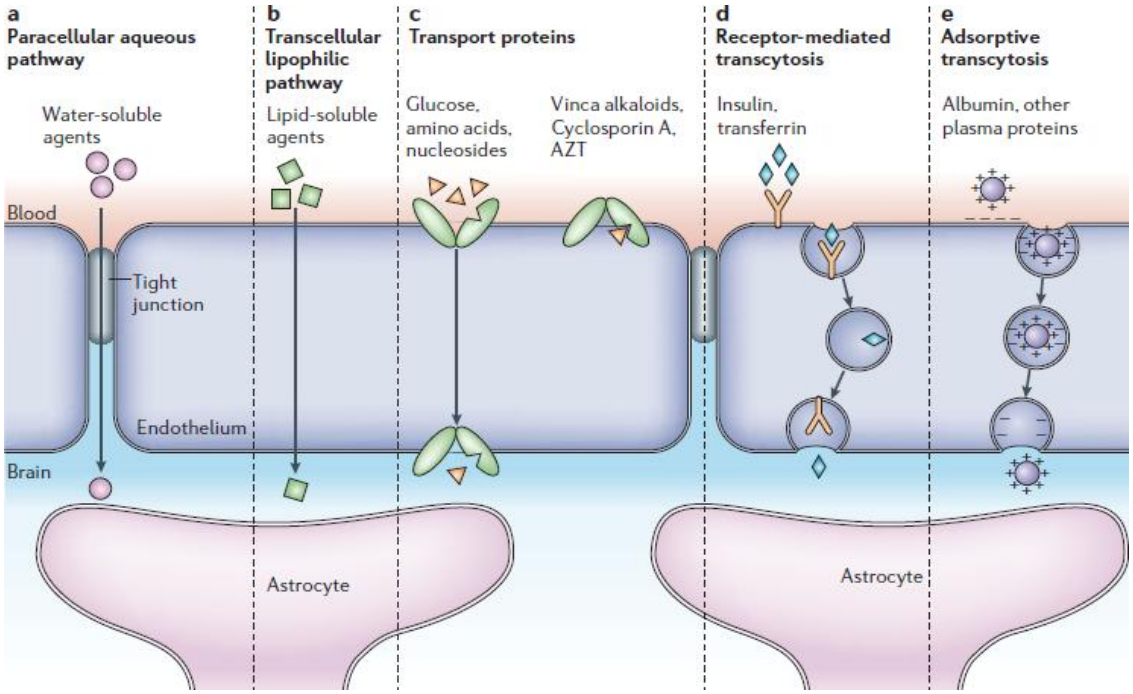

Fig. 3 different pathways across the BBB, from (Abbott, Ronnback et al. 2006), further explanation in the text

First there is the way of passive diffusion, which can only be used by small lipophilic molecules. Criteria for predicting a substance's ability to pass the barrier passively are the logD (partition coefficient between octanol and buffer at pH 7.4), the polar surface area (PSA) and the tendency of the molecule to form hydrogen bonds. In general a higher logD correlates with better permeation, a PSA greater than 80 $Å^2$ and the ability to form more than 6 hydrogen bonds decrease the possibility for passive diffusion. Additionally rotatable bonds and a molecular weight of more than 450 Da appear to restrain BBB permeability. Nevertheless, these are only guidelines and there are always exceptions to the rule. Apart from small, lipophilic substances, two essential gases, oxygen and carbon dioxide, diffuse passively along their concentration gradients. Hence, if the cerebral blood flow is ensured, the oxygen supply and carbon dioxide removal are guaranteed (Abbott, Patabendige et al. 2010).

The next pathway is the one via transport proteins which is, along with the mechanism of receptor-mediated transcytosis, responsible for the uptake of substrates and the efflux of unwanted substances (Abbott and Romero 1996). Drug transporters can be divided into two major families, the ATP-binding cassette transporters (ABC) and the solute carrier-family (SLC) (Eyal, Hsiao et al. 2009).

ABC-transporters characteristically need ATP to transport their substrates against concentration gradients. The most prominent member here is Pgp, others are multidrug resistance-associated proteins (MRPs) and breast cancer resistance protein (BCRP). Pgp is an efflux pump located at the luminal side of the capillaries with a wide range of substrates, for instance the cytostatics, vincristin and vinblastin, as well as anti-retroviral agents like indinavir and opioids such as morphine and loperamide (Abbott and Romero 1996; Eyal, Hsiao et al. 2009). These substances all penetrate the membrane of the capillaries, but are removed by Pgp. This explains why their concentration in the brain is much lower than would be expected from their logD values (Abbott, Patabendige et al. 2010). However Pgp not only has substrates, but inhibitors too, for example the cardiac agent verapamil and the immunosuppressant cyclosporine. Therefore the option of inhibiting Pgp transiently to provide greater uptake of several drugs into the brain can be considered as a therapeutic strategy for diseases like epilepsy. Nevertheless, the hazards of such a modulation have to be taken into account (Loscher and Potschka 2005). The second prominent member of the ABC-transporter family, which is located at the luminal membrane is the breast cancer resistance protein (BCRP). Many substrates overlap with the ones of Pgp, but in contrast BCRP is upregulated in tumour cells (Eyal, Hsiao et al. 2009). Finally there is the group of MRPs which are present at the luminal (MRP2, MRP4) and the basolateral (MRP1, MRP3, MRP5, MRP6) membrane (Loscher and Potschka 2005). Most of these proteins are organic anion transporters, but there are neutral substrates too. Additionally to ATP, some of them need cofactors for the transport. Again substrates overlap with the ones of Pgp and BCRP (Eyal, Hsiao et al. 2009).

In contrast to the ABC-transporters, members of the SLC-family do not need ATP to transport their substrates. Currently there are 43 subfamilies in the human body known which have mostly polar and essential substrates like glucose or amino acids (Kusuhara and Sugiyama 2005; Abbott, Patabendige et al. 2010). The SLC-family members expressed at the BBB play a

greater role in supplying the brain with nutrients, rather than keeping unwanted agents out. Examples here include the glucose transporter GLUT-1 cationic amino acid transporters (CAT1 and CAT3) and the large neutral amino acid transporter (system L) (Abbott, Patabendige et al. 2010). The glucose transporter is of special importance because of the high need for glucose in the brain. There are two isoforms selectively expressed in brain capillaries, GLUT-1 and GLUT-3 (Guo, Geng et al. 2005; Wolburg, Noell et al. 2009). The expression is regulated by metabolic demand and regional differences in glucose need. Therefore a malfunction or dysregulation following or caused by different diseases can become rate limiting for the metabolism in the brain. Diseases like that are Alzheimer's disease, ischemia or epilepsy (Guo, Geng et al. 2005).

Third in the possibilities of transcellular pathways is receptor-mediated transcytosis. In this case the molecule binds to a specific receptor which activates an endocytotic event. First receptor and ligand cluster together, then a caveolus is formed which leads to the shaping of a vesicle with both receptor and ligand in it. Inside this vesicle they are moved to the other side of the cell and exocytosed (Abbott, Patabendige et al. 2010). This pathway is for large molecules like insulin, albumin, low- and high-density lipoprotein or advanced glycation end products (Wolburg, Noell et al. 2009).

Finally there is another type of transcytosis, called adsorptive transcytosis. As well as with receptor-mediated transcytosis, the substrates in adsorptive transcytosis are macromolecules such as cationised albumin or cell penetrating peptides. But unlike receptor-mediated transcytosis, the transported molecule has to show excessive positive charging to form the caveolus and later the vesicle (Abbott, Patabendige et al. 2010).

In both cases the vesicles' contents have to be kept safe from being lysed by degradative mechanisms such as lysosomes. It appears to be a speciality in brain endothelial cells to actively route the vesicles away from acidic lysosomes as in peripheral tissues endosomes are very often directed there for breakdown (Abbott, Patabendige et al. 2010).

1.1.6 Role as metabolic barrier

Another important function of the BBB are its metabolic properties. These restrict traffic across the BBB even more than just the physical barrier, as substances may enter the endothelial cells but can be metabolised and therefore made ineffective. Up until now it has been shown that in rodent brains enzymes such as monoamine oxidase, catechol-O-methyl transferase or epoxide hydrolase act at the blood-brain interface. Less evidence has been found that monoamine oxidase, epoxide hydrolase and several cytochromes such as CYP1B1 appear at the human BBB (Eyal, Hsiao et al. 2009). Nevertheless, the levels of cytochromes in the BBB are generally 0.5-2% of those in the liver (Carvey, Hendey et al. 2009). Apart from that the cytochromes possibly play a major role in regulating endogenous GABA (γ-aminobutyric acid). Finally the cytochromes which are present in the BBB appear to be inducible, as the ones in the liver are (Carvey, Hendey et al. 2009).

1.1.7 Different approaches in studying the BBB

Recently, as technology has improved, research on the BBB has increased and several models have been designed to explore different aspects of the BBB. In general there are three major approaches for studying the BBB: *in vivo*, *in vitro* and *in silico*.

In vivo

Although *in vitro* and *in silico* methods cost less money and often do not require as much time and effort, in vivo experiments remain an important part of BBB research as they give the most reliable reference information to validate and test other models. There is a broad range of techniques which can be separated into two major groups: the first is based on equilibrium studies between brain and blood such as the extent of brain penetration and the second is focused on kinetic parameters such as permeability X surface area product. Another classification can be made by dividing the techniques into invasive and non-invasive. Only the non-invasive experiments can be done on humans as they permit to measure the brain uptake along with pharmacokinetic parameters without harming the body (Mensch, Oyarzabal et al. 2009). Most of the invasive methods imply injecting the drug in question

along with a vascular space marker, for instance tritium-labelled inulin or technetium-marked albumin, to ensure the BBB is intact (Kakee, Terasaki et al. 1997; Pan, Banks et al. 1997). These markers typically have low permeability across the BBB and increased values indicate a loss of BBB integrity (Bickel 2005; Sanderson, Dogruel et al. 2009). The injection is made intravenously in the carotid artery, which is used for example with the brain uptake index technique or in situ brain perfusion. After the given perfusion time the animal is decapitated and the amount of drug in the different brain regions is analysed (Mensch, Oyarzabal et al. 2009). Another method is the intracerebral microdialysis, which is performed on a living animal. A probe is implanted in the extracellular space of the brain. Here it is possible to choose which region is analysed by selecting where to place the probe. It consists of a semi-permeable membrane which is perfused with a physiological medium. The drug in question can be administered orally, intravenously or subcutaneously and by collecting the perfusate at the membrane it is determined how much of the drug has entered the brain (Alavijeh, Chishty et al. 2005; Mensch, Oyarzabal et al. 2009). Non invasive techniques like MRI (magnet resonance imaging) or PET (positron emission tomography) allow highly specific monitoring of a number of pharmacokinetic parameters. On the other hand they are very expensive and the tracers used show some problems in terms of stability (Bickel 2005; Mensch, Oyarzabal et al. 2009).

In vitro

Compared to *in vivo* techniques, *in vitro* experiments do not show a whole organism, but they allow more specific analysis of transporters, for instance. Possibilities for *in vitro* preparations are isolated brain microvessels, primary endothelial cells (human or animal) alone or in coculture with astrocytes, immortalized brain endothelial cells, cell lines with non-brain origin like Caco-2 cells (from human colon adenoma) or ECV304/C6 cells (from human bladder carcinoma) and non-cell based immobilized artificial membrane chromatography (IAM) or parallel artificial permeability assay (PAMPA). Isolated brain microvessels are the *in vitro* model closest to in vivo, but they lose activity while being isolated and the luminal side is difficult to assess (Mensch, Oyarzabal et al. 2009). The next step is isolating endothelial cells and culturing them alone or in combination with astrocytes. These primary cells do not have a TEER as high as in vivo and lose some of their characteristic properties while being extracted, but on the other hand, they do maintain

most of them and can be used for studying transporters (Bickel 2005; Mensch, Oyarzabal et al. 2009). In general the primary cells mostly used, are of bovine or porcine origine. An alternative to bovine and porcine cells are rats as sources, but they do not provide a comparable yield of cells (Cecchelli, Berezowski et al. 2007). Primary cells are very often used for transport studies in a transwell setting. As said before, the biggest problem is the low TEER. Solutions to this problem are mimicking the presence of astrocytes, as it is known that they interact with endothelial cells and regulate their properties. This can be done by culturing in astrocyte-conditioned media or co-culturing with astrocytes either in close proximity at the other side of the permeable membrane the endothelial cells are grown on or at the bottom of the well the membrane is placed in (Cecchelli, Berezowski et al. 2007). However, major disadvantages are the time-consuming process of isolating, seeding and incubating the cells (and astrocytes) and a variable reproducibility from batch to batch. As a result, immortalized cell lines, generated by transformation with viral proteins, are being developed as they overcome these problems (Bickel 2005). The most commonly used ones are the RBE4 line (rat) or hCMEC/D3 (human), which has been used for this study and is followed by a separate explanation later on. Cell lines in general can be characterised very well and they do express transporters, but again the TEER is a limiting factor. However, immortalized cell lines are usefule for biochemical and mechanistic studies. In an attempt to surmount the problem of the insufficient barrier properties other cell lines with non-brain origin have been tried, e.g. ECV304 or Caco-2. They have shown some properties of brain endothelial cells, but in general they cannot be used for predictions of brain permeability (Mensch, Oyarzabal et al. 2009).

In silico

Probably the most recent approach is the *in silico* one. Techniques in this field have evolved from experimental data and still rely on that. It is a promising field of research as generating data in a model costs significantly less effort, money and time than rendering experimental data (Mensch, Oyarzabal et al. 2009). A core element of *in silico* methods is the predicting of *in vivo* brain penetration. This can be achieved by creating screening libraries with compounds based on BBB permeability (Alavijeh, Chishty et al. 2005). Key features in a task like that are data quality and quantity, descriptors and modelling approaches (Mensch, Oyarzabal et al. 2009). On the other hand it is difficult to model the BBB permeability due to

the quality and quantity of the available data and the difficulty of creating a reasonable relationship between the molecular structure and the measured blood-brain partitioning (Mensch, Oyarzabal et al. 2009).

1.1.8 hCMEC/D3 cell line

The human cerebral microvascular endothelial cells / D3 are a stable immortalized cell line derived from human brain endothelial cells. They were transduced by lentiviral vectors transporting SV40 large T antigen and human telomerase reverse transcriptase (hTERT) to immortalize the cells. Of all the stable lines one was chosen for its expression of various transporters and endothelial markers e.g. von Willebrand factor and VE Cadherin, its growth capacity, contact inhibition at confluency and endothelial morphology. In addition this cell line has proved to maintain a stable phenotype throughout the course of 35 passages and forms capillary-like vascular cords (Weksler, Subileau et al. 2005). Additionally, the hCMEC/D3 cell line can be used for P-glycoprotein studies up to passage 38, afterwards the Pgp expression declines (Tai, Reddy et al. 2009). Although they express various tight junction proteins such as JAM-A and ZO-1, TEER values of cell monolayers are consistently low (around 40 $\Omega.cm^2$). However the cells do express functional intercellular junctions, which indicates that the cell line can be used for permeability studies with the exception of hydrophilic molecules sized smaller than 300 Da (Weksler, Subileau et al. 2005) or generally molecules smaller than 4 kDa (Tai, Reddy et al. 2009). The second experimental set-up for these cells is the drug accumulation study where the uptake of different drugs into the cells is measured. Again hCMEC/D3s show good values and can be used for experiments like that (Weksler, Subileau et al. 2005).

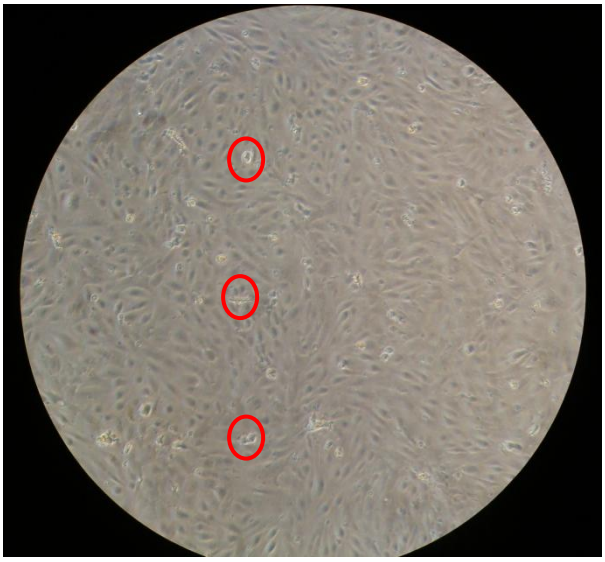

Fig. 5 hCMEC/D3 cells at confluency, marked areas: dead cells

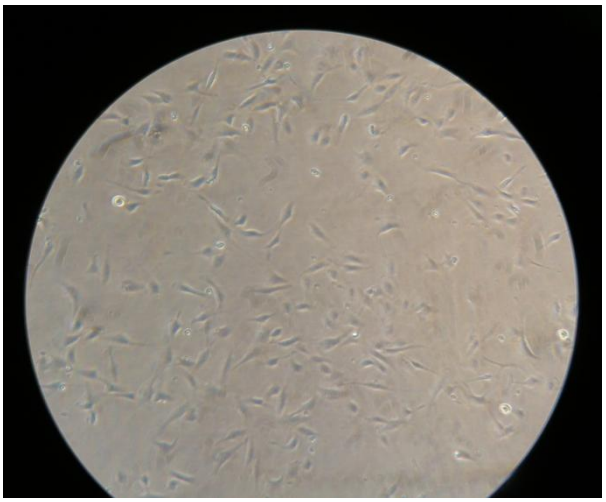

Fig. 4 hCMEC/D3 cells in a non-confluent state, free spaces between the cells are visible

1.2 Iron chelators

1.2.1 What is iron chelation?

Iron is an essential trace mineral in the human body which can be present as Fe^{2+} for reductions or Fe^{3+} for oxidations. Of the 4 – 5 grams iron in an adult about 2,5 grams can be found in the oxygen-transporting metalloprotein haemoglobin, about 1 gram is storage iron, bound to ferritin and hemosiderin, 130 milligrams are bound in myoglobin, the oxygen-binding protein found in muscles, the labile iron pool contains 2 - 3 milligrams and 4 milligrams appear bound to transferrin (Pschyrembel 2007; Kohgo, Ikuta et al. 2008). Usually the daily iron intake through normal diet is about 1 - 2 milligrams. As there is no active elimination pathway for iron, increased levels cannot be reduced (Galanello 2007). Normally iron is bound to transferrin when circulating, but when there is excessive iron supply, the capacity exceeds and iron is found free (Kohgo, Ikuta et al. 2008). One major problem in this case is the formation of radicals such as reactive oxygen species which are able to initiate and uphold inflammatory reactions and therefore cause tissue damage (Voest, Vreugdenhil et al. 1994). Another problem is the iron deposition in different organs mainly the liver, the heart, the brain and endocrinic glands causing dysfunction like carcinogenesis, fibrosis or cell death (Kohgo, Ikuta et al. 2008).

1.2.2 Structures and pharmacokinetics

At present three iron chelators are licensed for clinical use, namely Deferoxamine, Deferiprone, and Deferasirox.

Deferoxamine (also known as Desferrioxamine) was the first to be discovered. It has been the gold standard since the 1970s and saved a great number of patients with iron overload problems from death (Neufeld 2006; Dubey, Sudha et al. 2007). Deferoxamine is a hexadentate iron chelator where one molecule binds one atom of iron as ferric iron possesses six coordination sites which all need to be chelated in order to prevent the formation of radicals (Dubey, Sudha et al. 2007).

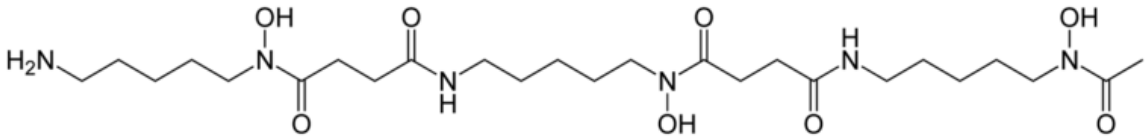

Formula 1 Deferoxamine

It is not active orally and therefore has to be administered parenteral, usually subcutaneously (Neufeld 2006). The short half-life of about 20 minutes requires an infusion time of 8 – 12 hours applied 5 – 7 nights a week (Beutler, Hoffbrand et al. 2003). This causes a major compliance and logistical problem compared to oral iron chelators. Another disadvantage is the charging of the Deferoxamine-iron chelate, which disables it to cross membranes and therefore iron-induced cardiomyopathy cannot be reversed in all patients.

In the early to mid 1980s Deferiprone (or CP20) was introduced and soon clinical studies began (Galanello 2007). Compared to Deferoxamine its major benefit was the ability of being orally active. Deferiprone is a bidentate chelator which requires three molecules to bind one atom of iron (Beutler, Hoffbrand et al. 2003). Resorption from the GIT is fast (15 minutes), plasma peak levels are 45 – 60 minutes and half-life is around 2 hours. Just 4% of the given oral dose is excreted bound to iron, even in heavily iron-overloaded patients (Beutler,

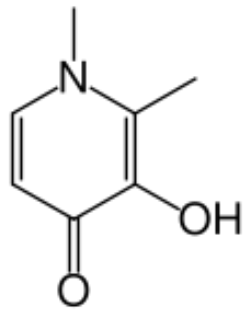

Formula 2 Deferiprone

Hoffbrand et al. 2003; Dubey, Sudha et al. 2007). The Deferiprone-iron complex is not charged, giving it the ability to remove iron from tissues and as a result protect the heart from toxic iron overload (Beutler, Hoffbrand et al. 2003; Neufeld 2006). In consequence of the relatively short half-life the dose of 75mg/kg, which is also the highest dose of all three chelators, has to be administered three times per day. It is eliminated via hepatic biotransformation as a glucuronidate and excreted with the urine (Galanello 2007).

Finally Deferasirox the youngest member of this family brings some new attributes to iron chelators. It is a tridentate chelator with a half-life of 12 – 16 hours, peak levels are reached after 1 – 3 hours. Subsequently, it is sufficient to administer it once daily (Beutler, Hoffbrand et al. 2003; Neufeld 2006; Gattermann 2009). The dosage regimen is 20 – 30 mg/kg which is the lowest dose of the described iron chelators. Deferasirox-iron complexes are completely excreted in the stool (Neufeld 2006). Due to its short time on the market it has not been reviewed so often yet, but recent clinical studies have been positive about efficacy and cost effectiveness (Dubey, Sudha et al. 2007). Also data about the ability to bind intracellular iron in tissues especially in the heart are not sufficient yet, but laboratory studies seem promising (Neufeld 2006).

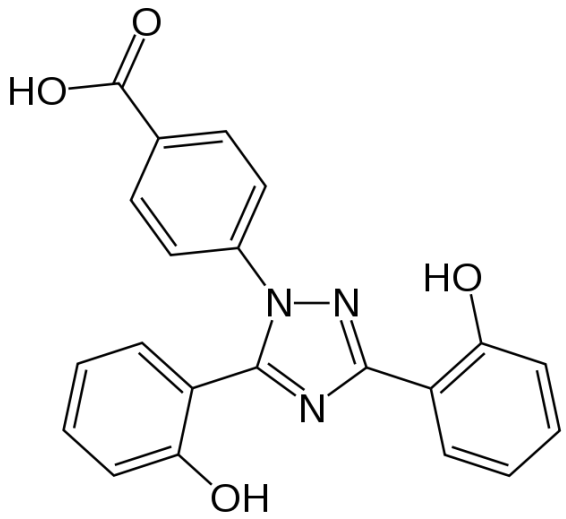

Formula 3 Deferasirox

1.2.3 Fields of application – diseases treated now

Iron chelators are used in treatment of iron overload caused by storage diseases or regular blood transfusions. In general increased iron storage and following pathological changes are called hemochromatosis. This definition has been modified over the years and it is still being discussed whether only patients who show clinical symptoms have hemochromatosis or already the ones who have the genotype (Beutler, Hoffbrand et al. 2003). However, a classification can be made into primary or hereditary and secondary hemochromatosis (Kohgo, Ikuta et al. 2008). Primary hemochromatosis is most commonly associated with a homozygous mutation of the HFE gene. Less frequent causes are juvenile hemochromatosis or African iron overload (Whittington and Kowdley 2002). In case of secondary hemochromatosis the state of iron overload is induced by blood transfusions required because of an anemic state of the patient. Several diseases, among others thalassemia, sickle-cell anemia, sideroblastic anemia or myelodysplastic syndrome can require transfusions to keep the patient alive (Beutler, Hoffbrand et al. 2003; Gattermann 2009). One millilitre blood contains about 0.5 milligrams iron (Kohgo, Ikuta et al. 2008). That means every transfusion unit (400 milliliters blood) contains 200 milligrams iron. A patient receiving 3 units every four weeks will therefore cumulate 7.8 grams iron in one year. Additionally there is the amount of iron absorbed by the gut and normally present in the body causing a severe overload (Vermylen 2008).

1.2.4 Application in non-iron overload states

Aside from the above-mentioned diseases, iron overload in the brain is said to be responsible for several neurodegenerative maladies (Shachar, Kahana et al. 2004). First of all there are Alzheimer's disease and Parkinson's disease which show different clinical conditions but share critical processes in genesis (Molina-Holgado, Gaeta et al. 2008). Furthermore, rare illnesses such as Friedreich's ataxia or Hallervorden-Spatz Syndrome show an iron-association in their development (Liu, Men et al. 2009). Additionally Huntington's disease, which has a prevalence of about 5 to 10 cases per 100.000, but has a higher number of people potentially at risk, seems to be iron-dependent too (Hersch and Rosas 2008; Liu,

Men et al. 2009). In the past years it has become clear, that a lot of neurodegenerative diseases are related to age which may be directly associated with oxidative stress (Molina-Holgado, Gaeta et al. 2008). As said before, free iron can cause the formation of radicals and therefore evoke oxidative stress-induced neurodegeneration (Shachar, Kahana et al. 2004).

Treatment options for the above-mentioned diseases are mostly handicapped by the presence of the blood-brain barrier as the therapeutic agents should reduce iron levels in the brain (Liu, Men et al. 2009). Therefore the possible ability of iron chelators crossing the BBB is of great interest, which has been an objective in this project too.

2 Materials and methods

2.1 Materials

2.1.1 Analytical apparatus

To analyse the amount of radioactivity in the cells, Perkin Elmer Liquid Scintillation Counter – TriCarb 2900TR, UK was used.

The protein assay was performed on a Labsystems Multiskan Ascent plate reader, UK, and interpreted by Ascent software.

HPLC was conducted on a Waters system with a 717plus Autosampler, a 2996 Photodiode Array Detector, a 600S Controller and a 626 Pump, all fabricated by Waters. The column used was a PLRP-S, 300 Å, 8 µm, 15 cm obtained from Waters.

2.1.2 Cells

The cells used to perform experiments, hCMEC/D3 cell line, were provided by Professor Couraud from the Institute Cochin, Paris, France.

2.1.3 Chemicals

CP20 and ethylmaltol were purchased from Sigma Aldrich, UK.

The EGM2-bulletkit containing EGM-medium, foetal bovine serum, Insulin-like Growth Factor (R3-IGF-1), Vascular Endothelial Growth Factor (VEGF), recombinant human Endothelial Growth Factor (rhEGF) and hydrocortisone was purchased from Lonza (Switzerland). The factors were added as recommended by the manufacturer. Phosphate-buffered saline (PBS-) plus calcium chloride and magnesium chloride, trypsin, basic human Fibroblast Growth Factor (bFGF), 4-(2-hydroxyethyl)-1-piperazineethanesulfonic acid (HEPES), Streptomycin and rat tail collagen were obtained by Gibco, Invitrogen, UK. All cultureware used, was provided by Nunc, Thermo Fisher, UK.

[^{14}C]sucrose with a specific activity of 412mCi/mmol was purchased from Moravek Biochemicals, US. OptiPhase Hi-Safe 2 scintillation fluid was obtained by Perkin Elmer, UK.

The reagents to perform the protein assay including the bovine serum albumin (BSA) standard and the reactive mix (reagent A containing sodium carbonate, sodium bicarbonate, bicinchoninic acid and sodium tartrate in 0.2N sodium hydroxide and reagent B which is a solution of 4% cupric sulphate), called BCA Protein assay, were purchased from Thermo Fisher, UK.

The contents of the HPLC buffer, 1-heptanesulfonic acid and hydrochloric acid, and acetonitrile (HPLC gradient grade) were obtained by Fisher Scientific, UK.

All other chemicals were supplied by Sigma Chemical Company, UK.

2.2 Methods

2.2.1 Cell culture

The hCMEC/D3 were cultured in EBM-2 endothelial growth medium from the EGM-2MV BulletKit. The medium was supplemented with HEPES, penicillin-streptomycin, 2.5% foetal bovine serum, insulin-like growth factor-1, vascular endothelial growth factor, epidermal growth factor, hydrocortisone and basic fibroblast growth factor (Poller, Gutmann et al. 2008). All cells used in the experiments were seeded at a density of 2.5×10^4 cells/cm^2 and were between passage 29 and 35 (Tai, Reddy et al. 2009). Before seeding cells were checked for viability by 0.4 % Trypan Blue solution in a haemocytometer. Cultureware was coated with rat tail collagen type 1 (diluted 1:10 with sterile distilled water) for two hours prior to seeding. Cells were cultured in an incubator with a saturated humidity at 37˚C in 5% CO_2 and 95% fresh air and grown to 100% confluency (determined visually) for experiments (confluency reached after approximately 4-5 days). Protein expression (BCA™ protein assay) and integrity of plasma membranes ([^{14}C]sucrose) were monitored to confirm cell viability (see experimental details below). At confluence the hCMEC/D3 cell line forms tight junctional complexes that prevent the paracellular movement of solutes with a MW in excess of 4 kDa (Weksler, Subileau et al. 2005; Tai, Reddy et al. 2009) and the movement of

solutes with lower molecular weights is unrestricted. As the present study is directed at cell uptake of test molecules this *in vitro* method is perfectly acceptable.

Usually one T-25 and one 96-well plate have been used, the flask for gaining a stock for the next splitting, the plate for use in an experiment. After splitting and seeding, the cells have been grown in a sterile incubator at 37°C and 5% CO_2 to imitate physiological conditions. The excess amount of cells was filled in 1 ml cryotubes, 100 µl DMSO were added and they were frozen at -80°C. After 24 hours the tubes were transferred into liquid nitrogen.

2.2.2 Uptake assay

Drug accumulation experiments were performed on confluent monolayers of hCMEC/D3s, grown in 60 wells of 96 well plates (Fig. 6, Fig. 7). Accumulation studies have been previously described (Chishty, Begley et al. 2004). A 200µl aliquot of CP20 (100, 500, 800 µM and 1mM) or ethylmaltol (100 and 800 µM) and [^{14}C]sucrose (321nM) in accumulation buffer (consisting of 135mM NaCl, 10mM HEPES, 5.4mM KCL, 1.5mM $CaCl_2$, 1.2mM $MgCl_2$, 1.1mM 2-deoxy-D-glucose, and distilled water, pH 7.4) was added to each well. Columns of well (6 wells per column, 10 columns per plate, with n=12 for each exposure time) were exposed to the CP20/[^{14}C]sucrose/buffer mix at five different time periods (5, 10, 15, 20 and 25 minutes). This allowed assessment of drug accumulation in the cells. The accumulation assays were performed on a temperature-controlled shaker (THERMOstar, BMG labtech, Offenburg, Germany) at 37˚C and 120 rpm.

Once each column of cells had been exposed for the correct amount of time, the wells were washed 3 times with ice-cold phosphate buffered saline to remove drugs and buffer that had not accumulated in the cells. The cells were then lysed by adding 250µl of 1% Triton per well to liberate any accumulated radiolabelled drug and solubilise the cell proteins. 100 µl of each well was then added to a scintillation vial and 4 ml scintillation fluid (Optiphase Hisafe 2) added and samples counted as described previously. Hereafter 100 µl were transferred into an HPLC vial and 50 µl stayed in the well to perform a BCA™ protein assay.

Fig. 6 empty 96-well plate

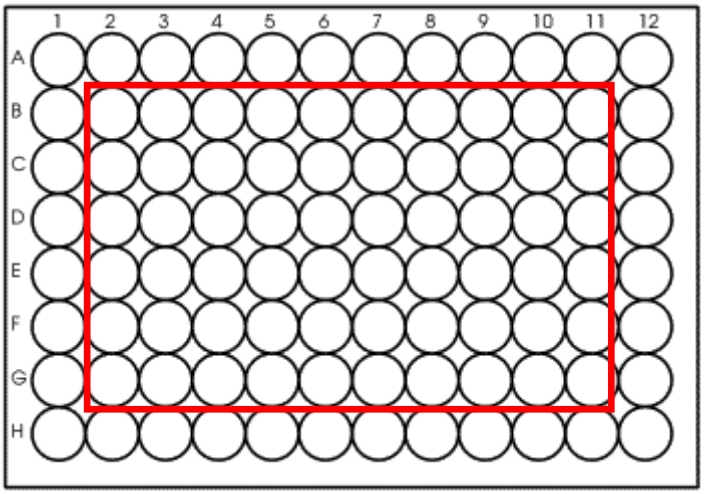

Fig. 7 schematic depiction of a 96-well plate, the red box shows the 60 wells used in the experiment

2.2.3 Protein assay

After lysing the cells, a protein assay was performed to establish the amount of protein in each well, which was used as a correction factor when calculating the amount of accumulated drug in the cells. It is based on the reduction of Cu^{2+} to Cu^{+} by peptide bonds in proteins when performed in an alkaline medium. The ion then reacts with bicinchoninic acid and produces a violet complex whose absorbance can be detected at 562 nm wavelength. In order to calculate the amount of protein found in each well, a calibration curve is made, based on the values from bovine serum albumin in different concentrations as standards. To obtain a convincing calibration curve, six different concentrations (0, 10, 15, 20, 25 and 30 µg/100µl) are prepared from a stock solution of 2 mg/ml.

	1	2	3	4	5	6	7	8	9	10	11	12
A	0	0	0	E	10	10	10	E	15	15	15	E
B	E	U7	U13	U19	U25	U31	U37	U43	U49	U55	U61	E
C	E	U8	U14	U20	U26	U32	U38	U44	U50	U56	U62	E
D	E	U9	U15	U21	U27	U33	U39	U45	U51	U57	U63	E
E	E	U10	U16	U22	U28	U34	U40	U46	U52	U58	U64	E
F	E	U11	U17	U23	U29	U35	U41	U47	U53	U59	U65	E
G	E	U12	U18	U24	U30	U36	U42	U48	U54	U60	U66	E
H	E	30	30	30	E	25	25	25	E	20	20	20

Table 1 schema of the array of standards

red: standards

green: samples

black: empty

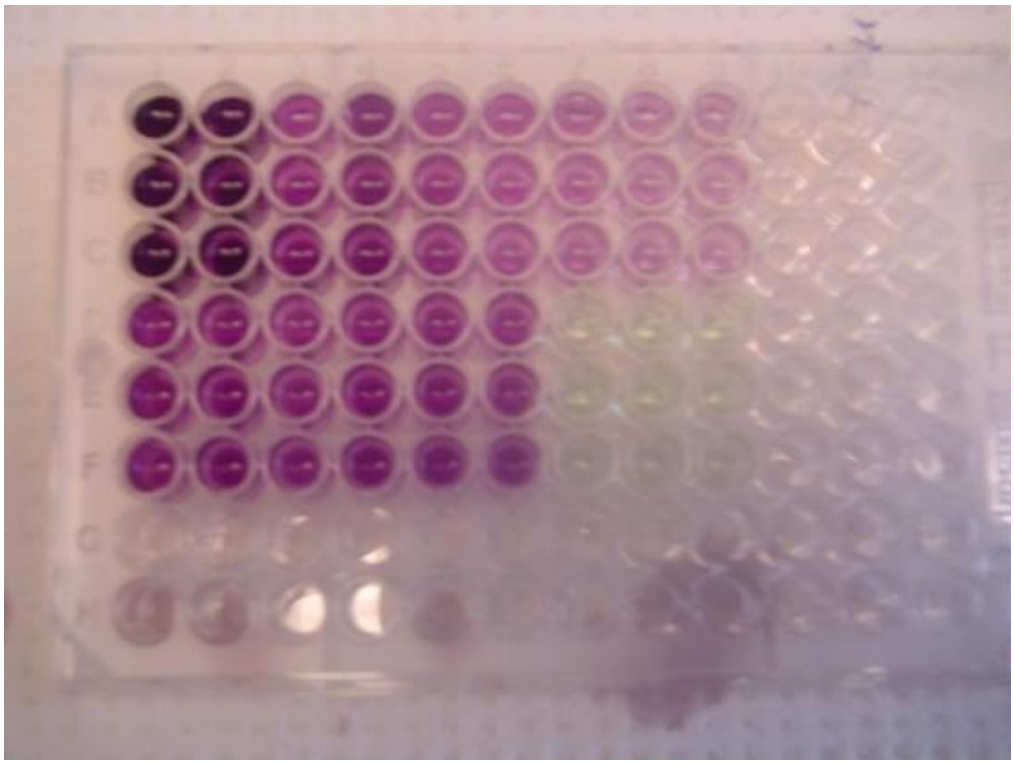

Fig. 8 completed protein assay, the darker the colour is, the more protein is present

2.2.4 Cytotoxicity assay

To gain an impression of how toxic the test compound is to the cells, a cytotoxicity assay can be performed. It uses (3-(4,5-dimethylthiazol-2-yl)-2,5-diphenyl tetrazolium bromide, MTT for short, to quantify the number of viable cells. At first the cells are incubated with the drug, in this case CP20, for the longest time point, 24 hours, to see the maximally toxic effect. Then MTT is dissolved in a solution of DMEM without phenol red and applied to the cells. Afterwards the plate is incubated for four hours at 37°C. In this time the tetrazolium salt is reduced to formazan, a blue-coloured product, by the succinate dehydrogenase, a mitochondrial enzyme. Finally the well contents are removed by blotting the plate into the sink and propan-2-ol is added to dissolve the blue formazan crystals. A few minutes later the absorbance is read at 540 nm. To obtain a correction value, the assay is performed only on half of the wells, having a corresponding protein assay well for each cytotoxicity assay well. As the measured product is only produced in viable cells, the colour intensity decreases with a higher number of dead cells.

2.2.5 HPLC system

100 µl of the cell lysate with Triton were transferred into an HPLC vial of which 50 µl have been injected into the system.

The analysis of the drug present in the cells was made by high-pressure liquid chromatography (HPLC). The HPLC system consisted of an autosampler, a pump, a controller, a photodiode array detector and a reversed-phase polymer column.

A linear gradient elution was applied using 1-heptanesulfonic acid sodium salt 5mM at pH 2 (adjusted using HCl conc.) as buffer A and acetonitrile. Elution started at 2% acetonitrile and 98% buffer and ended after 20 minutes with 35% acetonitrile, 65% buffer. To restore the initial conditions, 5 minutes post-run was made. The flow-rate was 1 ml/min, the compounds were monitored at 280 nm, room temperature (Liu, Liu et al. 1999).

HPLC chromatograms were produced and analysed by using Millenium software.

2.2.6 Statistical analysis

Statistical analysis was done with GraphPad Prism using two way ANOVA.

3 Results

3.1 Scintillation counter

In every experiment ^{14}C-labelled sucrose was added as a membrane integrity marker and a marker for non specific drug binding. To an aliquot of 100 µl cell lysate, scintillation fluid was added and the samples were analysed in a fluid scintillation counter. The amount of radioactivity was measured in disintegrations per minute (DPM).

3.1.1 Influence of time points

The influence of having five different time points (5, 10, 15, 20 and 25 minutes), was investigated by observing the sucrose values throughout that period. Therefore, three experiments have been chosen to give a representative depiction, shown in Fig. 9 and Fig. 10 (values of both figures see Appendix).

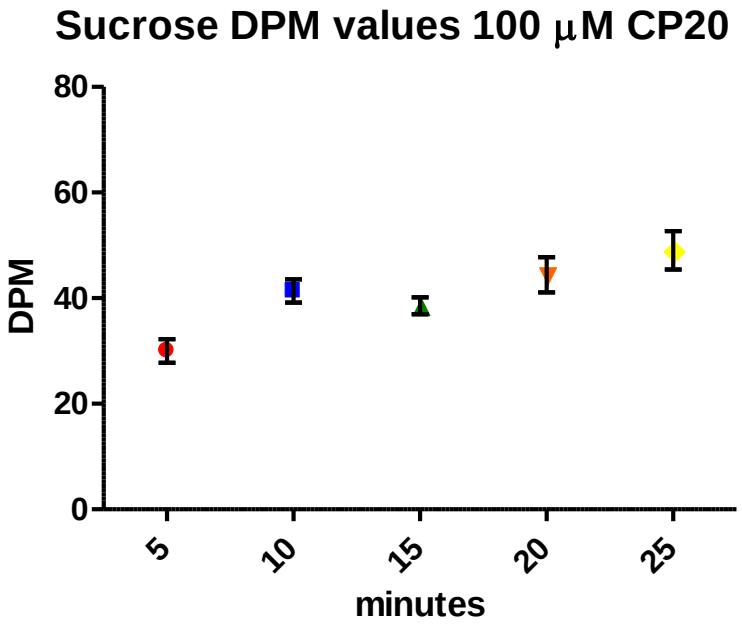

Fig. 9 The accumulation of [^{14}C]sucrose by hCMEC/D3 cells in the presence of 100µM CP20.

DPM mean values of three experiments, 100 µM CP20, mean ± SEM error bars are displayed, background uncorrected, n = 3 for each time point, x-axis: time in minutes, y-axis: radioactivity in DPM

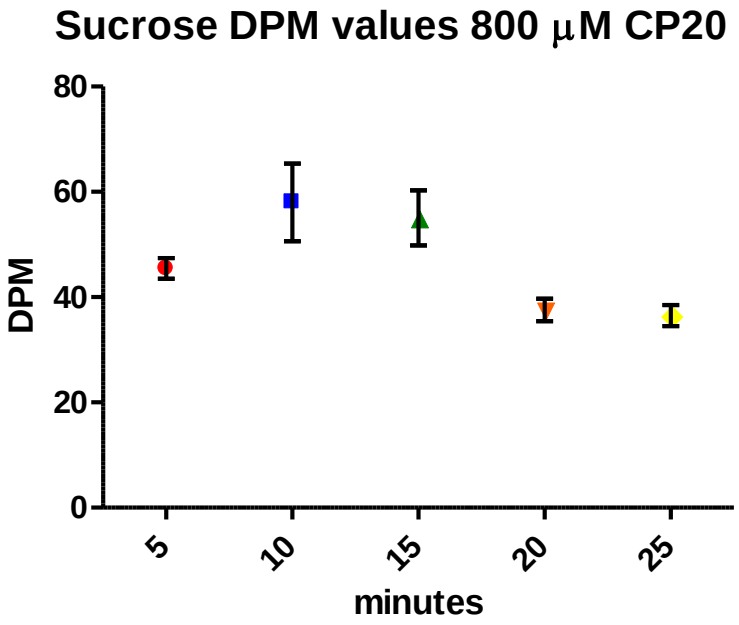

Fig. 10 The accumulation of [^{14}C]sucrose by hCMEC/D3 cells in the presence of 800µM CP20.

DPM mean values of three experiments, 800 µM CP20, mean ± SEM error bars are displayed, background uncorrected, n = 3 for each time point, x-axis: time in minutes, y-axis: radioactivity in DPM

In comparison to this data, the background and the buffer have to be considered. Background was distilled water, 250 µl and 4 ml scintillation fluid, which had a mean value of 46 DPM (± 10.096 SEM) and the buffer, used to incubate the cells, again 250 µl and 4 ml scintillation fluid, brought a mean value of 115,922.3 DPM (± 697.571 SEM). It is shown that the amount of radioactivity in the samples lies in the same range as the background. This indicates that the integrity of the cells was not violated during performing an uptake assay.

3.1.2 Influence of concentration

Another point of view was the presence of two different concentrations, 100 µM and 800µM. Fig. 11 shows the direct comparison.

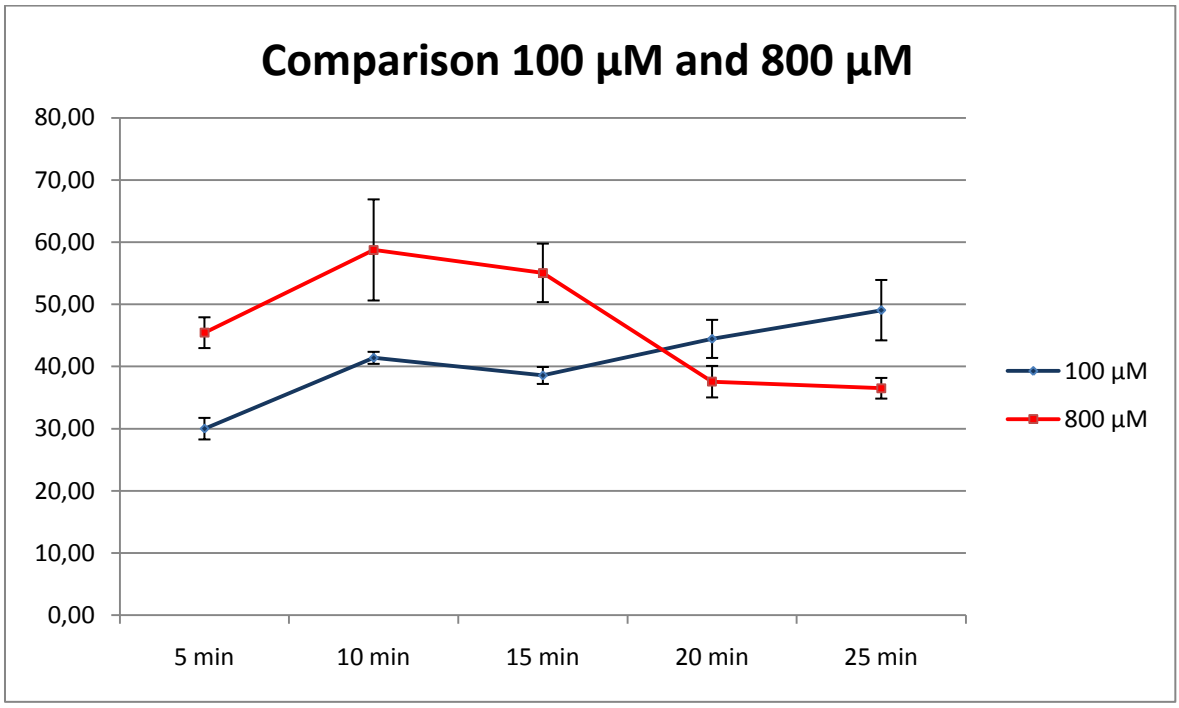

Fig. 11 The comparison of [^{14}C]sucrose accumulation by hCMEC/D3 cells in the presence of 100 µM and 800µM CP20.

DPM mean values of three experiments, 100 µM and 800 µM CP20, mean ± SEM error bars are displayed, background uncorrected, n = 3 for each time point, x-axis: time in minutes, y-axis: radioactivity in DPM

Again it is visible, that the differences seen in the diagram are very low and both curves stay in the range of the background values (46 DPM). The result of a two way ANOVA showed, that the effect of time has a significant effect on the uptake ($P<0.0001$), on the other hand the concentration does not ($P=0.4452$).

It occurred that samples showed higher values than the usual average, this may have been caused by spills during performing the uptake assay or other mistakes due to manually conducted experiments.

3.1.3 24 hour uptake

The experimental setting of a 24 hour uptake should give a higher concentration of CP20 in the cells, as they have a long period of time to equilibrate between buffer and cell. Regarding the sucrose it was assumed, that, as a marker, it would stay the same throughout the experiment.

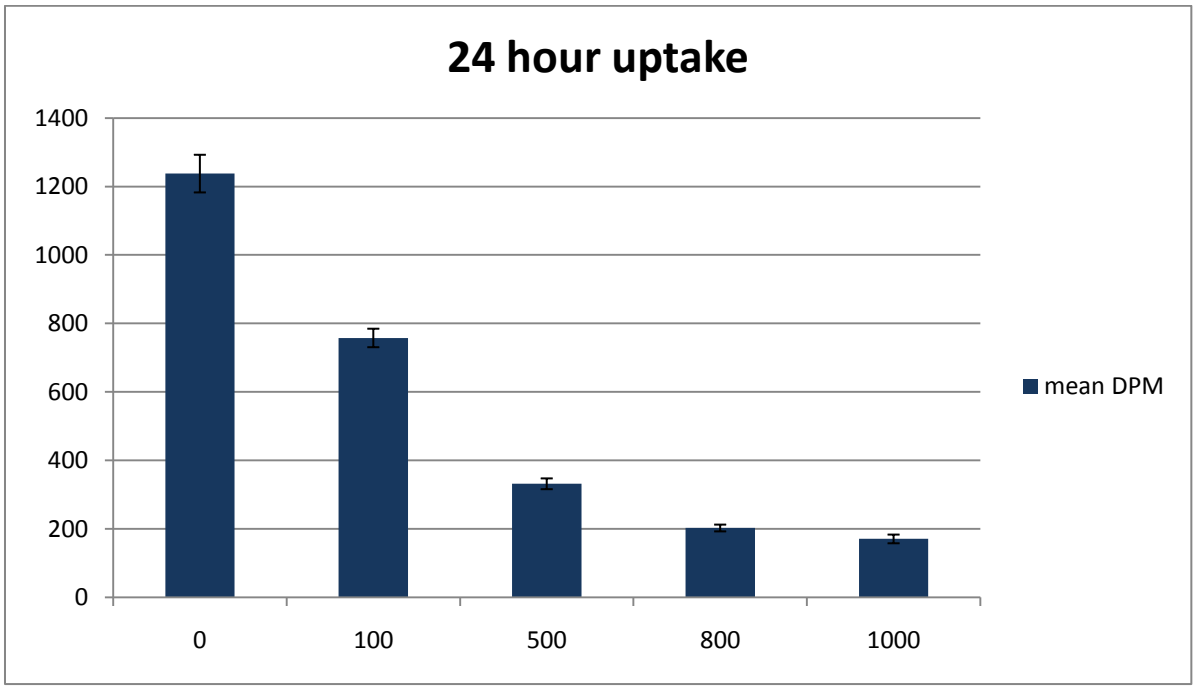

Fig. 12 The accumulation of [^{14}C]sucrose by hCMEC/D3 cells over 24 hours in the presence of 0, 100, 500, 800 and 1000µM CP20

24 hour uptake, DPM mean values, mean ± SEM error bars are displayed, background uncorrected, x-axis: concentration in µM, y-axis: radioactivity in DPM

As Fig. 12 shows, the more CP20 was present in the buffer, the less [^{14}C] sucrose could enter the cells. This observation could lead to a conclusion about a connection between the penetration into the cells of [^{14}C]sucrose and CP20 or maybe, more generally said, a statement about CP20's way of penetration. At present the type of mechanism that CP20 uses to cross the BBB is not yet known, which is a promising field to study.

3.2 Protein assay

The protein assay was done to establish a correction factor when calculating the amount of drug in the cells. It gives the amount of protein in one well, which is indicative for the amount of cells. This value is important to know considering the fact that a higher number of cells could take up more drug.

Additionally, the values can be observed throughout several experiments to monitor the amount of cells as a control for the performance of each experiment. Fig. 13 shows an example of the mean values from three experiments through the five time points (values see Appendix)

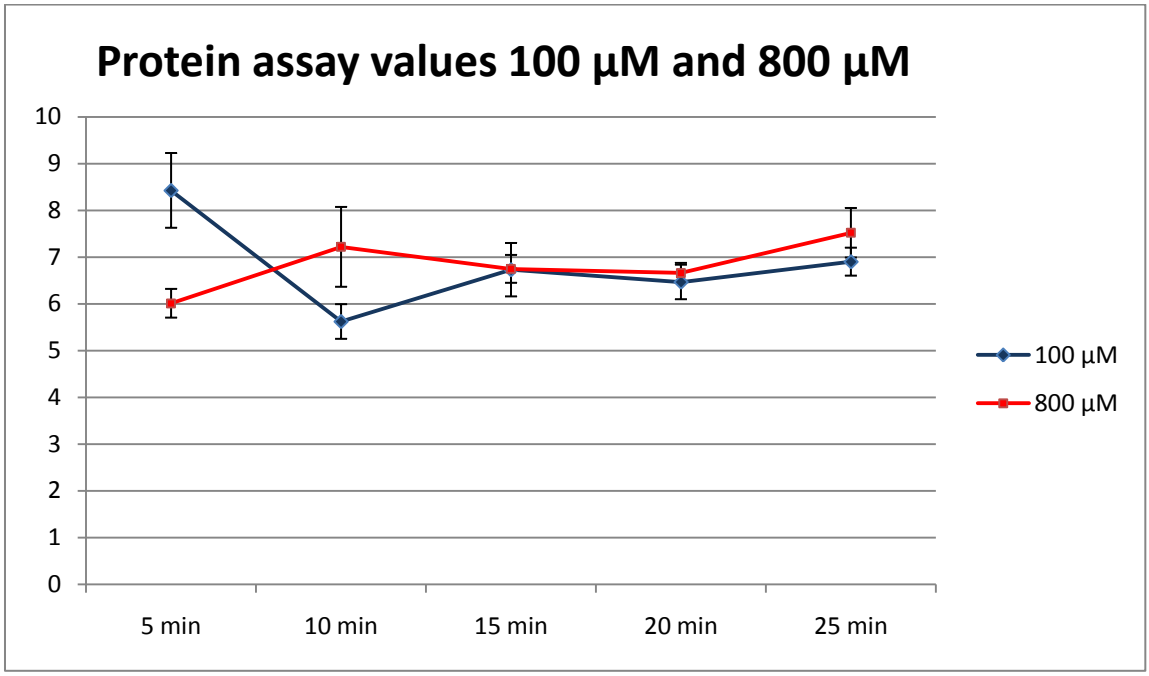

Fig. 13 Comparison of amount of protein in hCMEC/D3 cells after lysis, incubated with 100 µM and 800 µM CP20.

Protein assay values, comparison 100 µM and 800 µM CP20, n = 3 for each time point at each concentration, x-axis: time in minutes, y-axis: amount of protein in µg/100µl

Fig. 13 shows a constant protein value around 7 µg/ 100µl, outliers like the high value at 5 minutes with 100 µM CP20 can derive from a higher amount of cells in some wells. In cell culture a constant seeding density is desired, but it is not possible to ensure this and after seeding, the cell growth varies too.

3.3 HPLC

3.3.1 CP20 in water

Before analysing samples with cell lysate, the column was equilibrated (with buffer and acetonitrile at a flow rate of 0.2 ml/min) until the pressure was stabilised. After that CP20 100 µM in water was injected to localize the peak.

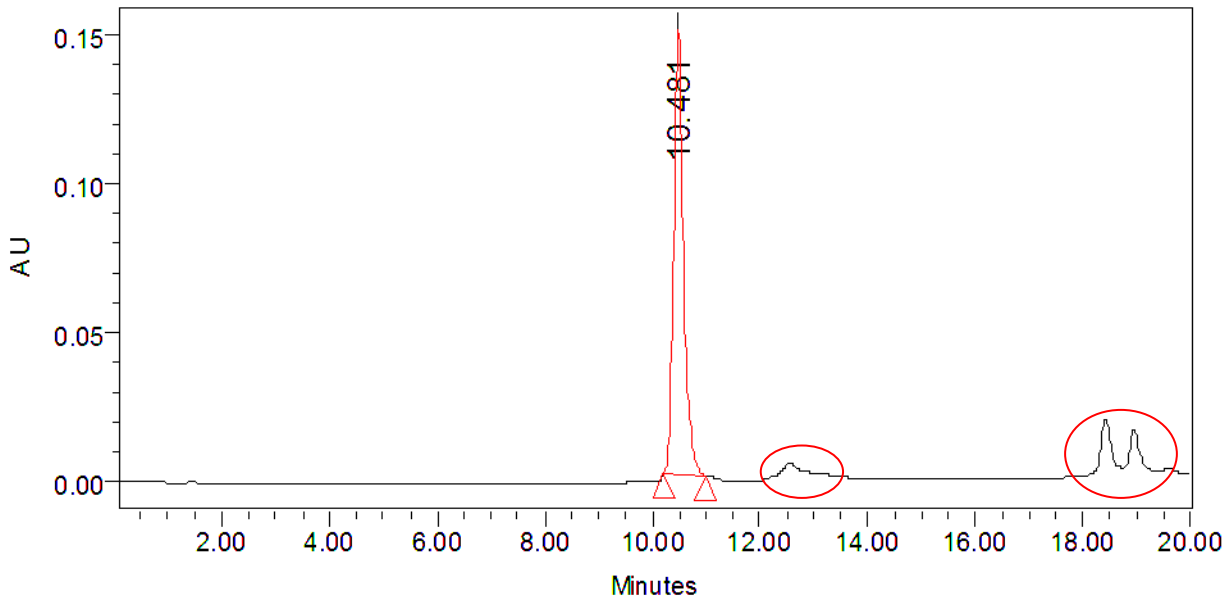

Fig. 14 CP20 100 µM in water, 50 µl injection volume, retention time: 10.481 minutes, marked in red circles are peaks of impurities caused by water

It was found at approximately 10.5 minutes showing a clear, symmetric peak (shown in Fig. 14), with a well defined area under the curve (AUC). The impurities shown in red circles are caused by various particles in the purified water as it is impossible to remove all foreign compounds. Fig. 15 shows a chromatogram of water in this system, which can be seen as background.

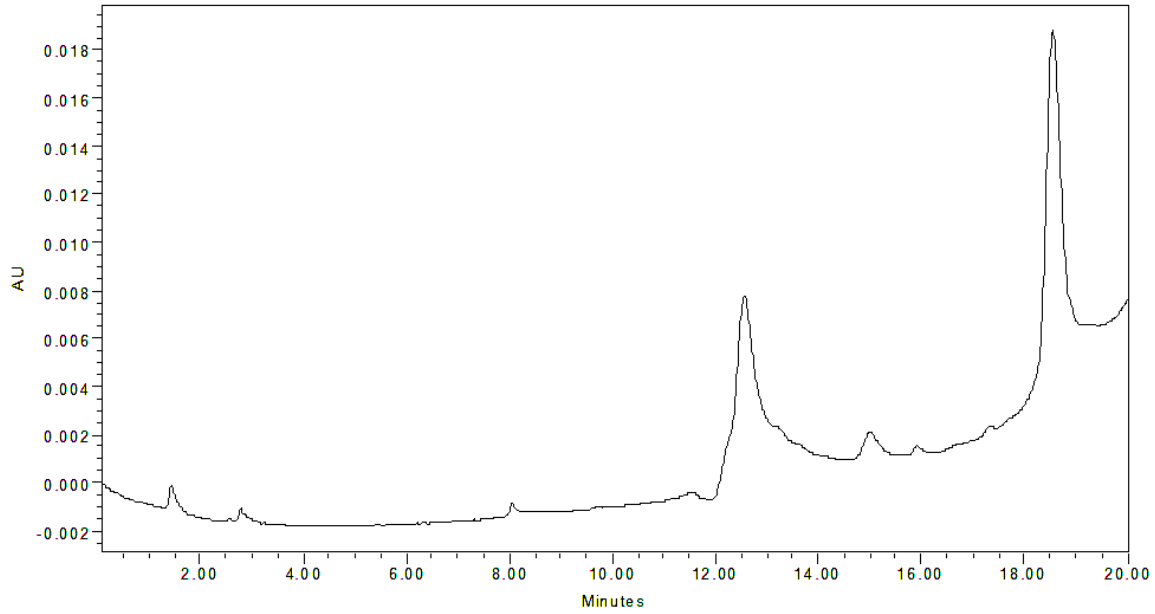

Fig. 15 chromatogram of purified water

The corresponding UV-spectrum shows a maximum around 280 nm, this can vary a little as seen in Fig. 16.

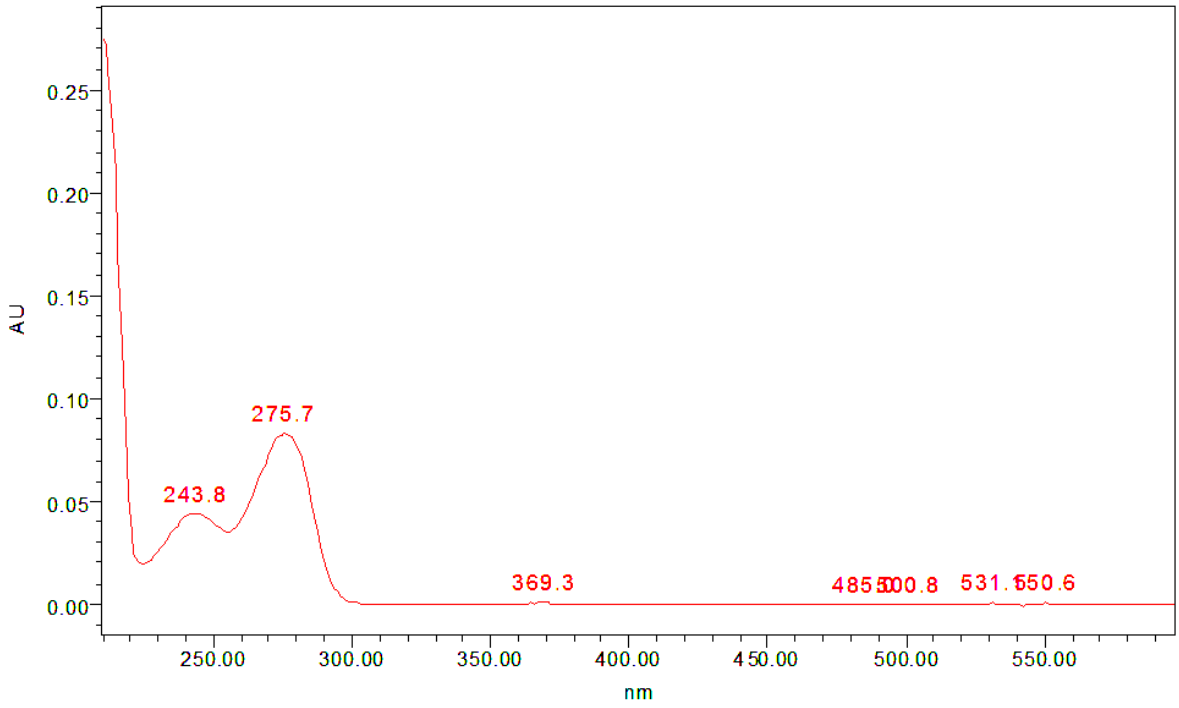

Fig. 16 UV-spectrum of CP20 in water

In comparison to 100 µM CP20, a lower concentration as shown in Fig. 17 also shows a significant peak around 10 minutes, but the impurities at 12 – 13 minutes and between 18 and 20 minutes are proportionally bigger.

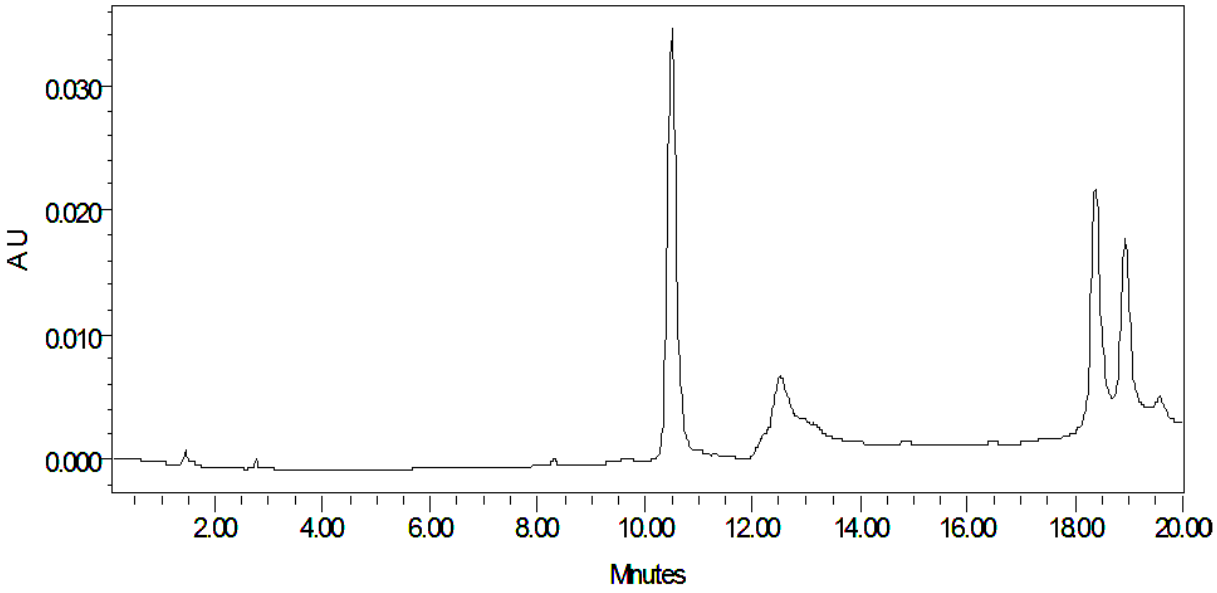

Fig. 17 CP20 20 µM in water, 50 µl injection volume

Finally a concentration of 3 µM (Fig. 18) does show a peak at 10.5 minutes, but the impurities caused by water and the solvents show peaks that are higher than the substance's. Therefore, other impurities, appearing at this time could easily overlap and hide the CP20 peak at concentrations like that.

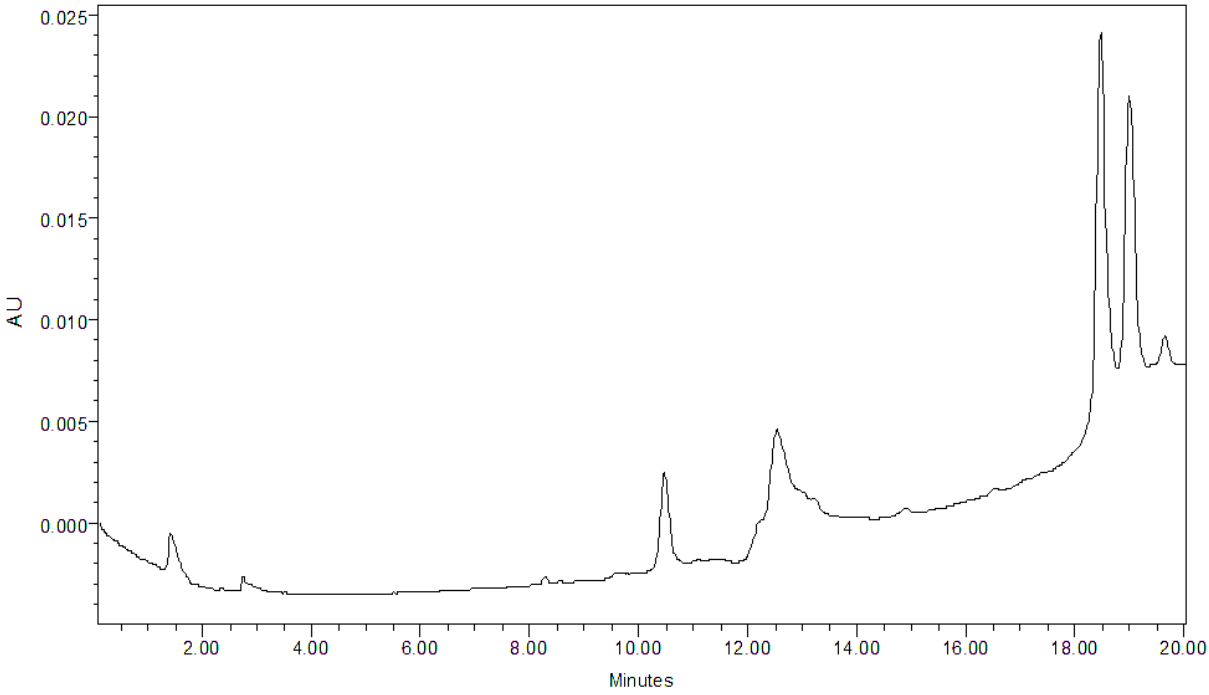

Fig. 18 CP20 3 µM in water, 50 µl injection volume

In order to be able to quantify the amount of CP20 in an unknown sample, a calibration curve was made using concentrations of 3, 5, 7, 10, 20, 30, 40, 50, 60, 70, 80, 90 and 100 µM in triplicates. As seen in Fig. 18, 3 µM can be seen as the detection limit of CP20 in this system, as a lower concentration might not produce an accurate peak with a measurable area under the curve. After analysing, the AUC was determined for each sample, mean values for each concentration were calculated and plotted (Fig. 19). The straight line and the R^2 value, the coefficient of determination show that the AUC levels correlate with the concentrations.

Chromatograms of all concentrations see Appendix.

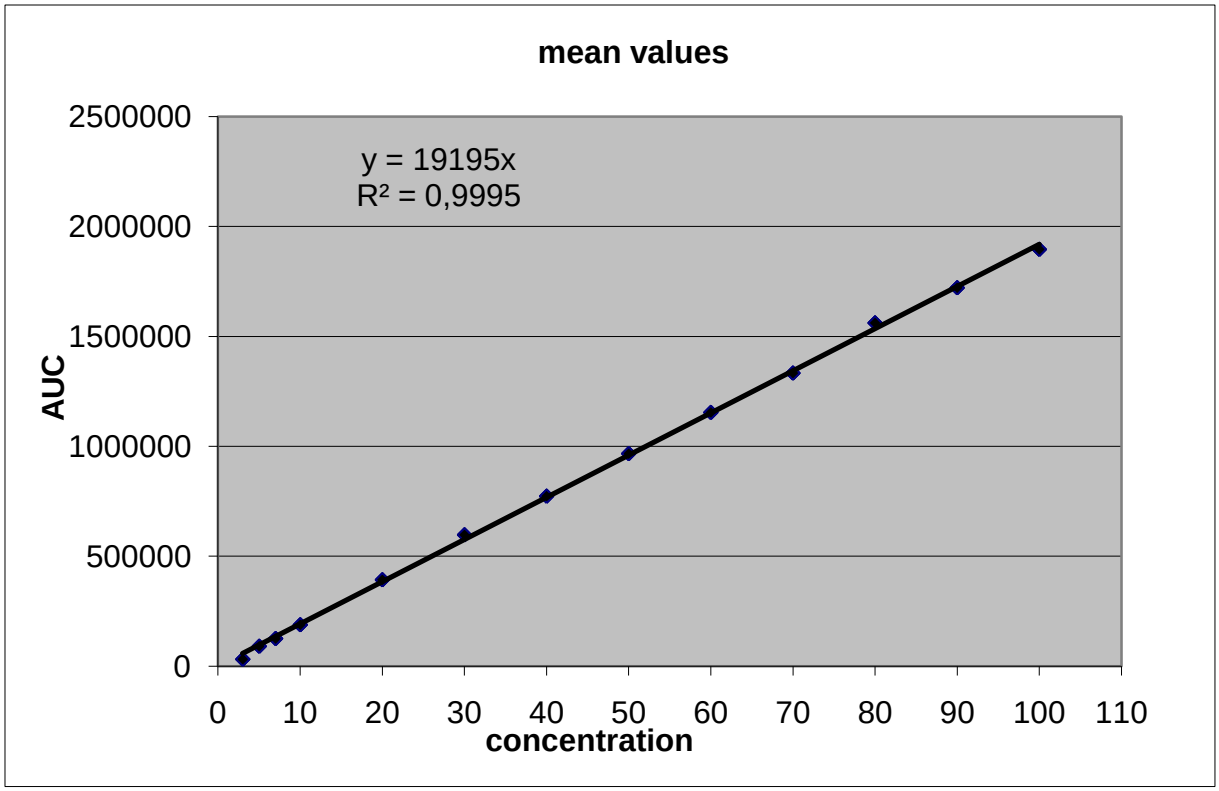

Fig. 19 calibration curve CP20 in water

3.3.2 First experiment data

After having set up the calibration curve, the first sample set was being run. Each well of the 60 ones incubated, represented a separate sample of 100 µl cell lysate of which 50 µl have been injected into the HPLC. Fig. 20 shows a chromatogram of a sample incubated with 800µM CP20 for 25 minutes, Fig. 21 shows the chromatogram of 100 µM CP20, again incubated for 25 minutes.

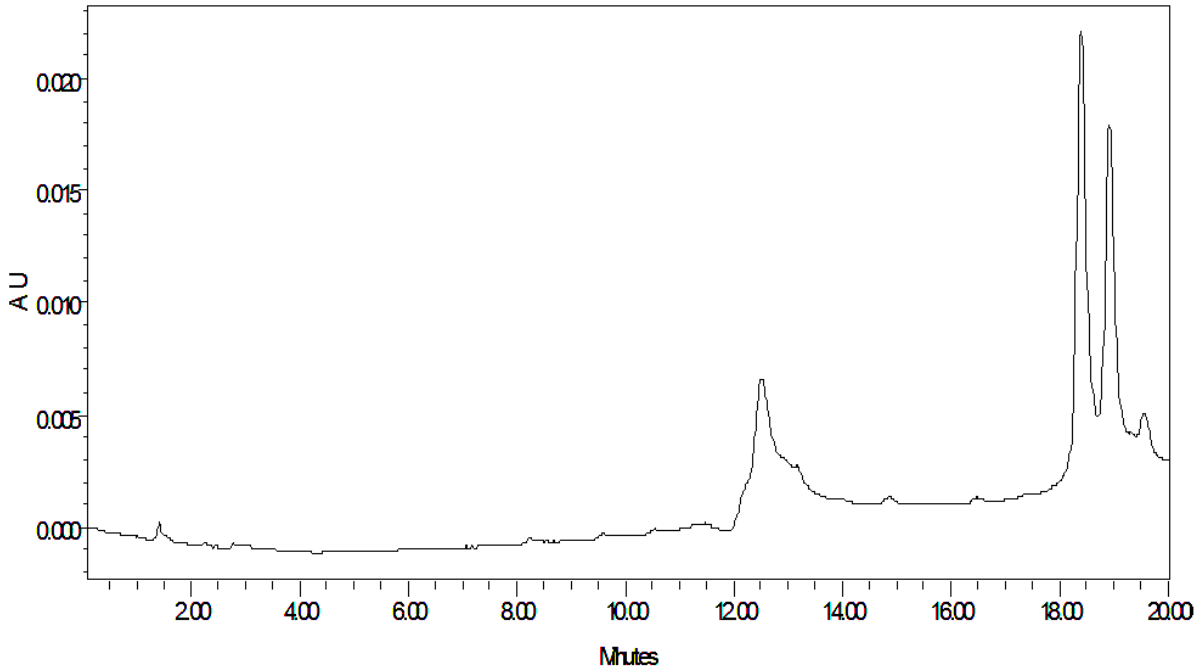

Fig. 20 cell lysate 800 µM CP20, 25 minutes incubation time, 50 µl injection volume

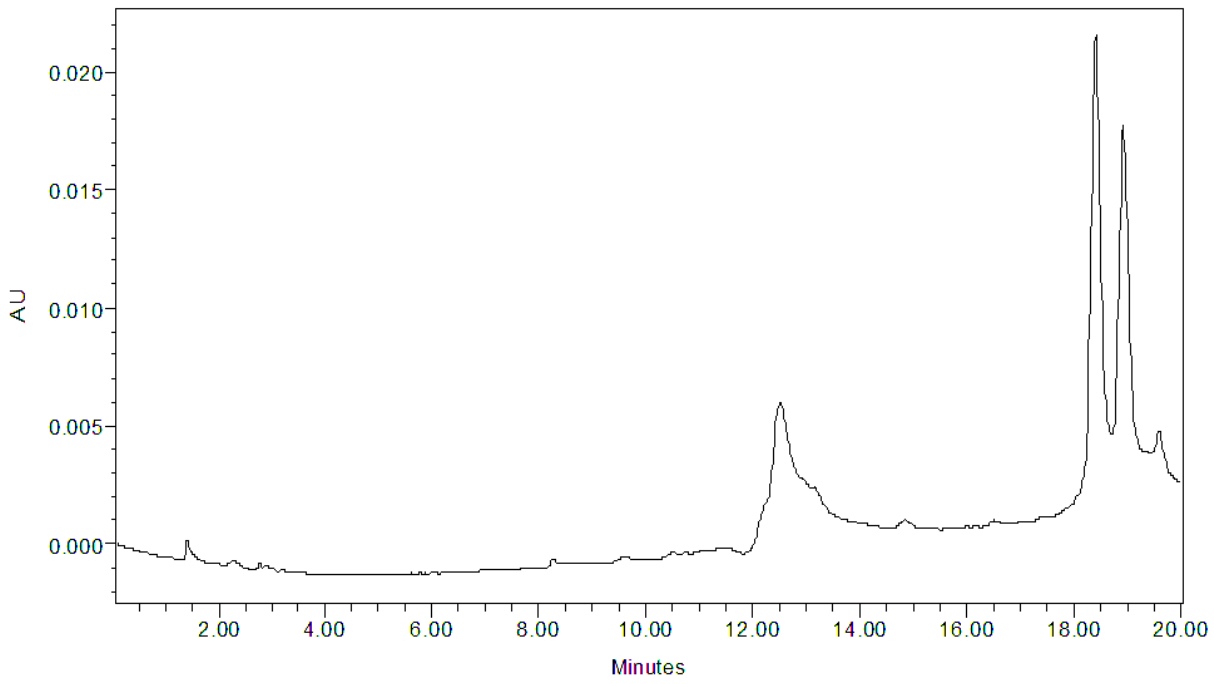

Fig. 21 cell lysate 100 µM CP20, 25 minutes incubation time, 50 µl injection volume

The corresponding UV-spectrum of the peak at 12.5 minutes is shown in Fig. 22.

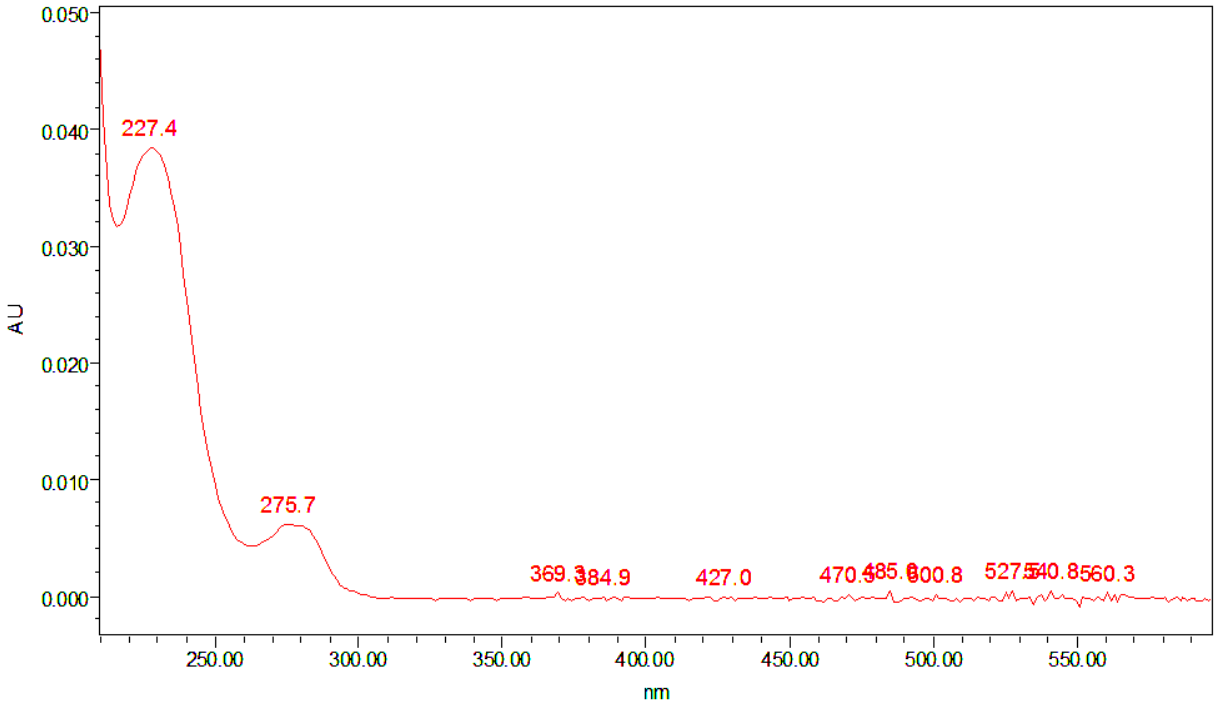

Fig. 22 UV-spectrum of the peak at 12.5 minutes in Fig. 21

Compared to the UV-spectrum in Fig. 16, a maximum at 227.4 nm occurs. In addition, the peak is shifted from 10.5 minutes to 12.5 minutes. This might be due to the fact that a cell lysate has been injected, which, compared to purified water, contains several compounds that might interact with CP20 and slow it down in its retention time.

3.3.3 Buffer and Triton samples

In order to evaluate the influence of the solutions the cells have been treated with, Triton and the physiological buffer used for the uptake assay have been studied separately. Therefore, samples of the buffer alone, 100 µM CP20 in the buffer, Triton alone and 100 µM CP20 in Triton have been analysed.

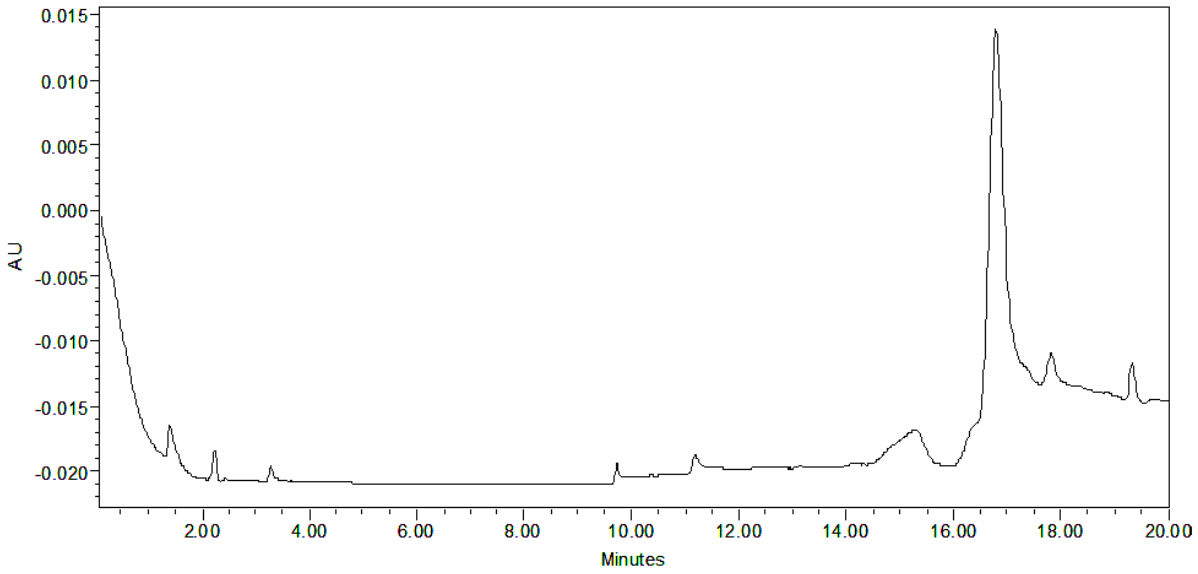

Fig. 23 physiological buffer from uptake assay alone, 50 µl injection volume

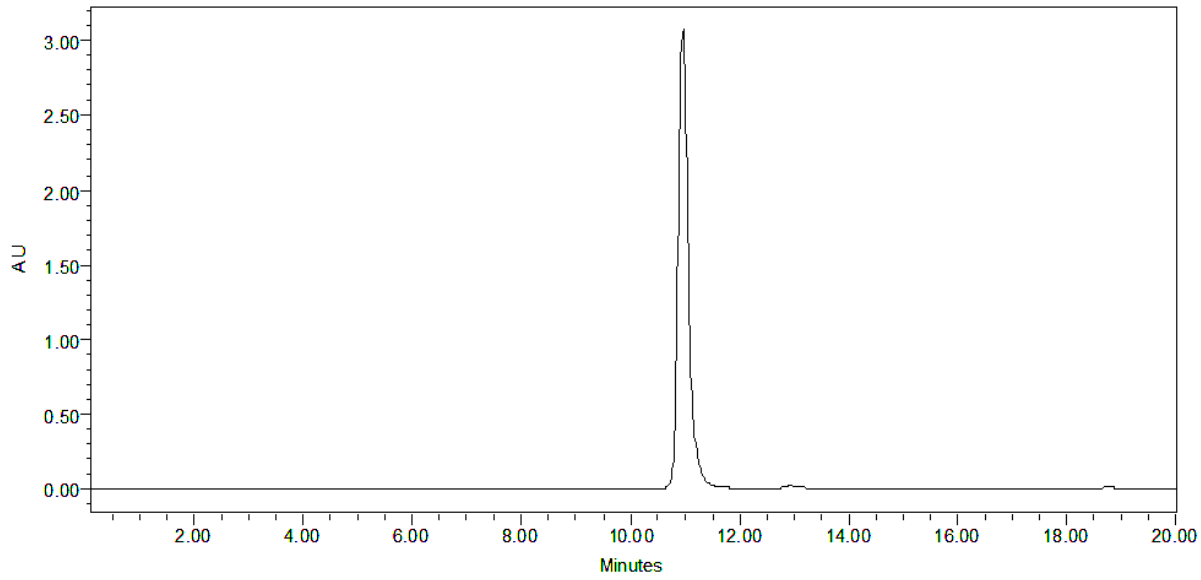

Fig. 24 CP20 100 µM in buffer from uptake assay, 50 µl injection volume, retention time: 10.962 minutes

The buffer alone shows a chromatogram similar to the one of purified water concerning the quantity, location and height of impurity peaks. This means the buffer can be seen as background.

However, 100 µM CP20 in the buffer firstly show a slight shift of the peak towards 11 minutes and secondly the AUC is almost twice as much compared to the sample “CP20 100µM in water”.

Fig. 25 and Fig. 26 show the same experiment with Triton.

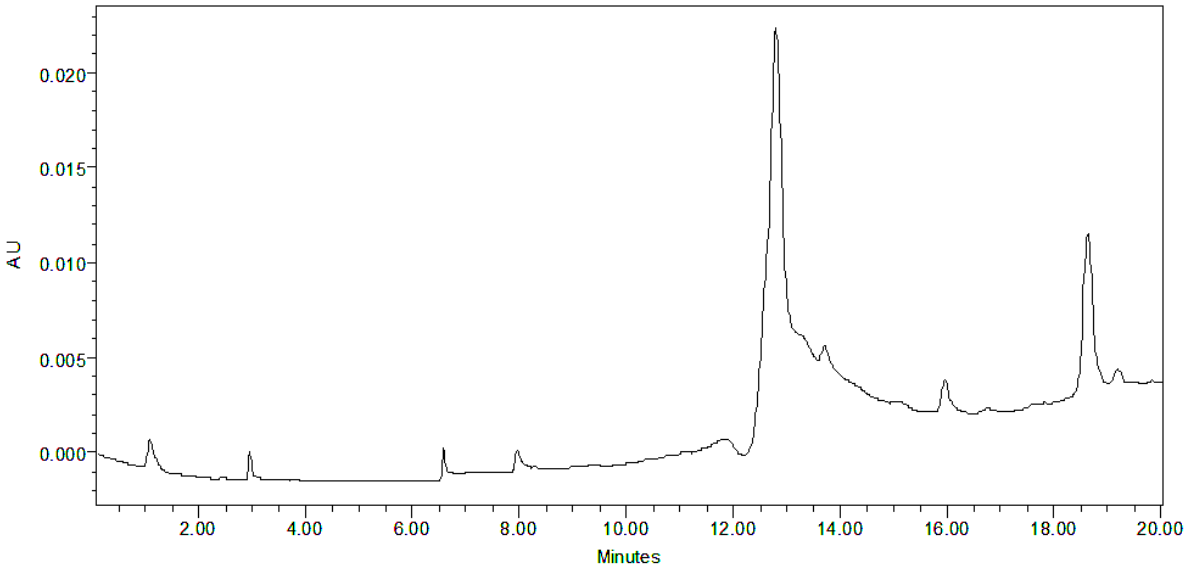

Fig. 25 chromatogram Triton alone

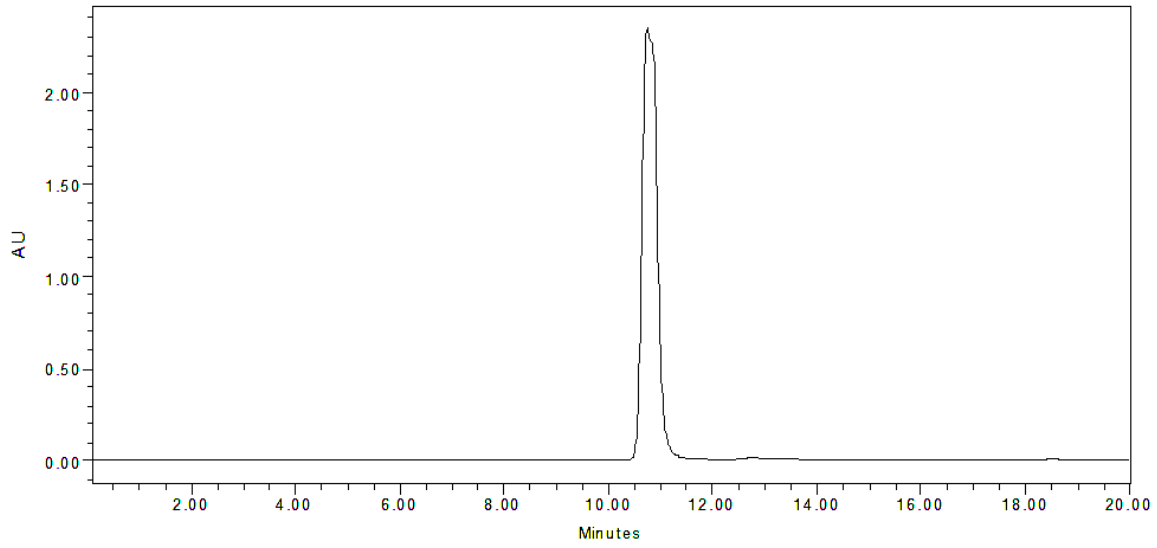

Fig. 26 CP20 100 µM in Triton 1%, 50 µl injection volume, retention time 10.742 minutes

In this case, Triton alone shows a peak at a similar time point to the peak in the experimental data (Fig. 21), but it shows a higher AUC. Compared to the peaks of CP20 in water, the peak generated by Triton alone would overlap a CP20 peak up to a concentration of 10 µM (see Appendix Fig. 44 to Fig. 56).

Additionally, CP20 in Triton shows a slight delay in retention time and again it shows a much bigger AUC (about 2.5 times bigger than in the calibration curve).

To get more data on how CP20 is acting in the HPLC system when dissolved in Triton, a calibration curve with the same concentrations as the one used for quantifying CP20 in water, was carried out.

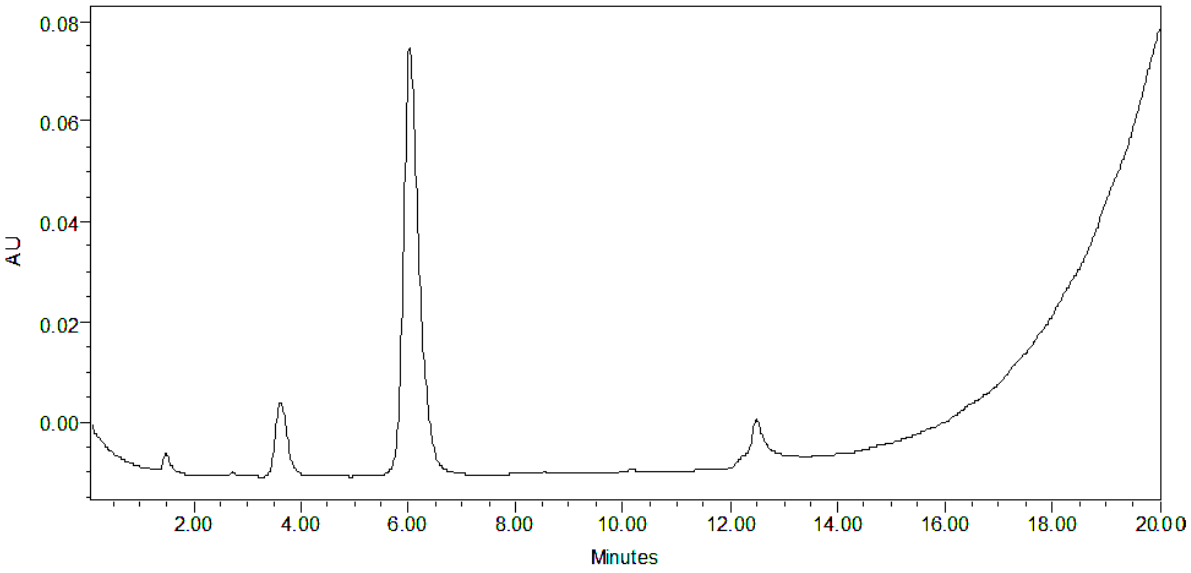

Fig. 27 CP20 100 µM in Triton, 50 µl injection volume

Instead of seeing a peak around 10 – 12 minutes, CP20 now appears to leave the column at a retention time of 6.037 minutes. In order to ensure that it is CP20, the UV-spectrum was checked and showed a maximum at 275.5 nm, the same as it did with CP20 in water (Fig. 28).

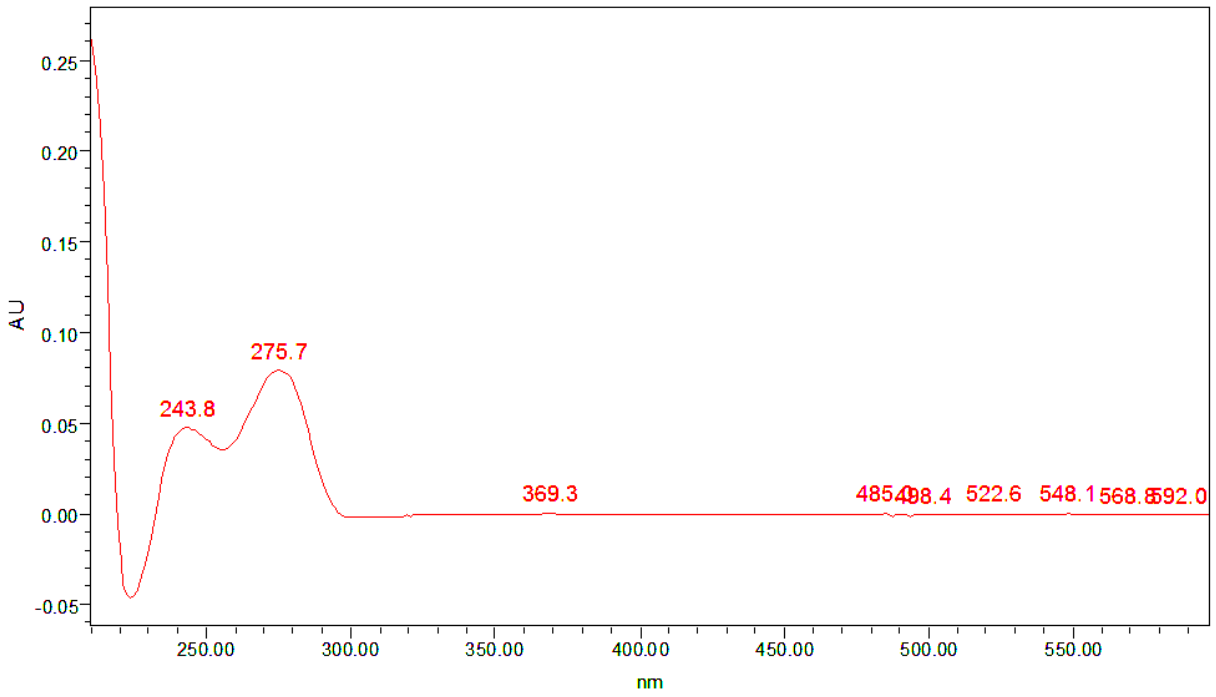

Fig. 28 UV-spectrum of the peak at 6 minutes from Fig. 27

This shift was seen throughout all the samples, here an example of a concentration of 20 µM (Fig. 29).

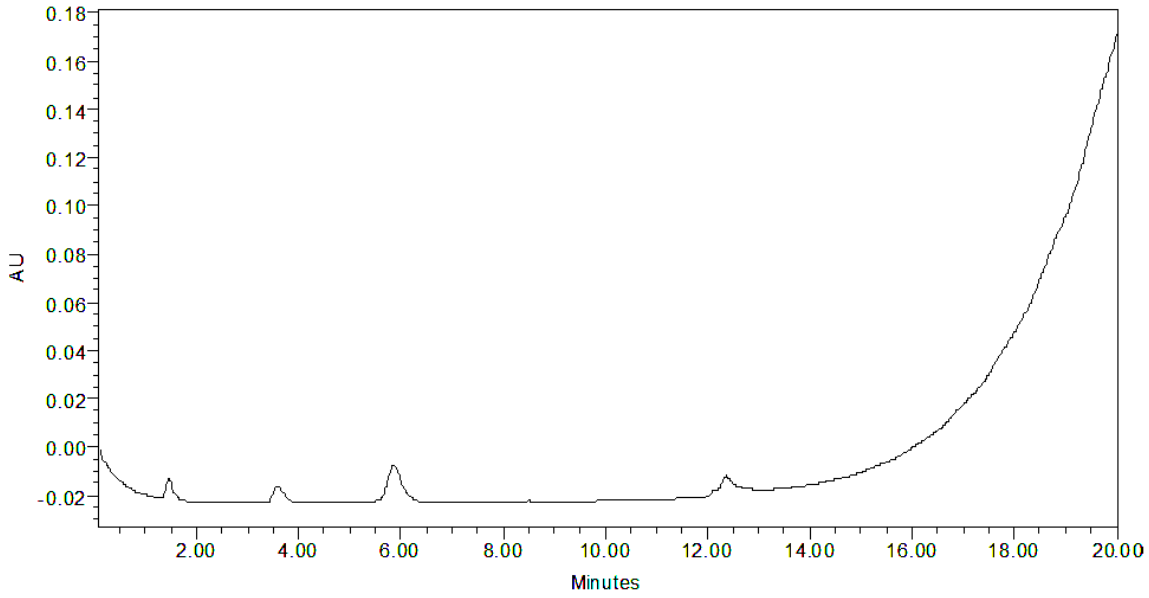

Fig. 29 CP20 20 µM in Triton, 50 µl injection volume

Furthermore, the peak was not visible after injecting a concentration lower than 20 µM (Fig. 30), compared to the calibration curve done in water, where 3 µM CP20 were detectable.

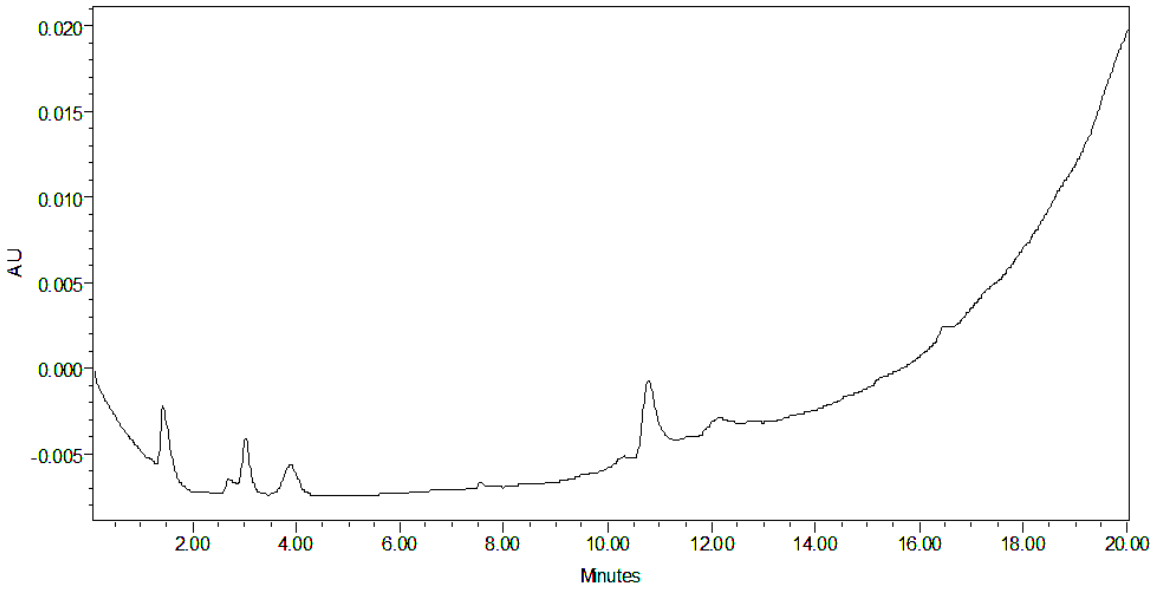

Fig. 30 CP20 3 µM in Triton, injection volume 50 µl

According to the results up to this point, a reproducible analysis of cell samples was not possible due to the following observations. Firstly, the peak of CP20 in presence of Triton was not found to be consistent in its retention time over separate experiments. Secondly, the UV-maximum at 227.4 nm found in the sample data could not be assigned to a compound in the lysate and is therefore made it harder to assure that the peak was CP20 only without impurities. Thirdly after performing the experiments from above and analysing the UV-spectra, it was found that Triton-x100 has its UV-maximum at 275 nm (product information from Sigma) and therefore interferes with CP20 (UV-maximum at 280 nm). Due to this result, an accurate quantification of CP20 could not be done as it was seen impossible to determine the AUC of a peak by comparing the UV-spectra.

3.3.4 Detergents

As a result of the previous conclusions, it was the aim to find a detergent, which would not interfere with CP20 in the UV-spectrum.

Limitations in that respect are:

- a UV-maximum much lower or much higher than 280 nm
- the ability to perform a protein assay after lysing the cells, which means the detergents should break up the cells, but should not break up the proteins
- possibly not an amphiphilic detergent, as Triton is amphiphilic and this might have caused some of the problems in the HPLC system

According to these principles, sodium-dodecyl sulphate (SDS), 3-[3-Cholamidopropyl)-dimethyl-ammonio]-1-propansulphonate (CHAPS), Saponine and distilled water have been chosen.

SDS is an anionic detergent, often used for separating proteins in a polyacrylamide gel electrophoresis (SDS-PAGE). In this setting SDS is used to unfold proteins and it is able to destroy the protein-DNA complex (Pang, Al-Mahrouki et al. 2006), which can therefore influence the amount of protein in the cells regarding the protein assay. CHAPS is a mild detergent and nondenaturating surfactant, designed for membrane protein purification (Giacomelli, Vermeer et al. 2000). Saponin is found to be a mild detergent and was chosen for that attribute (Mercanti and Cosson 2010), but on the other hand, it is a mixture of several compounds and cannot give a specific UV-spectrum. Finally distilled water can break up cells by osmotic lysis and has the advantage of not bringing in any additional compounds.

In order to find the appropriate lysis buffer, the cells were incubated with all four detergents and additionally with Triton in order to have a control group. The concentrations used, were 2.5% SDS in 0.2M NaOH (Guerlava, Izac et al. 1998), 1% CHAPS in 10mM TRIS (Pang, Al-Mahrouki et al. 2006) and 10 g/l saponin in water (Wright, Finglas et al. 2000). Of the 60 wells available, each detergent was used on 12 wells. The incubation time was 45 minutes. In this case ECV304 cells were used.

The result of the protein assay is shown in Fig. 31.

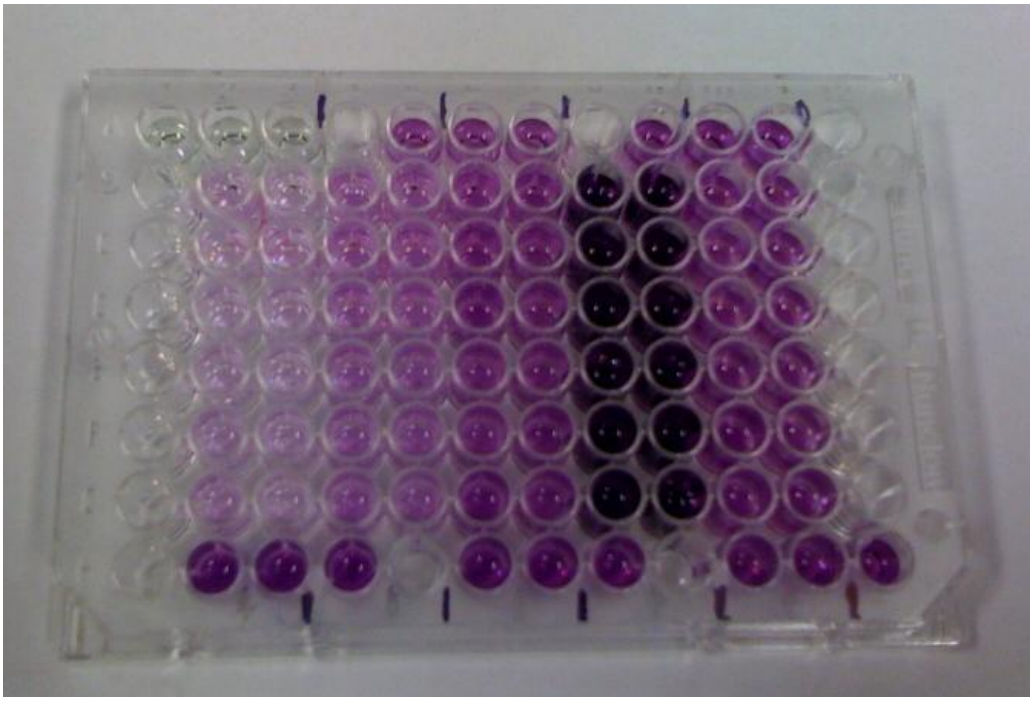

Fig. 31 finished protein assay with five different detergents, first two rows: SDS, second: CHAPS, third: distilled water, fourth: saponin, fifth: Triton

As seen in the picture (Fig. 31), distilled water brought the result the nearest to what Triton did. The Triton control group had a mean protein value of 18.47 µg/100 µl. SDS showed very low values (mean value of -0.015 µg/100 µl) with a few below the detection limit. This result may be due to SDS' ability to denature proteins and there were no protein structures left, which could react with bicinchoninic acid. CHAPS performed slightly better, having a mean value of 5.82 µg/100 µl. However, distilled water with a value of 15.33 µg/100 µl is the closest to the Triton results. Saponin could not be analysed as the contents of the wells instantly turned dark purple after adding the reactive mix, which lead to the assumption that the compounds themselves reacted with bicinchoninic acid and therefore disguised the reaction with protein compounds.

In order to get an impression of how the detergents would react in the HPLC system, they have all been injected and analysed, parallel to performing the protein assay.

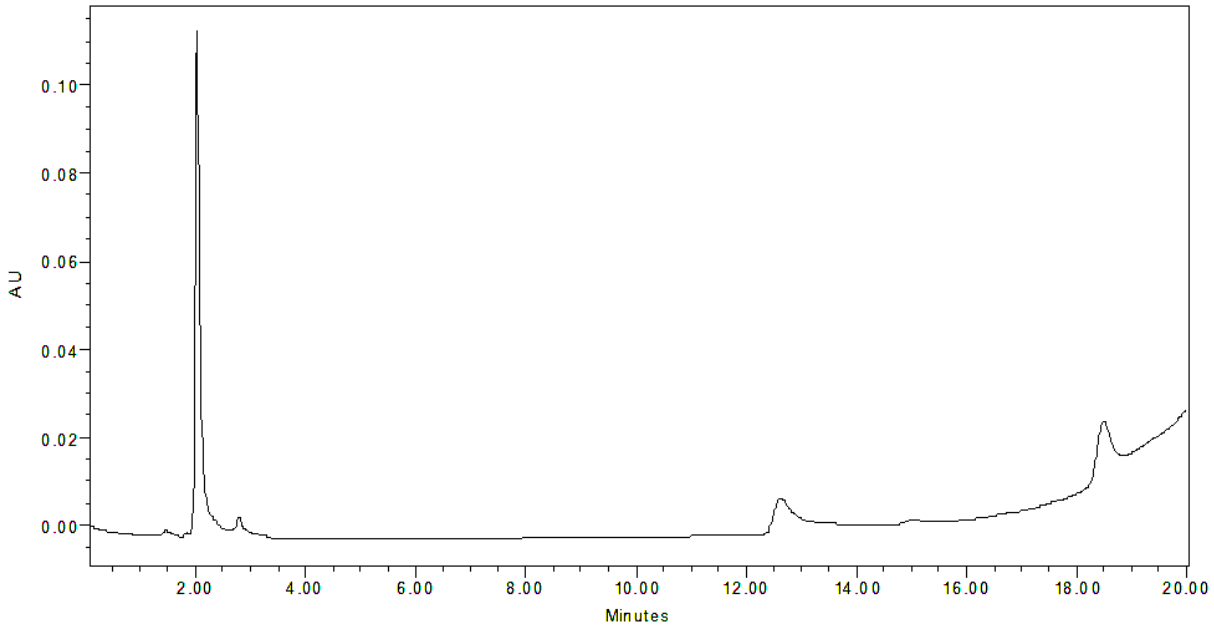

Fig. 32 SDS 2.5% in 0.2M NaOH, 50 µl injection volume

The chromatogram of the SDS sample (Fig. 32) showed a big peak around two minutes, but that can be neglected regarding the fact that CP20 has a retention time of about 10.5 minutes and SDS would therefore not interfere with the compound. The smaller peaks at 12.5 minutes and 18.5 minutes had a low AUC and even a concentration of 3 µM CP20 could be detected next to them.

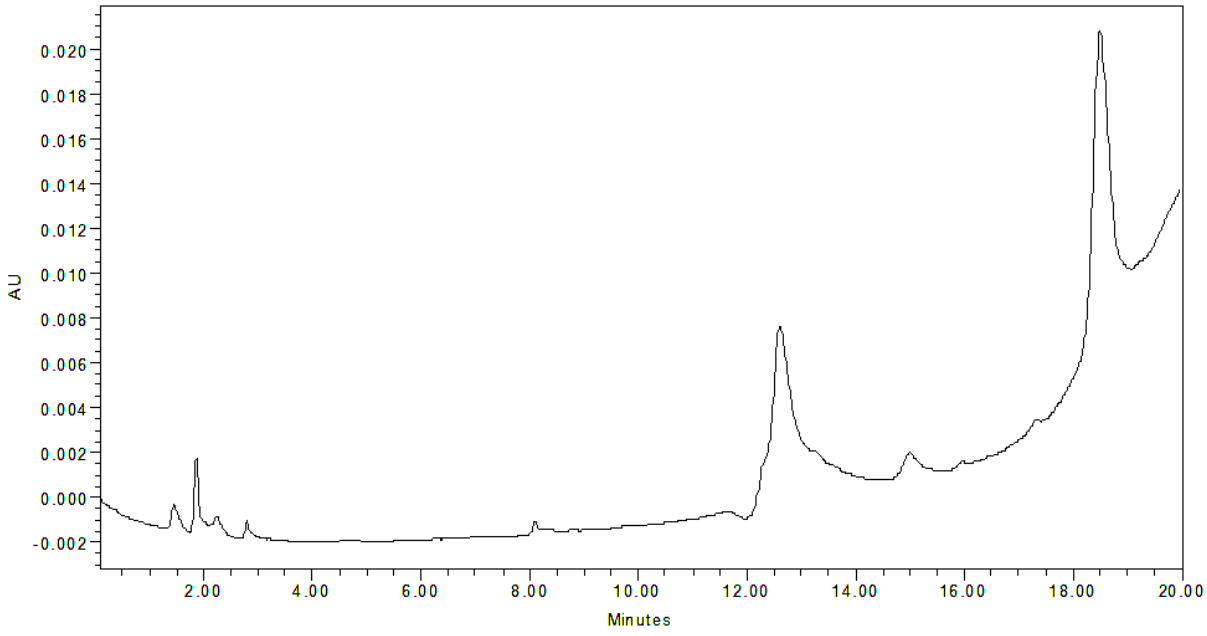

Fig. 33 1% CHAPS in 10mM TRIS, 50 µl injection volume

Comparing the samples of CHAPS (Fig. 33) and distilled water (Fig. 34), they showed a similar location and number of peaks, where the AUCs resembled too. As discussed earlier the peaks in the chromatogram of distilled water can be seen as background and therefore so can be the ones of CHAPS.

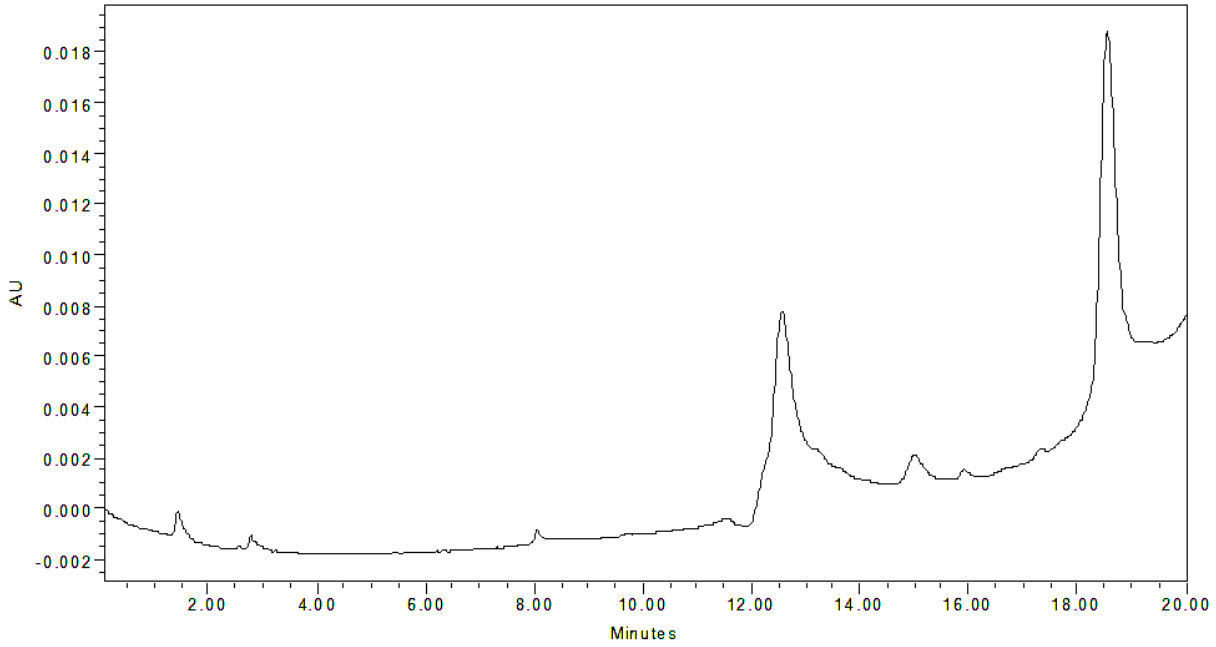

Fig. 34 distilled water, 50 µl injection volume

Finally saponin showed a chromatogram (Fig. 35) with many peaks at various timepoints and with considerable AUCs in respect of the CP20 peak.

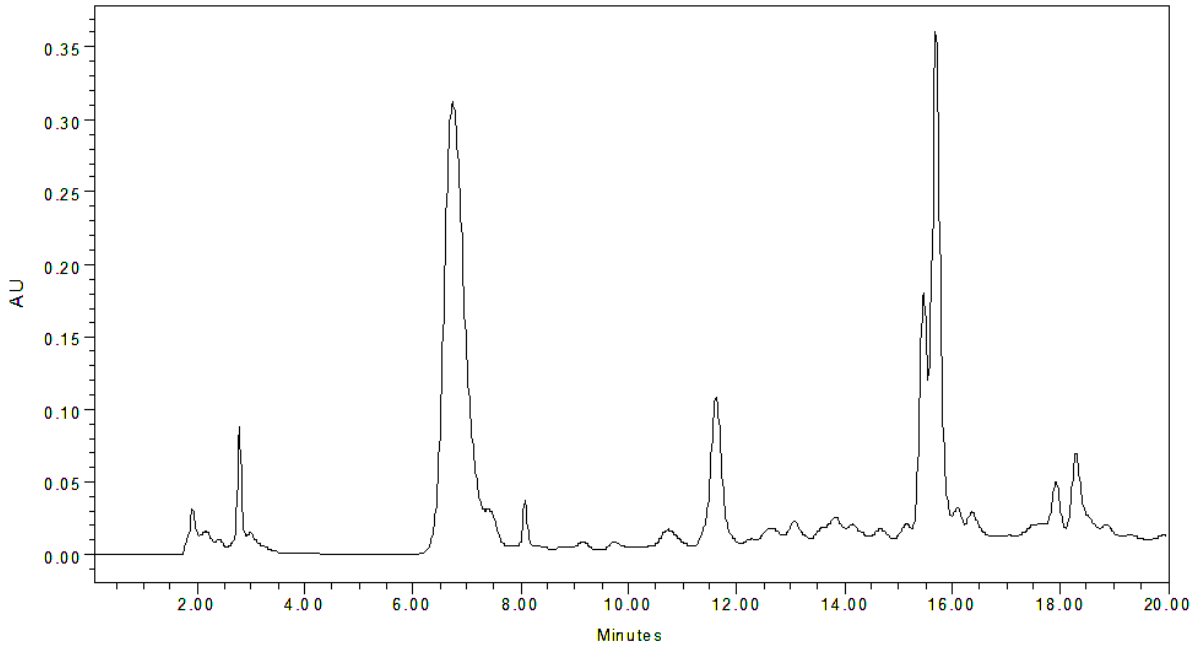

Fig. 35 10 g/l saponin in water, 50 µl injection volume

According to the data gained in the past experiments, distilled water was chosen as lysing agent by reason of its good performance in the protein assay and its HPLC chromatogram giving the least chances of impurities which could influence CP20's retention time.

3.3.5 Results of experiments with distilled water

After deciding to continue with distilled water, the procedure of an uptake assay stayed the same, only the lysing agent was changed.

The experiment showed a relatively low mean value of protein concentration (2.65 µg/100 µl) and the HPLC samples did not show a CP20 peak. Fig. 36 shows a representative sample.

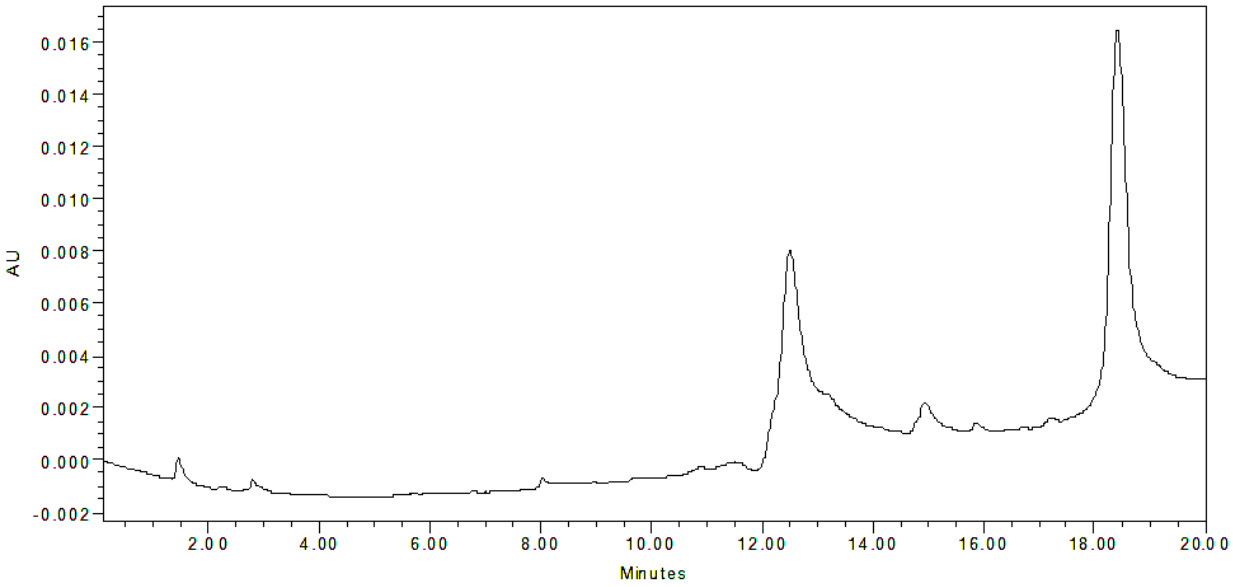

Fig. 36 cell lysate with distilled water, 800 µM, 15 minutes incubation time, 50 µl injection volume

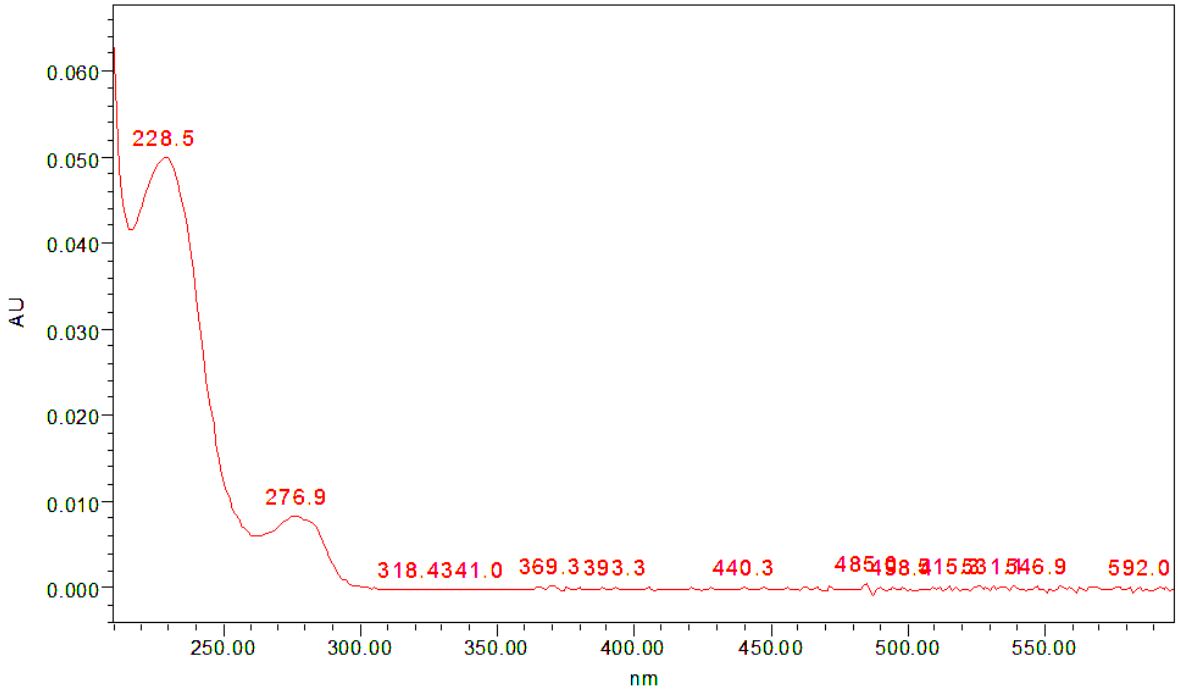

Fig. 37 UV-spectrum of the peak at 12.5 minutes in Fig. 36

The UV-spectrum showed a similar maximum at 228.5 nm than it did in the experiment data with Triton. Up to this point, the maximum could not have been identified or assigned to a specific compound. It could be assumed, that the cells themselves may cause this maximum.

3.3.6 Additional samples

This section shows additional samples that were either analysed before the realisation of the Triton problem or performed after in order obtain more data.

Pooled samples

After the first experimental data analysed by HPLC, it was the aim to make the peak CP20 gives more visible. Therefore, samples from one sample set were pooled, taking together 6 wells (all of the same timepoint) and then injecting 500 µl instead of 50 µl.

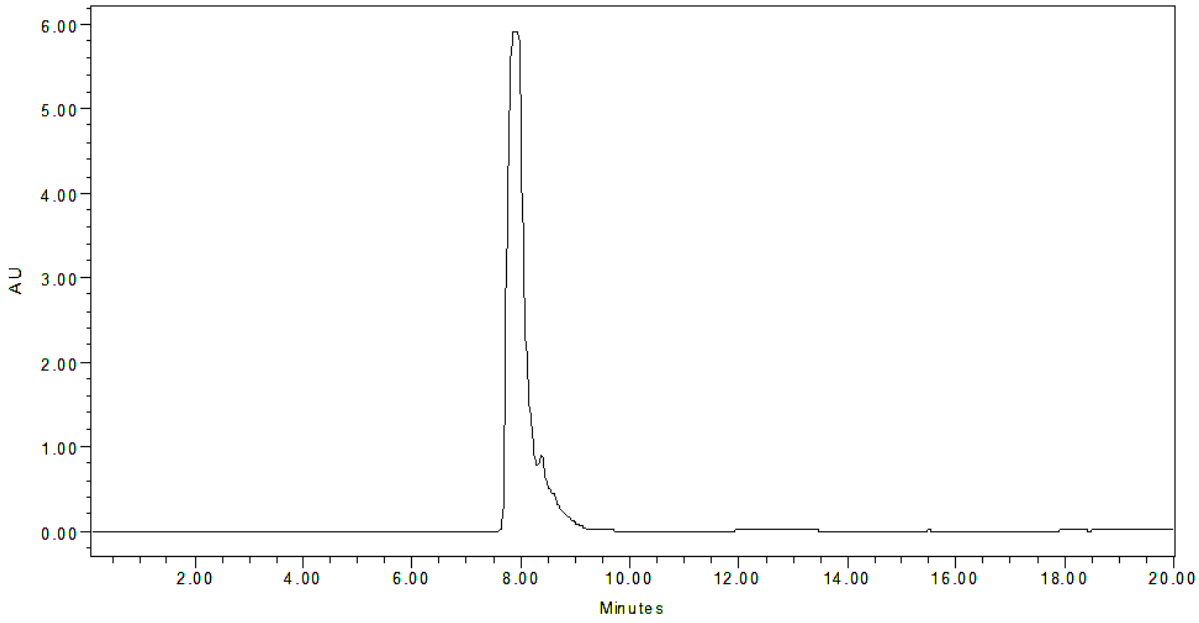

Fig. 38 pooled sample, 800 µM CP20, 15 minutes incubation time, 500 µl injection volume

The chromatogram showed a significant peak around 8 minutes, which did not show a symmetric AUC and after analysing the UV-spectrum of the peak (Fig. 39) could not be identified as CP20.

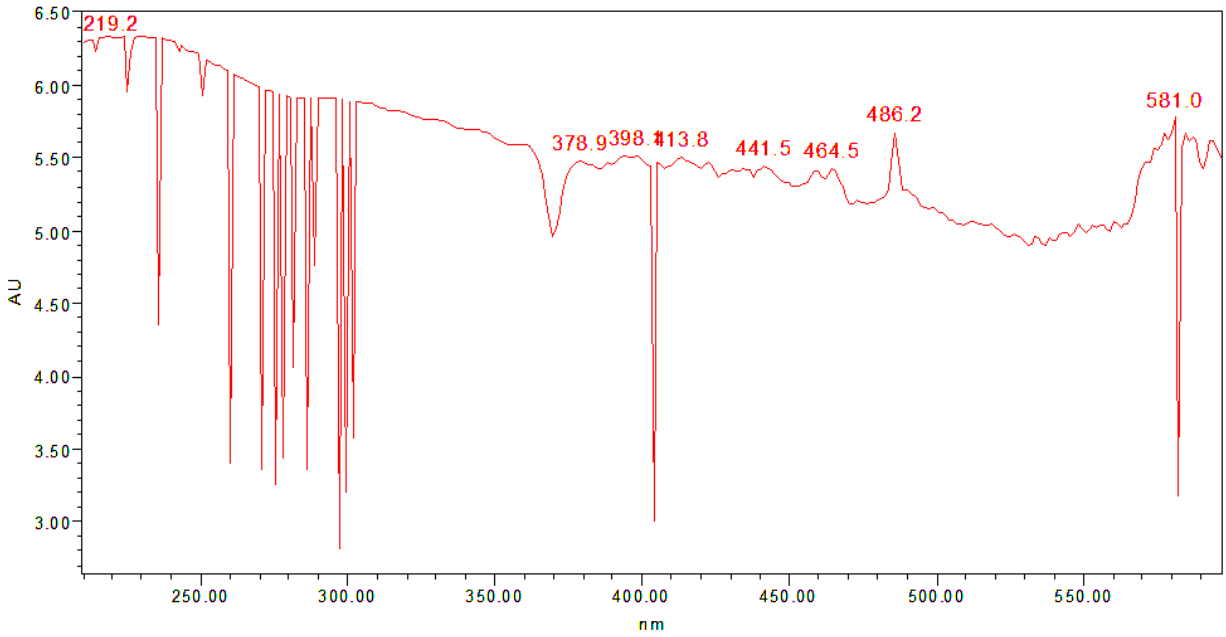

Fig. 39 UV-spectrum of the peak at 8 minutes in Fig. 38

Protein precipitation

According to the data from the pooled samples, it was tried to reduce the impurities by precipitating the proteins present in the cell lysate with trifluoroacetic acid. Fig. 40 shows the chromatogram.

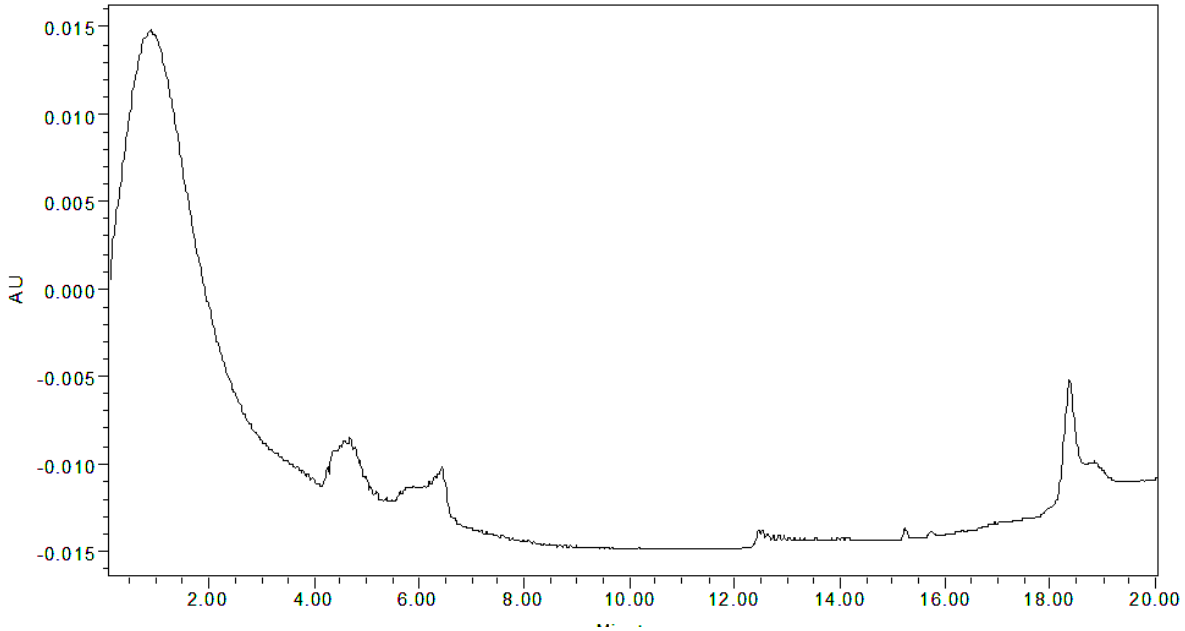

Fig. 40 protein precipitated, pooled sample, 800 µM CP20, 15 minutes incubation time, 50 µl injection volume

In this case the attempt to purify the sample resulted in getting more peaks from impurities instead of obtaining a better defined peak of CP20.

24 hour uptake

This experiment was done to evaluate the possibility that the chosen timepoints (5 to 25 minutes) may have been too short for CP20 to enter the cells. The protocol for the uptake assay stayed the same only the incubation time was elongated to 24 hours. In order to gain an insight on the effects of different concentrations, 100 µM, 500 µM, 800 µM and 1 mM CP20 were each applied to twelve wells. Additional 12 wells were done as a control group without CP20.

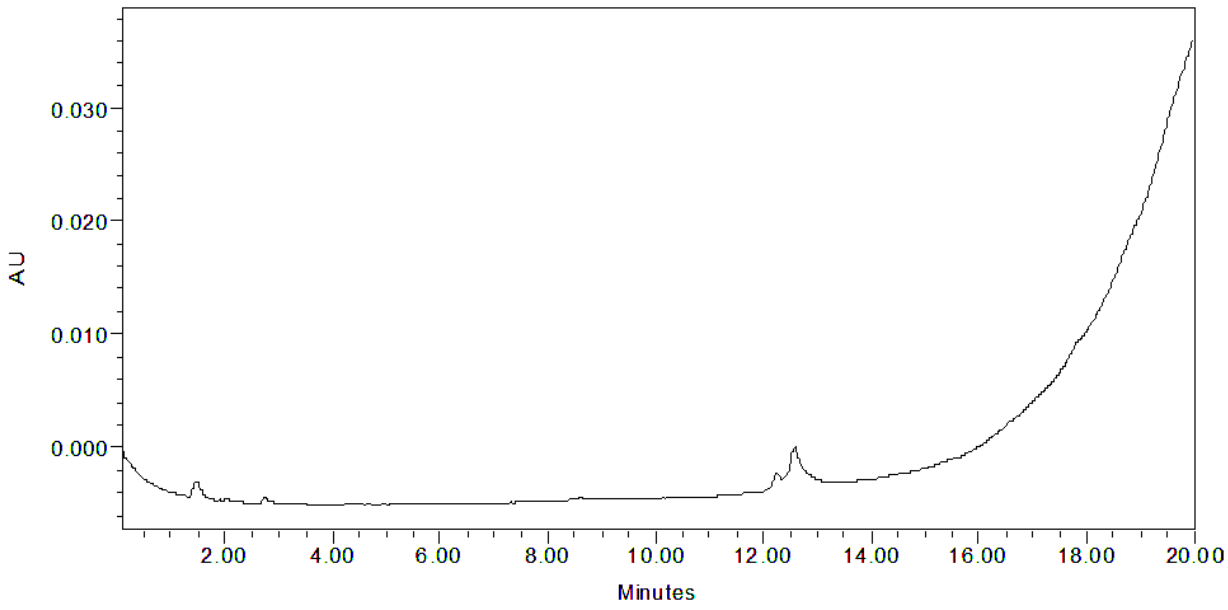

Fig. 41 24 hour uptake sample, 500 µM CP20, 50 µl injection volume

As seen in Fig. 41 the chromatogram did not show a significant CP20 peak. Additionally the end of the curve is drawn upwards, which was detected in all the samples. This phenomenon could be due to an accumulation of Triton in the column which could not leave the system.

Ethylmaltol experiment

The last experiment was done with ethylmaltol instead of CP20. Based on experiments with maltol and CP21, which has an additional methyl group compared to CP20 (Hider 1991), in multilamellar liposomes, it was suspected, that ethylmaltol would penetrate the cells very quickly.

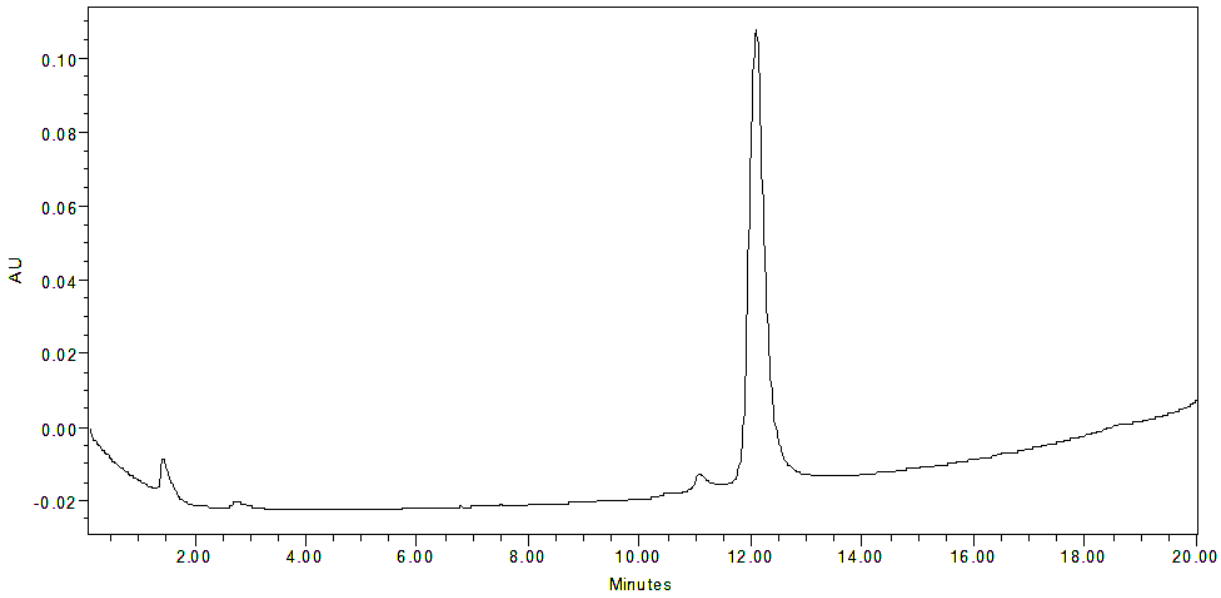

Fig. 42 ethylmaltol, 100 µM in water, 50 µl injection volume

At first ethylmaltol's peak in the HPLC system had to be detected. Fig. 42 shows a chromatogram of 100 µM ethylmaltol in water. Similar to CP20, it came out around 12 minutes.

Then an uptake assay was performed, following the protocol from CP20, with the concentrations of 100 µM and 800 µM and lysed with Triton.

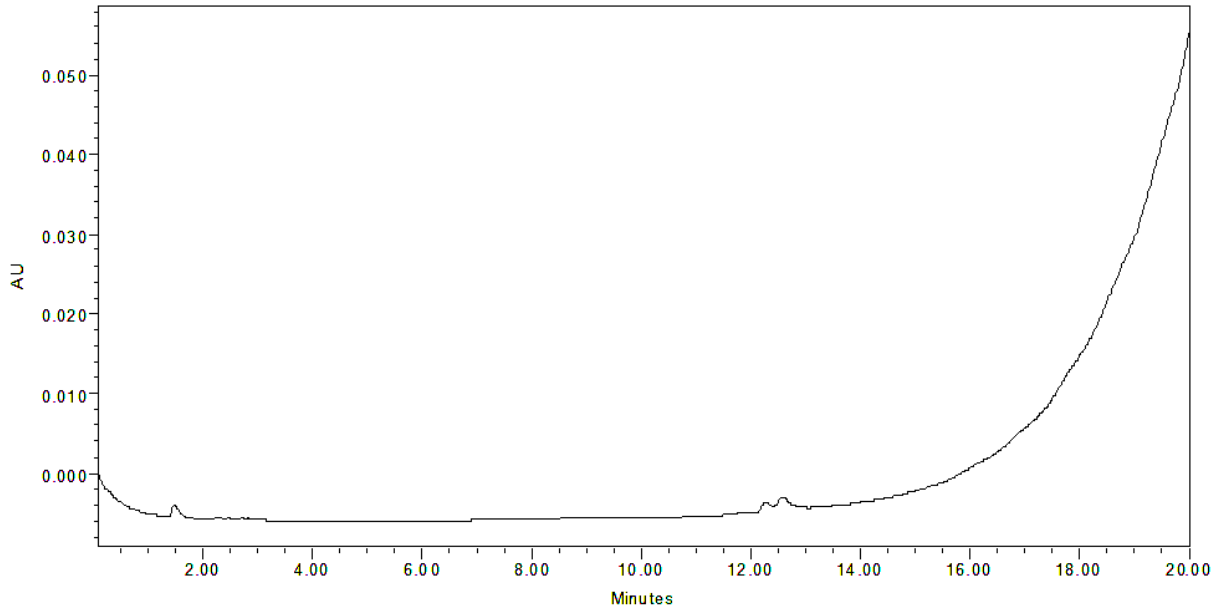

Fig. 43 cell lysate, 800 µM ethylmaltol, 15 minutes incubation time, 50 µl injection volume

Unfortunately the chromatogram did not show a significant peak of ethylmaltol and again the curve drew upwards at the end of the run.

4 Discussion

The aim of this project was to establish whether iron chelators are able to cross the human blood-brain barrier based on an *in vitro* system.

Protecting the brain from harmful compounds is a major purpose of the BBB, which is important to maintain all physiological functions. On the contrary it is a difficult task to ensure the penetration of drugs into the brain in order to enable an optimal effect in the body. Therefore, permeation through the BBB is a major limitation to drug delivery and subsequently a promising field of research.

Iron chelators, up to the present used in various diseases with iron overload states, are now considered as a valuable strategy for the treatment of neurodegenerative diseases (Hider, Ma et al. 2008). It has been found, that iron plays a crucial role in creating oxidative stress, which is a factor in the genesis of diseases like Alzheimer's disease or Parkinson's disease. Consequently it is of great interest to evaluate the possibility of transporting iron chelators through the BBB, in the brain.

In vivo experiments with guinea pigs showed that CP20 can permeate the BBB and suggest that it passively diffuses across the endothelium (Roy 2010). To expand on this data, examining how the compound would act in an human setting would provide even more compelling information. A human endothelial cell line was chosen and incubated with a buffer containing CP20. The aim was to find out how much drug would accumulate in the cells.

In general the experimental settings have produced valuable data except for the analysis by HPLC. Here it was a problem to detect CP20 because of various factors of which the choice of detergent was the most obstructive one. After eliminating Triton from the experimental setting, the search for another detergent with similar features but better performance in the HPLC system was done. The results from the protein assay and the HPLC analysis showed that distilled water, compared to SDS, CHAPS and saponin, had the best attributes to continue. It seemed to lyse the cells in an equivalent quality of Triton and did not interfere with CP20 in the HPLC chromatogram. Although distilled water seemed promising when tested on ECV304 cells, the protein values with hCMEC/D3 cells were significantly lower than

the usual average generated with Triton, which lead to the conclusion that the cells have not been split up completely.

An interesting experiment was the 24 hour uptake as it showed a decreasing amount of radioactivity in the samples when more drug was added. Further studies may be able to find out how CP20 enters the cells and can therefore explain why this phenomenon occurred. In this project however, there was not enough time to pursue this observation more.

As a result of the work done, a few suggestions for further experiments can be made in order to achieve the goal of characterising CP20's ability to cross the BBB in an *in vitro* setting.

4.1 Changes to the experimental setting

As said before, the lysing agent was not ideal for an analysis with HPLC. Therefore it remains crucial to find a better way of lysing the cells without interfering with the HPLC chromatogram. An option not mentioned in this report is sonication. In this case the cells get ruptured by mechanical action which would not give any additional compounds that might produce or overlap peaks. This method needs to be coordinated with the protein assay to confirm the efficacy of the lysis.

4.2 Changes in the cell system

The hCMEC/D3 cell line was chosen because it is human and it has many features of the BBB *in vivo*. As described in various papers (Weksler, Subileau et al. 2005) the endothelial cells do not form a tight monolayer and have a low TEER. Therefore, the cells are not ideal for transwell systems which would allow measurements of transendothelial permeability. Nevertheless, a transwell system might help getting better results regarding the HPLC. The biggest advantage in this case is that the sample used, does not contain cell compounds as the experimental setting is focused on the drug passing through the cells, not staying in them. The samples would contain physiological buffer, but as seen in Fig. 23 and Fig. 24 the

buffer does not interfere with CP20 and can be seen as background. Here it is a difficult decision whether to stay close to human conditions or accept animal cells which do not represent the settings in the human body this accurate, but allow other techniques. In order to set up a transwell experiment, other cell lines, involving cells with non human origin for instance derived from mice or rats (Terasaki, Ohtsuki et al. 2003), are well established at present.

The co-culture with astrocytes is another option, whether the endothelial cells are human or animal. This should improve the barrier tightness as astrocytes influence endothelial cells *in vivo* and heighten the integrity (Butt, Jones et al. 1990). Mimicking this specific influence can be done by co-culturing as said before or adding astrocyte conditioned culture medium to a culture of endothelial cells (Mensch, Oyarzabal et al. 2009).

4.3 Changes in the analysis

As said before, the HPLC analysis was the major problem in the experiments. In order to avoid this problem, it may be interesting to use other methods like radiolabelling of the compound or fluorescence measurements to quantify the amount of CP20 in the cells.

Since sucrose was radiolabelled and analysed by a liquid scintillation counter, it would be a possibility to test a compound that is radiolabelled too. This would ease the process as the sample can be analysed at once and does not have to be divided and would therefore minimize the risk of human error. It has to be considered, that the drug used, would need to be labelled with another radio isotope (such as tritium) than carbon-14 in order to be able to count the two compounds separately.

5 Abstract

The Blood-Brain Barrier (BBB) is an important partition of the blood circulation and the brain environment. It makes sure unwanted agents like xenobiotics or microorganisms cannot enter the brain whereas substrates needed for physiological functions are supplied in sufficient amounts. The pharmaceutical industry, as well as academia, have great interest in research on the BBB in terms of selective drug targeting. For some drugs it is important they do not enter the brain because if they did, it would cause sideeffects. In other cases penetration into the brain is essential for the drug's effect such as therapeutical agents treating neurodegenerative diseases like Alzheimer's disease or Parkinson disease.

In order to obtain insight in the mechanisms of the BBB, various systems have been developed. *In vitro* cultures have undergone a rapid development in the past years and it was possible to create an immortalized human cell line of microvascular endothelial cells appearing at the BBB. These cells have proven to possess a large number of features which occur in the living human body. However, one attribute has not yet been fully mimicked with these cells, the ability to form the extraordinary impermeable tight junctions which are an important characteristic of the BBB. Therefore experiments done in this study investigated the drug uptake into the cells.

The compound analysed was deferiprone (or CP20), an iron chelator widely used for diseases like thalassaemia where frequent blood transfusions are required. As a result the body is soon developing an iron overload state which, untreated, can cause death. Recent studies have found out that iron overload in the brain is a participant in the formation of neurodegenerative diseases. Hence research about iron chelators crossing the BBB is of great interest.

Radiolabelled sucrose was used as a vascular space marker and a marker for non specific drug uptake and was analysed by a liquid scintillation counter. CP20 was analysed in an HPLC system.

In the course of experiments it was discovered that the system used, had some problems with the analysis of the compound. It was attempted to change the lysing agent, Triton, as it was interfering with CP20 in the HPLC chromatogram and had the same maximum in the UV-

spectrum. Distilled water was chosen as a replacement but it did not show more promising results.

So as to vary the experimental setting and overcome the issues mentioned above, precipitating the proteins in the sample or pooling several samples was tried. Nevertheless these efforts did not show the desired effect and CP20 could not be detected or quantified in the chromatograms.

An experiment worth pursuing was the 24 hour uptake, showing a decreasing amount of sucrose with an increasing amount of CP20. Due to a lack of time it was not analysed further in this study.

Taken together the ability of CP20 crossing the BBB could not be studied in these circumstances, nevertheless changes in the experimental setting might bring new insights to this subject and therefore to treatment of neurodegenerative diseases.

6 Zusammenfassung

Die Blut-Hirn Schranke (BHS) stellt eine wichtige Teilung zwischen Blutzirkulation und Gehirn dar. Sie sorgt dafür, dass nicht erwünschte Stoffe wie Xenobiotika oder Mikroorganismen nicht ins Gehirn kommen, Substrate, die für die physiologische Funktion erforderlich sind, jedoch in genügender Zahl geliefert werden. Sowohl die pharmazeutische Industrie als auch die universitäre Forschung sind sehr an der Erforschung der BHS bezüglich „drug targeting“ interessiert. Für manche Stoffe ist es wichtig, dass sie nicht ins Gehirn gelangen, da sonst Nebenwirkungen auftreten könnten. In anderen Fällen ist es notwendig Medikamenten Zutritt zum Gehirn zu verschaffen um den gewünschten Effekt zu erreichen. Beispiele dafür sind Pharmazeutika, die zur Therapie von neurodegenerativen Krankheiten wie Alzheimer oder Parkinson verwendet werden.

Um die BHS und ihre Funktionen zu verstehen und erforschen wurden verschiedene Systeme entwickelt. In den vergangenen Jahren hat es eine große Entwicklung im Bereich der *in vitro* Kulturen gegeben und es war möglich eine immortalisierte, menschliche Zelllinie von mikrovaskulären Endothelzellen, die in der BHS vorkommen, zu erschaffen. Diese Zellen haben bewiesen, dass sie viele der im lebendigen, menschlichen Körper vorkommenden Attribute innehaben. Trotzdem gibt es bis zum heutigen Tag keine Möglichkeit die außergewöhnlich dichten „tight junctions“, die eine wichtige Eigenschaft der BHS darstellen, nachzuahmen. Deshalb wurde in dieser Studie die Aufnahme eines Stoffes in die Zellen untersucht.

Der zu untersuchende Stoff war Deferipron (oder CP20), ein Eisenchelator, der weit verbreitet bei der Therapie von Krankheiten wie Thalassämie eingesetzt wird, wo die Patienten regelmäßige Bluttransfusionen benötigen. Durch diese Transfusionen stellt sich im Körper ein Übermaß an Eisen ein, das unbehandelt zum Tod führen kann. Neuere Studien belegen, dass übermäßig viel Eisen im Gehirn ein Faktor bei der Entstehung von neurodegenerativen Krankheiten sein kann. Daher ist die Erforschung der Möglichkeiten, wie Eisenchelatoren die BHS überwinden, von großer Bedeutung.

Radioaktiv markierte Saccharose wurde als vaskulärer Gefäßmarker verwendet und durch einen Flüssig-Szintillationszähler vermessen. CP20 wurde auf einem HPLC-System analysiert.

Im Verlauf der Experimente wurde herausgefunden, dass es einige Probleme bezüglich der Analyse des Stoffes in dem verwendeten System gab. Daher wurde versucht, das zur Lyse verwendete Detergens Triton zu ändern, da es im HPLC-Chromatogramm CP20 störte und dasselbe UV-Maximum aufwies. Als neues Detergens wurde destilliertes Wasser genutzt, das aber auch nicht das gewünschte Ergebnis brachte.

Um die Bedingungen der Experimente zu ändern und die oben beschriebenen Hindernisse zu überbrücken, wurde Proteinfällung oder Vereinigung mehrerer Proben versucht. Jedoch konnten auch diese Versuche nicht zu einer Verbesserung führen und CP20 konnte in den Chromatogrammen nicht detektiert oder quantifiziert werden.

Ein weiteres Experiment, das der genaueren Untersuchung unterzogen werden könnte, ist das der 24-Stunden-Aufnahme, das eine verringerte Saccharose-Konzentration bei erhöhter CP20-Konzentration aufwies. Durch einen Mangel an Zeit wurde diese Beobachtung in dieser Studie nicht weiter verfolgt.

Abschließend ist zu sagen, dass es unter diesen Umständen nicht möglich war eine Aussage über die Fähigkeit von CP20 die BHS zu übertreten, zu treffen. Änderungen im Aufbau der Experimente könnten aber neue Erkenntnisse bezüglich dieses Themas und folglich auch in der Therapie von neurodegenerativen Erkrankungen bringen.

7 References

Abbott, N. (2002). "Astrocyte-endothelial interactions and blood-brain barrier permeability." J Anat **200**(5): 527.

Abbott, N. J., A. A. Patabendige, et al. (2010). "Structure and function of the blood-brain barrier." Neurobiol Dis **37**(1): 13-25.

Abbott, N. J. and I. A. Romero (1996). "Transporting therapeutics across the blood-brain barrier." Mol Med Today **2**(3): 106-113.

Abbott, N. J., L. Ronnback, et al. (2006). "Astrocyte-endothelial interactions at the blood-brain barrier." Nat Rev Neurosci **7**(1): 41-53.

Alavijeh, M. S., M. Chishty, et al. (2005). "Drug metabolism and pharmacokinetics, the blood-brain barrier, and central nervous system drug discovery." NeuroRx **2**(4): 554-571.

Bernacki, J., A. Dobrowolska, et al. (2008). "Physiology and pharmacological role of the blood-brain barrier." Pharmacol Rep **60**(5): 600-622.

Beutler, E., A. V. Hoffbrand, et al. (2003). "Iron deficiency and overload." Hematology Am Soc Hematol Educ Program: 40-61.

Bickel, U. (2005). "How to measure drug transport across the blood-brain barrier." NeuroRx **2**(1): 15-26.

Butt, A. M., H. C. Jones, et al. (1990). "Electrical resistance across the blood-brain barrier in anaesthetized rats: a developmental study." J Physiol **429**: 47-62.

Carvey, P. M., B. Hendey, et al. (2009). "The blood-brain barrier in neurodegenerative disease: a rhetorical perspective." J Neurochem **111**(2): 291-314.

Cecchelli, R., V. Berezowski, et al. (2007). "Modelling of the blood-brain barrier in drug discovery and development." Nat Rev Drug Discov **6**(8): 650-661.

Chishty, M., D. J. Begley, et al. (2004). "Interaction of nucleoside analogues with nucleoside transporters in rat brain endothelial cells." J Drug Target **12**(5): 265-272.

Dubey, A. P., S. Sudha, et al. (2007). "Deferasirox: the new oral iron chelator." Indian Pediatr **44**(8): 603-607.

Eyal, S., P. Hsiao, et al. (2009). "Drug interactions at the blood-brain barrier: fact or fantasy?" Pharmacol Ther **123**(1): 80-104.

Galanello, R. (2007). "Deferiprone in the treatment of transfusion-dependent thalassemia: a review and perspective." Ther Clin Risk Manag **3**(5): 795-805.

Gattermann, N. (2009). "The treatment of secondary hemochromatosis." Dtsch Arztebl Int **106**(30): 499-504, I.

Giacomelli, C. E., A. W. P. Vermeer, et al. (2000). "Micellization and Adsorption Characteristics of CHAPS." Langmuir **16**(11): 4853-4858.

Guerlava, P., V. Izac, et al. (1998). "Comparison of different methods of cell lysis and protein measurements in Clostridium perfringens: application to the cell volume determination." Curr Microbiol **36**(3): 131-135.

Guo, X., M. Geng, et al. (2005). "Glucose transporter 1, distribution in the brain and in neural disorders: its relationship with transport of neuroactive drugs through the blood-brain barrier." Biochem Genet **43**(3-4): 175-187.

Hawkins, B. T. and T. P. Davis (2005). "The blood-brain barrier/neurovascular unit in health and disease." Pharmacol Rev **57**(2): 173-185.

Hersch, S. M. and H. D. Rosas (2008). "Neuroprotection for Huntington's disease: ready, set, slow." Neurotherapeutics **5**(2): 226-236.

Hider, R. C., Hall A. D. (1991). Iron chelating agents in medicine: The application of bidentate hydroxypyridin-4-ones. Perspectives on Bioinorganic Chemistry, JAI Press Ltd. **1:** 209 - 253.

Hider, R. C., Y. Ma, et al. (2008). "Iron chelation as a potential therapy for neurodegenerative disease." Biochem Soc Trans **36**(Pt 6): 1304-1308.

Kakee, A., T. Terasaki, et al. (1997). "Selective brain to blood efflux transport of para-aminohippuric acid across the blood-brain barrier: in vivo evidence by use of the brain efflux index method." J Pharmacol Exp Ther **283**(3): 1018-1025.

Kohgo, Y., K. Ikuta, et al. (2008). "Body iron metabolism and pathophysiology of iron overload." Int J Hematol **88**(1): 7-15.

Kusuhara, H. and Y. Sugiyama (2005). "Active efflux across the blood-brain barrier: role of the solute carrier family." NeuroRx **2**(1): 73-85.

Liu, D. Y., Z. D. Liu, et al. (1999). "Gradient ion-pair high-performance liquid chromatographic method for analysis of 3-hydroxypyridin-4-one iron chelators." J Chromatogr B Biomed Sci Appl **730**(1): 135-139.

Liu, G., P. Men, et al. (2009). "Metal chelators coupled with nanoparticles as potential therapeutic agents for Alzheimer's disease." J Nanoneurosci **1**(1): 42-55.

Loscher, W. and H. Potschka (2005). "Blood-brain barrier active efflux transporters: ATP-binding cassette gene family." NeuroRx **2**(1): 86-98.

Mensch, J., J. Oyarzabal, et al. (2009). "In vivo, in vitro and in silico methods for small molecule transfer across the BBB." J Pharm Sci **98**(12): 4429-4468.

Mercanti, V. and P. Cosson (2010). "Resistance of Dictyostelium discoideum membranes to saponin permeabilization." BMC Res Notes **3**(1): 120.

Molina-Holgado, F., A. Gaeta, et al. (2008). "Neuroprotective actions of deferiprone in cultured cortical neurones and SHSY-5Y cells." J Neurochem.

Neufeld, E. J. (2006). "Oral chelators deferasirox and deferiprone for transfusional iron overload in thalassemia major: new data, new questions." Blood **107**(9): 3436-3441.

Pan, W., W. A. Banks, et al. (1997). "Permeability of the blood-brain and blood-spinal cord barriers to interferons." J Neuroimmunol **76**(1-2): 105-111.

Pang, Z., A. Al-Mahrouki, et al. (2006). "Selection of surfactants for cell lysis in chemical cytometry to study protein-DNA interactions." Electrophoresis **27**(8): 1489-1494.

Poller, B., H. Gutmann, et al. (2008). "The human brain endothelial cell line hCMEC/D3 as a human blood-brain barrier model for drug transport studies." J Neurochem **107**(5): 1358-1368.

Pschyrembel, W. (2007). Klinisches Wörterbuch, Gruyter.

Roy, S. (2010). Iron chelator design: Evaluation of blood-brain barrier permeability and neuroprotective properties. Pharmacy. London, King's College London. **PhD**.

Rubin, L. L., D. E. Hall, et al. (1991). "A cell culture model of the blood-brain barrier." J Cell Biol **115**(6): 1725-1735.

Sanderson, L., M. Dogruel, et al. (2009). "Pentamidine movement across the murine blood-brain and blood-cerebrospinal fluid barriers: effect of trypanosome infection, combination therapy, P-glycoprotein, and multidrug resistance-associated protein." J Pharmacol Exp Ther **329**(3): 967-977.

Shachar, D. B., N. Kahana, et al. (2004). "Neuroprotection by a novel brain permeable iron chelator, VK-28, against 6-hydroxydopamine lession in rats." Neuropharmacology **46**(2): 254-263.

Smith, M. W. and M. Gumbleton (2006). "Endocytosis at the blood-brain barrier: from basic understanding to drug delivery strategies." J Drug Target **14**(4): 191-214.

Stamatovic, S. M., R. F. Keep, et al. (2008). "Brain endothelial cell-cell junctions: how to "open" the blood brain barrier." Curr Neuropharmacol **6**(3): 179-192.

Tai, L. M., P. S. Reddy, et al. (2009). "Polarized P-glycoprotein expression by the immortalised human brain endothelial cell line, hCMEC/D3, restricts apical-to-basolateral permeability to rhodamine 123." Brain Res **1292**: 14-24.

Terasaki, T., S. Ohtsuki, et al. (2003). "New approaches to in vitro models of blood-brain barrier drug transport." Drug Discov Today **8**(20): 944-954.

Ueno, M. (2009). "Mechanisms of the penetration of blood-borne substances into the brain." Curr Neuropharmacol **7**(2): 142-149.

Vermylen, C. (2008). "What is new in iron overload?" Eur J Pediatr **167**(4): 377-381.

Voest, E. E., G. Vreugdenhil, et al. (1994). "Iron-chelating agents in non-iron overload conditions." Ann Intern Med **120**(6): 490-499.

Weksler, B. B., E. A. Subileau, et al. (2005). "Blood-brain barrier-specific properties of a human adult brain endothelial cell line." FASEB J **19**(13): 1872-1874.

Whittington, C. A. and K. V. Kowdley (2002). "Review article: haemochromatosis." Aliment Pharmacol Ther **16**(12): 1963-1975.

Wolburg, H., S. Noell, et al. (2009). "Brain endothelial cells and the glio-vascular complex." Cell Tissue Res **335**(1): 75-96.

Wright, A. J., P. M. Finglas, et al. (2000). "Erythrocyte folate analysis: saponin added during lysis of whole blood can increase apparent folate concentrations, depending on hemolysate pH." Clin Chem **46**(12): 1978-1986.

8 Curriculum vitae

Name:	Elisabeth Priester
Day of birth:	October, 6th 1987
Nationality:	Austria, Germany
Address:	Hirschengasse 10/2/8 1060 Vienna
Academic studies:	
Oct 2005 – Jun 2010:	Diploma study Pharmacy at University of Vienna Althanstraße 14, 1090 Vienna
Oct 2009 – Jan 2010:	Erasmus student at King's College London Hodgkin Building, Guy's Campus London SE1 1UL Diploma thesis: "*Penetration of Hydroxypyridinones through the Blood-Brain Barrier based on a cell monolayer system*"
Education:	
Sept 1993 – Jun 1997:	Elementary School: VS Eisenstadt, Bahngasse 2 – 4, 7000 Eisenstadt
Sept 1997 – Jun 2005:	Secondary School: BG/BRG/BORG Eisenstadt, Kurzwiesenweg 1, 7000 Eisenstadt
Work experience:	
Aug 2006:	Internship at Sanochemia Pharmazeutika AG, Landeggerstraße 7, 2491 Neufeld/Leitha
Jul 2007:	Internship at Apotheke der Barmherzigen Brüder Eisenstadt, Esterhazystraße 26, 7000 Eisenstadt
Aug 2008:	Internship at Salvator-Apotheke Eisenstadt, Hauptstraße 4, 7000 Eisenstadt
Jul 2009 - Aug 2009:	Internship at Sanochemia Pharmazeutika AG, Landeggerstraße 7, 2491 Neufeld/Leitha

Appendix

1 HPLC chromatograms

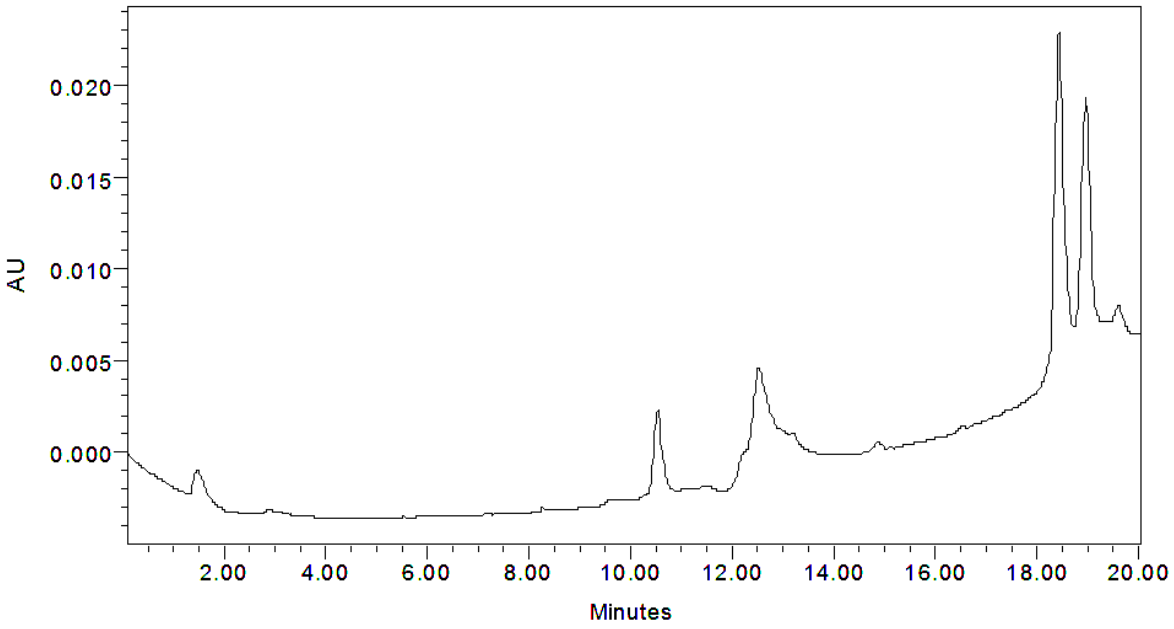

Fig. 44 CP20 3 µM in water, 50 µl injection volume

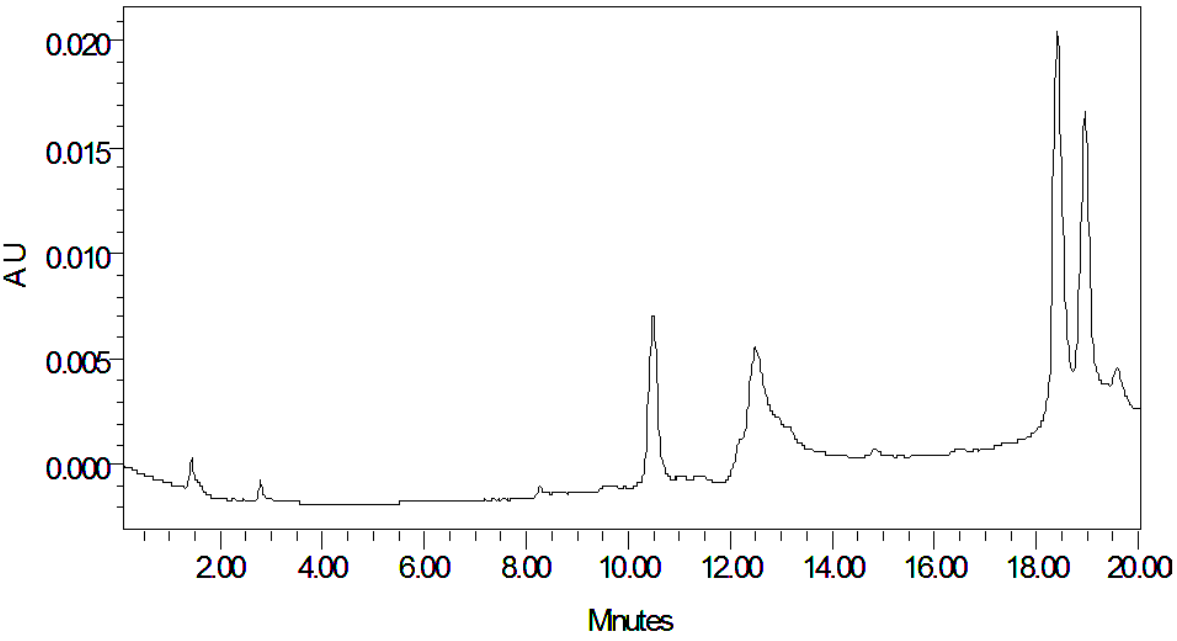

Fig. 45 CP20 5 µM in water, 50 µl injection volume

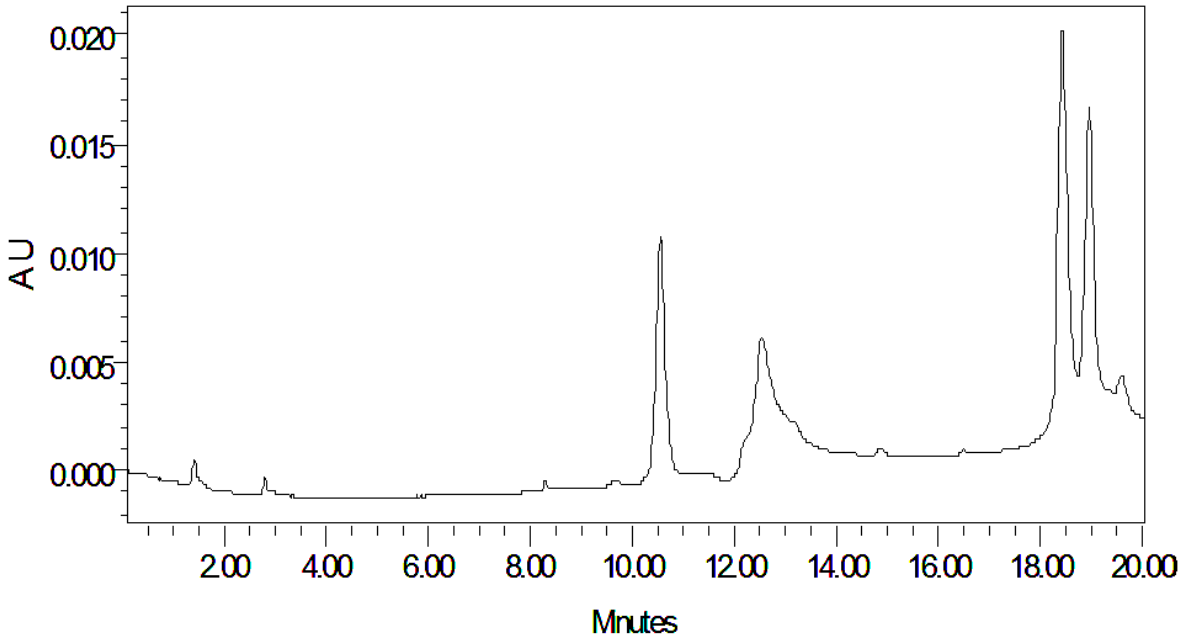

Fig. 46 CP20 7 µM in water, 50 µl injection volume

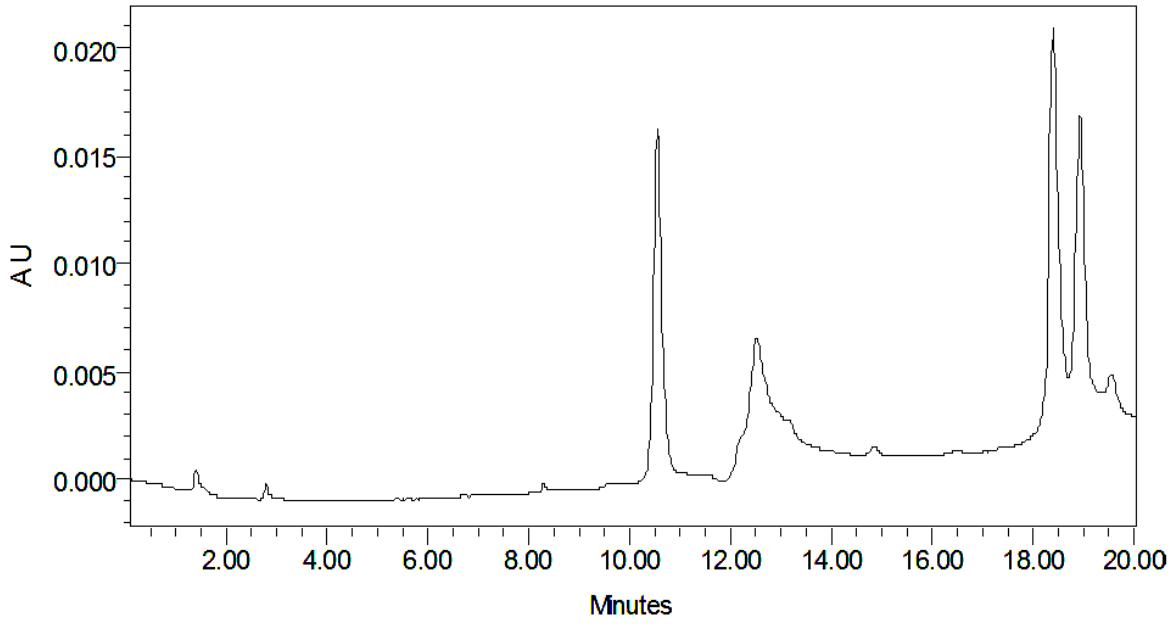

Fig. 47 CP20 10 µM in water, 50 µl injection volume

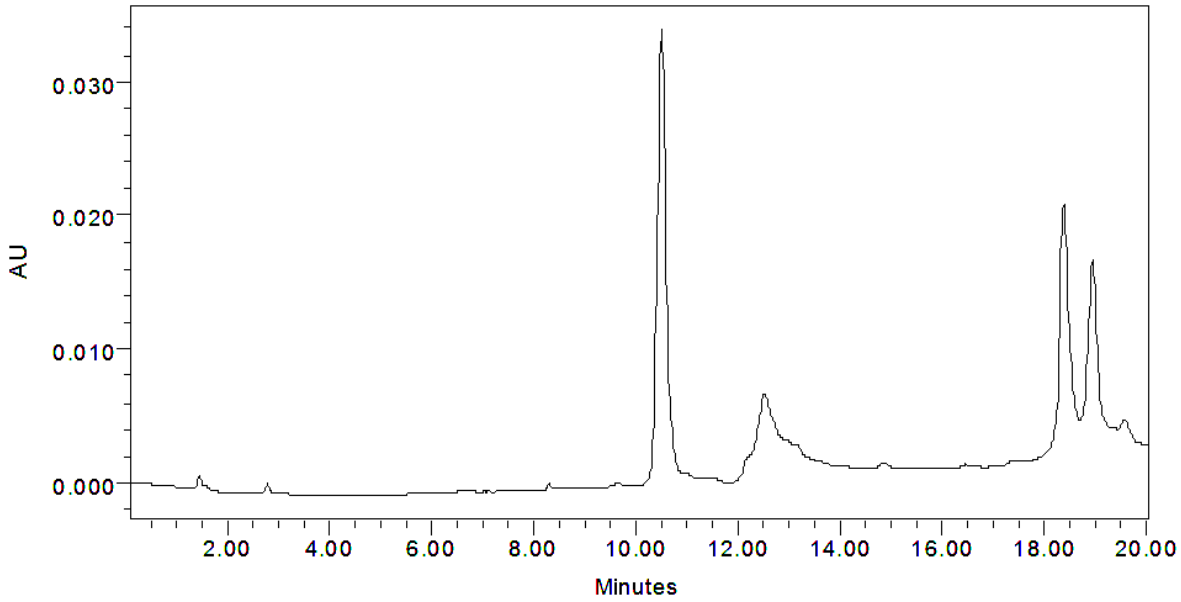

Fig. 48 CP20 20 µM in water, 50 µl injection volume

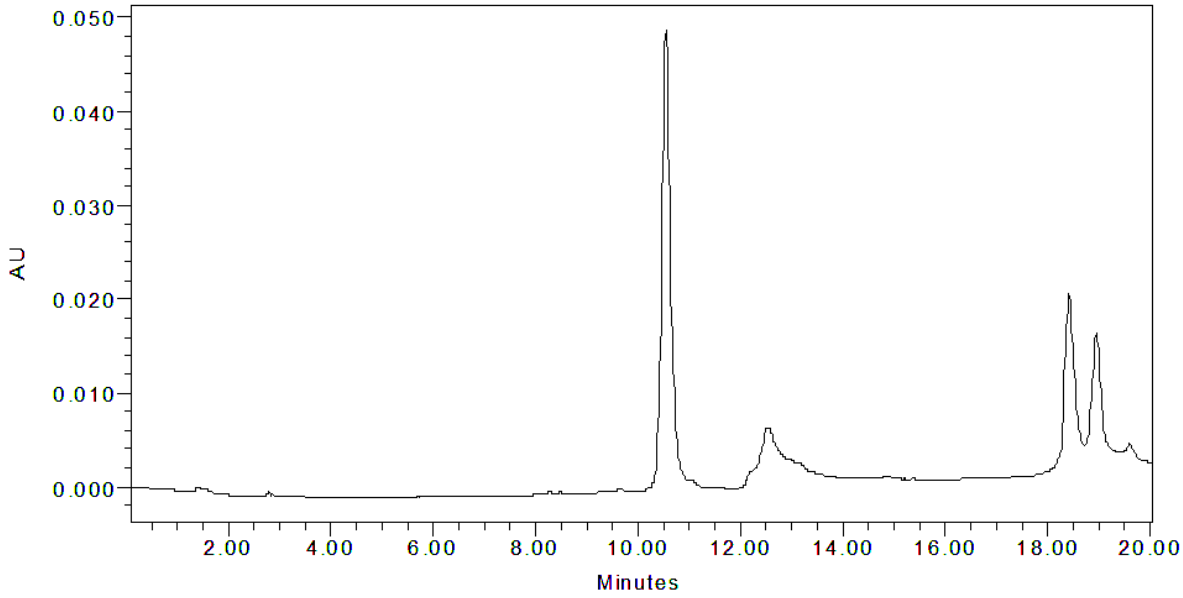

Fig. 49 CP20 30 µM in water, 50 µl injection volume

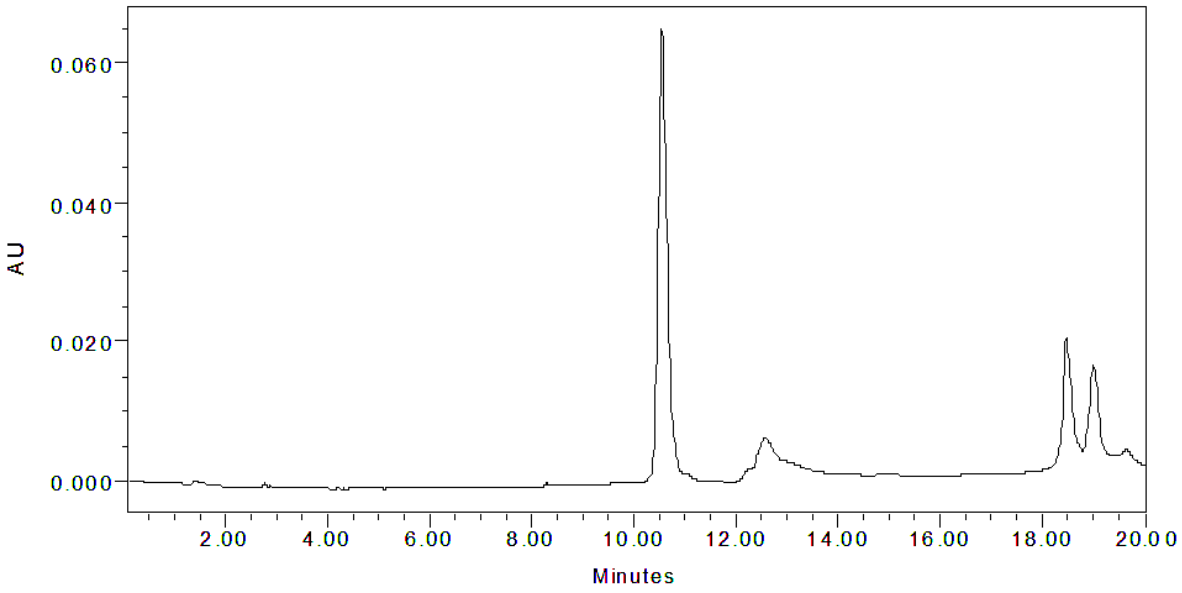

Fig. 50 CP20 40 µM in water, 50 µl injection volume

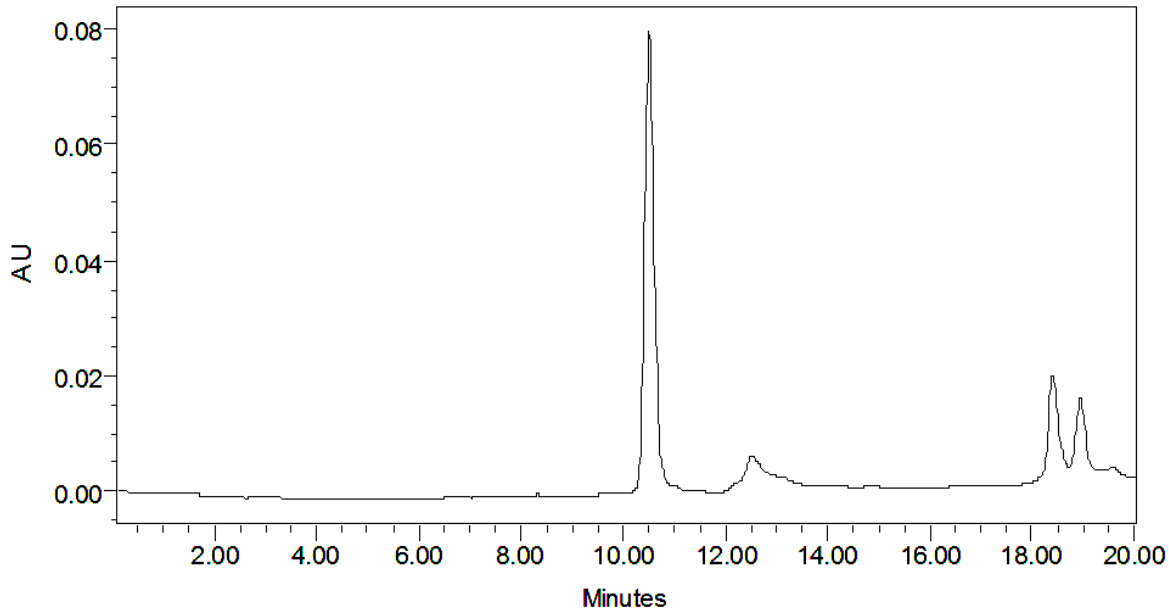

Fig. 51 CP20 50 µM in water, 50 µl injection volume

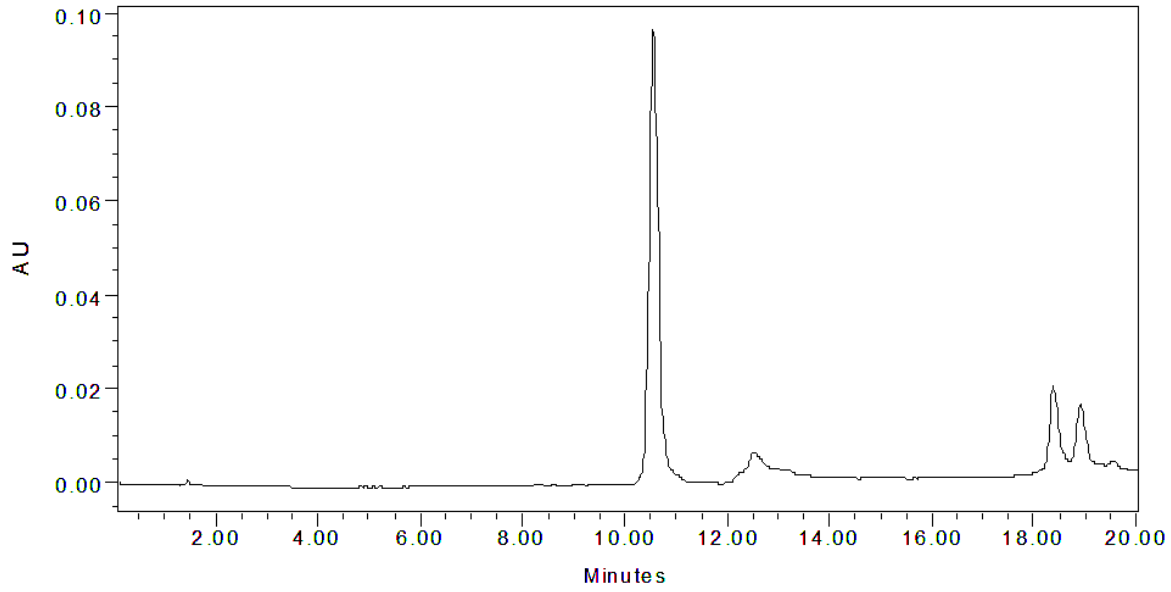

Fig. 52 CP20 60 µM in water, 50 µl injection volume

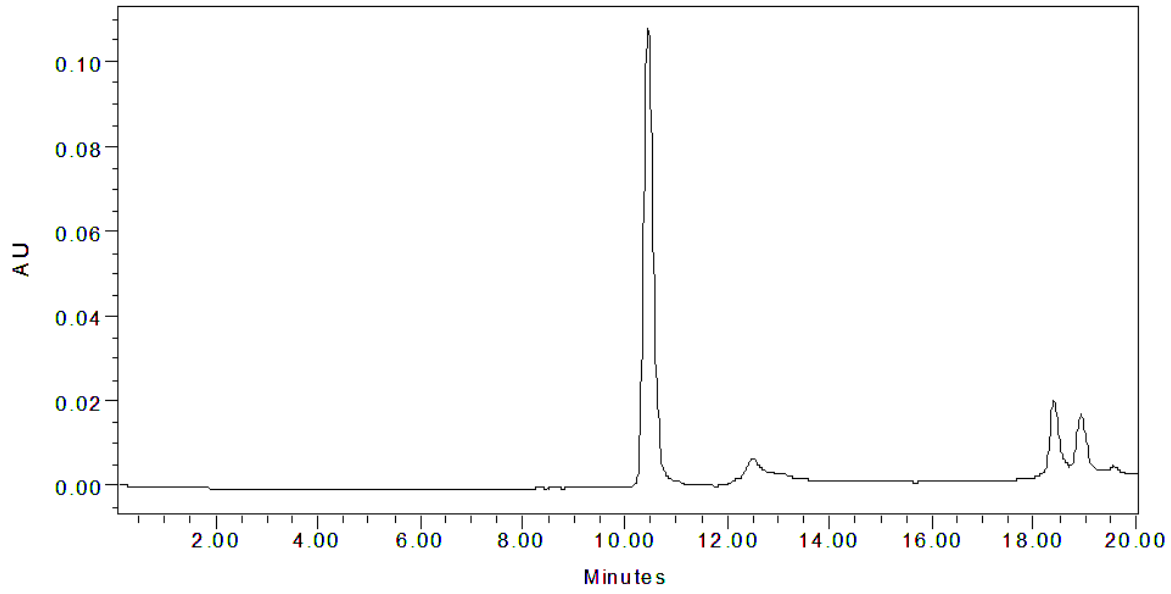

Fig. 53 CP20 70 µM in water, 50 µl injection volume

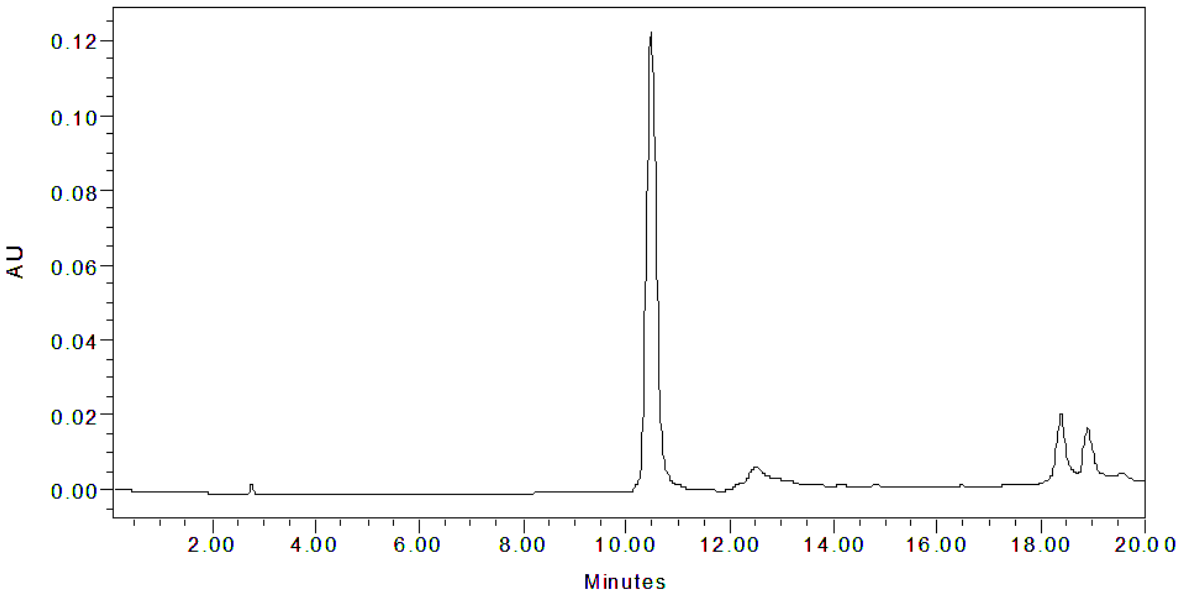

Fig. 54 CP20 80 µM in water, 50 µl injection volume

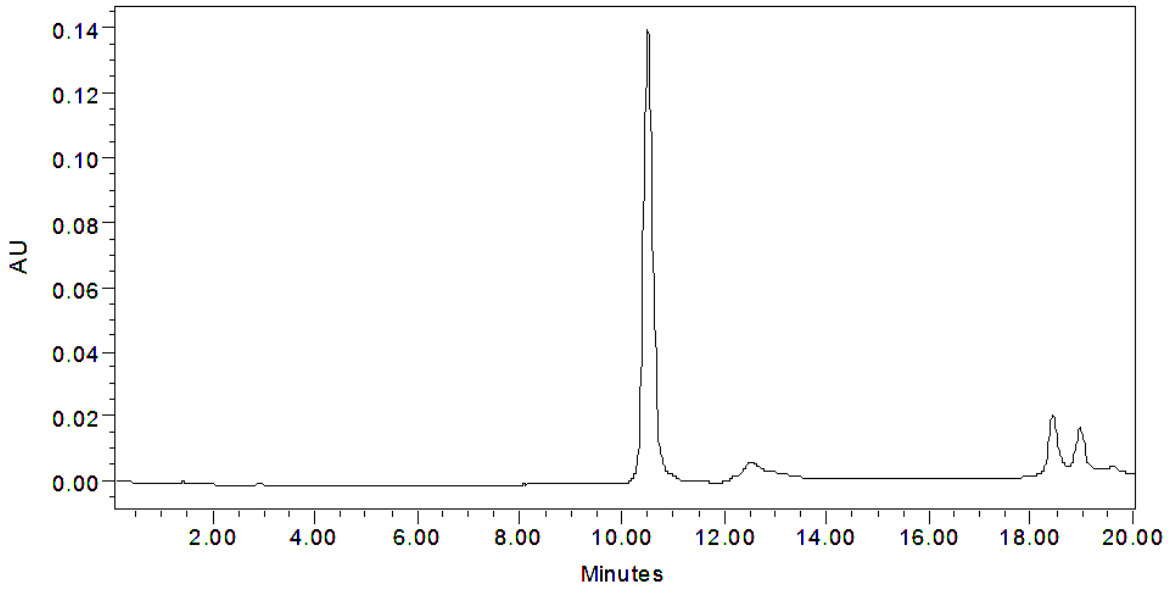

Fig. 55 CP20 90 µM in water, 50 µl injection volume

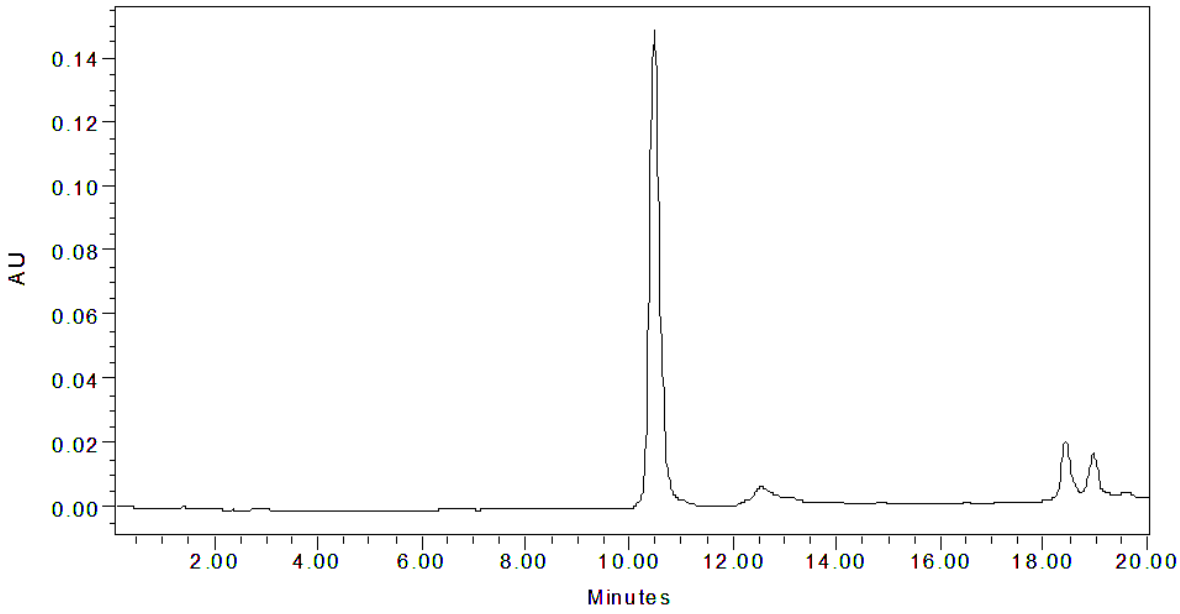

Fig. 56 CP20 100 µM in water, 50 µl injection volume

2 Calibration curve AUCs

calibration curve CP20		
concentration:	AUC:	average:
5µM:	31581	
	28948	31307
	33392	
5µM:	92531	
	90289	90366,33
	88279	
7µM:	120901	
	127722	125410,3
	127608	
10µM:	185466	
	194853	188152,3
	184138	
20µM:	395421	
	393019	392906,3
	390279	
30µM:	575452	
	619486	597580,3
	597803	
40µM:	787764	
	786988	773388,7
	745414	
50µM:	967377	
	993794	967121,3
	940193	
60µM:	1153716	
	1146018	1154411
	1163499	
70µM:	1290341	
	1362762	1333550
	1347547	
80µM:	1561967	
	1584492	1562041
	1539663	
90µM:	1751993	
	1697272	1721930
	1716525	
100µM:	1949649	
	1848424	1896597
	1891718	

Table 2 AUCs of the calibration curve CP20 in water

3 Scintillation counter results

14C DPM in hCMEC/D3 P, + 100 µM CP20					
Time	19.11.2009	23.11.2009	27.11.2009	**total av.**	Average timepoints
25	40	41	49	43,33	49,06
25	86	83	41	70,00	
25	64	55	49	56,00	
25	52	31	35	39,33	
25	49	36	35	40,00	
25	52	47	38	45,67	
20	48	36	40	41,33	44,44
20	38	50	32	40,00	
20	43	39	41	41,00	
20	94	41	40	58,33	
20	56	49	38	47,67	
20	51	29	35	38,33	
15	58	40	32	43,33	38,56
15	44	38	38	40,00	
15	49	41	32	40,67	
15	42	34	33	36,33	
15	35	33	35	34,33	
15	39	33	38	36,67	
10	41	48	41	43,33	41,39
10	43	44	36	41,00	
10	44	40	28	37,33	
10	55	40	31	42,00	
10	36	67	29	44,00	
10	44	45	33	40,67	
5	27	22	57	35,33	30,00
5	28	24	41	31,00	
5	29	23	35	29,00	
5	22	23	32	25,67	
5	22	20	33	25,00	
5	26	34	42	34,00	
average:	45,233333	39,533333	37,3	40,69	

Table 3 DPM values 100 µM CP20

14C DPM in hCMEC/D3 P, + 800 µM CP20					
Time	19.11.2009	23.11.2009	27.11.2009	**total av.**	Average timepoints
25	29	27	33	29,67	36,50
25	23	25	53	33,67	
25	41	34	38	37,67	
25	44	33	40	39,00	
25	44	48	30	40,67	
25	45	39	31	38,33	
20	40	33	35	36,00	37,56
20	39	40	32	37,00	
20	42	38	28	36,00	
20	36	28	28	30,67	
20	36	39	34	36,33	
20	40	69	39	49,33	
15	36	44	38	39,33	55,06
15	86	40	41	55,67	
15	125	46	41	70,67	
15	60	72	43	58,33	
15	51	46	36	44,33	
15	60	68	58	62,00	
10	40		47	43,50	58,75
10	51	54	33	46,00	
10	50	79	38	55,67	
10	59	47	83	63,00	
10	62	42	39	47,67	
10	169	56	65	96,67	
5	40	39	45	41,33	45,44
5	42	40	38	40,00	
5	56	52	41	49,67	
5	56	62	36	51,33	
5	42	43	31	38,67	
5	52	54	49	51,67	
average:	53,2	46,103448	40,766667	46,66	

Table 4 DPM values 800 µM CP20

4 Protein assay results

PA in hCMEC/D3 P, +100 µM CP20					
Time	19.11.2009	23.11.2009	27.11.2009	**Average**	av time
25	5,9	9,69	3,82	6,76	6,90
25	7,81	10,63	5	7,82	
25	4,19	9,42	4,92	7,17	
25	4,19	7,93	3,77	5,85	
25	5,66	8,75	3,92	6,34	
25	6,25	10,67	4,28	7,48	
20	5,31	11,08	3,97	7,53	6,47
20	5,8	10,05	4,92	7,49	
20	4,41	7,18	3,79	5,49	
20	7,03	7,78	3,43	5,61	
20	5,68	7,35	4,72	6,04	
20	4,97	7,5	5,82	6,66	
15	5	6,22	2,61	4,42	6,73
15	4,56	13,23	4,18	8,71	
15	6,17	9,52	4,77	7,15	
15	4,26	9,76	3,64	6,70	
15	4,61	8,63	3,92	6,28	
15	6,22	9,54	4,72	7,13	
10	5,88	4	4,85	4,43	5,62
10	3,75	10,05	3,74	6,90	
10	5	8,19	3,95	6,07	
10	4,97	6,1	3,36	4,73	
10	4,02	7,54	3,87	5,71	
10	5,31	6,92	4,87	5,90	
5	4,14	10,6	4,59	7,60	8,43
5	5,56	9,37	8,11	8,74	
5	4,58	12,17	4,46	8,32	
5	5,88	10,05	4,13	7,09	
5	5,02	9,11	4,28	6,70	
5	5,27	9,83	14,4	12,12	

Table 5 Protein assay values 100 µM CP20

PA in hCMEC/D3 P, +800 µM CP20					
Time	19.11.2009	23.11.2009	27.11.2009	**Average**	
25	4,61	10,82	7,88	9,35	7,52
25	4,38	10,65	4,33	7,49	
25	5,56	9,01	5,21	7,11	
25	4,26	8,1	3,82	5,96	
25	4,21	8,53	4,46	6,50	
25	5,95	6,41	11,01	8,71	
20	5,51	10,19	4,59	7,39	6,66
20	4,46	9,78	3,2	6,49	
20	3,38	8,77	3,38	6,08	
20	4,41	8,68	5,77	7,23	
20	3,09	9,04	3,69	6,37	
20	4,7	8,31	4,51	6,41	
15	5,14	9,11	6,23	7,67	6,75
15	5,27	9,08	5,62	7,35	
15	3,94	9,13	4,56	6,85	
15	4,41	7,01	4,31	5,66	
15	3,16	10,05	3,38	6,72	
15	3,8	8,75	3,72	6,24	
10	5,49	13,66	6,39	10,03	7,22
10	4,51	9,42	8,36	8,89	
10	4,31	9,81	4,51	7,16	
10	3,28	9,76	4,18	6,97	
10	3,31	5,04	3,02	4,03	
10	5,88	7,5	4,95	6,23	
5	5,71	9,61	4,98	7,30	6,01
5	5,12	6,94	4,03	5,49	
5	5,22	8,05	4,03	6,04	
5	5,05	7,3	4,1	5,70	
5	4,73	7,62	5,1	6,36	
5	4,41	6,39	3,97	5,18	

Table 6 Protein assay values 800 µM CP20